

SCHOOL OF CIVIL ENGINEERING



JOINT HIGHWAY RESEARCH PROJECT

JHRP-75-3

PORE SIZE DISTRIBUTION OF
COMPACTED SOILS AFTER CRITICAL
REGION DRYING

R. N. Bhasin



PURDUE UNIVERSITY
INDIANA STATE HIGHWAY COMMISSION

PORE SIZE DISTRIBUTION OF COMPACTED SOILS AFTER CRITICAL REGION DRYING

File: 6-6-8

C. F. Scholer
M. B. Scott
K. C. Sinha
H. R. J. Walsh
L. E. Wood
E. J. Yoder
S. R. Yoder

1. Report No.	2. Government Accession No.	3. Recipient's Catalog No.	
4. Title and Subtitle PORE SIZE DISTRIBUTION OF COMPACTED SOILS AFTER CRITICAL REGION DRYING		5. Report Date March 1975	
		6. Performing Organization Code C-36-5H	
7. Author(s) R. N. Bhasin		8. Performing Organization Report No. JHRP-75-3	
9. Performing Organization Name and Address Joint Highway Research Project Civil Engineering Building Purdue University West Lafayette, Indiana 47907		10. Work Unit No.	
		11. Contract or Grant No. HPR-1(12) Part II	
12. Sponsoring Agency Name and Address Indiana State Highway Commission 100 North Senate Avenue Indianapolis, Indiana 46204		13. Type of Report and Period Covered Final Report	
		14. Sponsoring Agency Code CA 370	
15. Supplementary Notes Conducted in cooperation with the U.S. Department of Transportation, Federal Highway Administration, Research Study Titled "Pore Size Distribution and Its Effect on Behavior of Compacted Clayey Soils".			
16. Abstract The major objective of this research was to develop an improved insight into the soil compaction process in terms of the pore size distribution resulting from variations of the soil compaction variables, and of the changes in this parameter arising as a result of exposing compacted soils to soaking under a moderate surcharge, thus partly simulating service conditions. The mercury intrusion technique was used to obtain pore size distributions on dried specimens of a number of naturally occurring soils, each compacted at a number of water contents by the Standard Proctor method and/or by 3 levels of compactive effort in the Modified Proctor method. The wet specimens were dried by transforming soil water to water vapor in the critical region without effecting change in the total porosity and probably in the size distribution of pores. It was shown that different soils compacted to a given percentage compaction, but to different total porosities, on the dry side of Standard Proctor optimum moisture contents have significantly different pore size distributions. On the other hand, these soils compacted at Standard Proctor optimum moisture contents to different total porosities had pore size distributions similar to each other except that the content of pores below 0.1 μ m varied with the clay			
17. Distribution Statement Pore Size Distribution; Mercury Intrusion; Critical Region Drying; Compacted Soils; Compacted Soils after Soaking; Compaction Process		18. Distribution Statement Type of Distribution	
19. Security Classif. (of this report) Unclassified	20. Security Classif. (of this page) Unclassified	21. No. of Pages 220	22. Price

Final Report
PORE SIZE DISTRIBUTION OF COMPACTED SOILS AFTER
CRITICAL REGION DRYING

by

Rakhishwar Nath Bhasin
Graduate Instructor in Research

Joint Highway Research Project

Project No.: C-36-5H

File: 6-6-8

Prepared as Part of an Investigation

Conducted by

Joint Highway Research Project
Engineering Experiment Station
Purdue University

in cooperation with the
Indiana State Highway Commission
and the

U.S. Department of Transportation
Federal Highway Administration

The contents of this report reflect the views of the author who is responsible for the facts and the accuracy of the data presented herein. The contents do not necessarily reflect the official views or policies of the Federal Highway Administration. This report does not constitute a standard, specification, or regulation.

Purdue University
West Lafayette, Indiana
March 26, 1975



ACKNOWLEDGEMENTS


The writer is indebted to Dr. C. W. Lovell, his major professor, and to Dr. S. Diamond, both of whom directed this research, for their unswerving support and understanding during the course of this study.

Sincere thanks are due to Dr. A. G. Altschaeffl for valuable counsel and financial support during the later part of this study, and to Dr. J. L. White and to Dr. G. A. Leonards for support.

The writer is grateful to Mr. James R. Hooper for his generous assistance in the design of the critical region drying equipment used in this research.

The financial support for this research was provided by the Indiana State Highway Commission, and the Federal Highway Administration of the U.S. Department of Transportation. The research was administered through the Joint Highway Research Project, Engineering Experiment Station, Purdue University, Lafayette, Indiana. Their support is acknowledged and appreciated.

Most of all, the writer expresses his deepest appreciation and gratitude to the three charming ladies, namely, his wife Tripta and his daughters Arpna and Archna, for their understanding and encouragement during this study.



Digitized by the Internet Archive
in 2011 with funding from
LYRASIS members and Sloan Foundation; Indiana Department of Transportation

TABLE OF CONTENTS

	Page
LIST OF TABLES	viii
LIST OF FIGURES	xi
LIST OF ABBREVIATIONS	xvi
ABSTRACT	xvii
CHAPTER I. INTRODUCTION	1
CHAPTER II. LITERATURE REVIEW	4
Soil Compaction	4
General	4
Domains in Compacted Soils	6
Role of Soil Aggregations in Soil Compaction	7
Compaction Process Details	8
Use of Air Dried Soil in Laboratory Compaction	8
Soil Mixing	10
Curing of Mixed Soil	11
Uniformity in Laboratory Impact Compacted Samples	12
Field Compaction versus Laboratory Impact Compaction	13
Critical Region Drying	14
Theory	14
Historical Development	16
Thermal Stability of Clay Minerals	17
Thermal Expansion of Clay Minerals	19
Constant Volume Soaking of Compacted Soils	20
Solubility of Air in Water	21
Pore Size Distribution	21
Significance of Pore Size Distribution	21
Methods to Determine Pore Size Distributions	22
Optical and Electron Microscopy	23
Capillary Condensation	24
Capillary Suction	25
Mercury Intrusion	26
Total Porosity Determinations Using the Mercury Intrusion Equipment	33
Soaking under a Nominal Surcharge Pressure	34

	Page
CHAPTER III. SOILS STUDIED.	36
General	36
Edgar Plastic Kaolin.	39
Grundite.	39
Reddish-Brown Limestone Residual Clay	39
Boston Blue Clay.	40
Crosby Silty Clay	40
Volclay Bentonite	40
CHAPTER IV. APPARATUS AND EXPERIMENTAL PROCEDURES . . .	42
Mixing and Curing	42
Mixing	42
Curing	44
Preparation and Protection of Compacted Samples . .	44
Soaking and Swelling of Compacted Samples	46
Preparation of Samples for Critical Region Drying .	47
Compacted Soil	47
Compacted Soil After Soaking	51
Soil Aggregations.	51
Critical Region Drying.	53
The Apparatus.	53
The Technique.	58
Pore Size Distribution.	72
The Apparatus.	72
The Technique.	78
Reduction of Data to Pore Size Distributions .	82
CHAPTER V. RESULTS.	85
Soil Mixing and Aggregation	85
Compacted Soil.	90
Effect of Drying Procedures	93
Pore Size Distribution.	101
Influence of Soil Processing and Soil Mixing	
Artifacts on Pore Size Distribution	105
Pore Size Distributions of Soil Aggregations .	107
Pore Size Distributions of Soils Compacted	
by the Standard Proctor Method.	111
Edgar Plastic Kaolin.	112
Crosby Silty Clay	116
Boston Blue Clay.	120
Grundite.	122
Reddish-Brown Limestone Residual Clay .	126
Comparison of Pore Size Distributions of	
Different Soils Compacted to Approximately	
Equal Total Porosities at Different Water	
Contents by the Standard Proctor Method .	128

Pore Size Distributions of Edgar Plastic Kaolin Compacted by the Modified Proctor Method and by Methods Based on It134
Pore Size Distributions of Compacted Soils After Soaking Under a Nominal Sur-charge Pressure142
Edgar Plastic Kaolin.152
Grundite.155
Comparisons of the Pore Size Distributions of Soaked Specimens of Edgar Plastic Kaolin Compacted at Nearly Equal Water Contents by Higher Compactive Efforts155
CHAPTER VI. DISCUSSION OF RESULTS157
Effectiveness of Critical Region Drying157
Changes in the Total Porosity of Compacted Soils on Oven Drying and on Freeze Drying.160
Comparisons of Pore Size Distributions of Critical Region Dried and Oven Dried Soils163
Constancy of Space in Fine Pores for Critical Region Dried Soils166
Influence of Mixing Water Content on Total Porosity and on Pore Size Distributions of Aggregations167
Influence of Compaction on Pore Size Distributions of Aggregations.168
Influence of Molding Water Content on Pore Size Distributions of Compacted Soils169
Comparisons of the Pore Size Distributions of Soils Compacted to the Same Total Porosity on the Dry and Wet Sides of Standard Proctor Optimum.173
Influence of Soil Type on Pore Size Distributions Obtained at About Standard Proctor Optimum. . .	.174
Influence of Soil Type on Pore Size Distributions Obtained for Dry-Side Samples Compacted to 95% or Less of Standard Proctor Maximum Dry Density.175
Influence of Soil Type on Pore Size Distributions Obtained for Wet-Side Samples Compacted to About 95% or Less of Standard Proctor Maximum Dry Density.176
Influence of Increasing Compactive Effort on Pore Size Distributions of Edgar Plastic Kaolin176
Influence of Molding Water Content on Total Porosity of Soaked Samples of Compacted Soils. . .	.178
Influence of Molding Water Content on Pore Size Distributions of Soaked Samples of Compacted Soils.180
Summary of Results.181

	Page
CONCLUSIONS	185
RECOMMENDATIONS FOR FURTHER STUDY	188
LIST OF REFERENCES.	189
APPENDIX A - TABULATED PORE SIZE DISTRIBUTION DATA. . .	204

LIST OF TABLES

Table		Page
III-1	Classification Properties of Soils Studied . .	37
V-1	Variation of the Dry Unit Weight and the Degree of Saturation for Edgar Plastic Kaolin and Grundite Aggregations Formed at Different Water Contents	89
V-2	The Optimum Moisture Contents and the Maximum Dry Densities of the Compacted Soils	92
V-3	Comparison of the "As-Molded" Porosity of Grundite and Crosby Silty Clay Compacted at Different Water Contents by the Standard Proctor Method with the Porosities Obtained After Oven Drying, Freeze Drying, and Critical Region Drying of Small Samples	95
V-4	Comparison of the "As-Molded" Porosity of Edgar Plastic Kaolin, Grundite, Crosby Silty Clay, Reddish-Brown Limestone Residual Clay, and Volclay Bentonite Compacted at Different Water Contents by the Standard Proctor Method with the Porosity Obtained After Critical Region Drying of Small Samples	96
V-5	Degrees of Saturation of Edgar Plastic Kaolin and Grundite Compacted at Different Water Contents, and Soaked Under a Surcharge Pressure of Either 3/16 Or 3/4 psi.	150
Appendix		
A-1	Distribution of Pore Space for Edgar Plastic Kaolin and Grundite Aggregations Manufactured at Different Water Contents, and Dried by the Critical Region Method	204
A-2	Percent Distribution of Pore Space for Edgar Plastic Kaolin and Grundite Aggregations Manufactured at Different Water Contents, and Dried by the Critical Region Method.	205

Appendix
Table

Page

A-3	Distribution of Pore Space for Edgar Plastic Kaolin, Crosby Silty Clay, Boston Blue Clay, Grundite, and Reddish-Brown Limestone Residual Clay Compacted at Different Water Contents by the Standard Proctor Method, and Critical Region Dried	206
A-4	Percent Distribution of Pore Space for Edgar Plastic Kaolin, Crosby Silty Clay, Boston Blue Clay, Grundite, and Reddish-Brown Limestone Residual Clay Compacted at Different Water Contents by the Standard Proctor Method, and Critical Region Dried.	208
A-5	Mean Pore Diameters of the Space in Pore Sizes Above and Below 0.1 Micrometers for Edgar Plastic Kaolin and Grundite Aggregations, and for Edgar Plastic Kaolin, Crosby Silty Clay, Boston Blue Clay, Grundite, and Reddish-Brown Limestone Residual Clay Compacted at Different Water Contents by the Standard Proctor Method, and Critical Region Dried.	210
A-6	Distribution of Pore Space for Edgar Plastic Kaolin Compacted at Different Water Contents by Methods Based on the Modified Proctor Compaction Method, and Critical Region Dried	212
A-7	Percent Distribution of Pore Space for Edgar Plastic Kaolin Compacted at Different Water Contents by Methods Based on the Modified Proctor Compaction Method, and Critical Region Dried.	213
A-8	Mean Pore Diameters of the Space in Pore Sizes Above and Below 0.1 Micrometers for Edgar Plastic Kaolin Compacted by the Methods Based on Modified Proctor Compaction, and Critical Region Dried	214
A-9	Distribution of Pore Space for Edgar Plastic Kaolin and Grundite Compacted at Different Water Contents, and Soaked Under a Surcharge Pressure of Either 3/16 Or 3/4 psi	215
A-10	Percent Distribution of Pore Space for Edgar Plastic Kaolin and Grundite Compacted at Different Water Contents, and Soaked Under a Surcharge Pressure of Either 3/16 Or 3/4 psi	217

Appendix
Table

Page

A-11	Mean Pore Diameters of the Space in Pore Sizes Above and Below 0.1 Micrometers for Edgar Plastic Kaolin and Grundite Compacted at Different Water Contents, and Soaked Under a Surcharge Pressure of Either 3/16 Or 3/4 psi .	219
------	---	-----

LIST OF FIGURES

Figure		Page
III-1	Grain Size Distribution for Soils Studied. . . .	38
IV-1(a)	Liquid-Solids Twin-Shell Blender	43
IV-1(b)	Mixing Operation Details of Dispersion Blades. .	43
IV-2	A Soil Sample Assembled for the Soaking Test Showing Porous Stone, Latex Membrane, and Stainless Steel Connectors	48
IV-3	Sample Preparation Accessories: Slotted Steel Cylinder (Left Top), 1/2 Inch Diameter Plastic Lathe Heads (Left Bottom), and Lathe for Rough Trimming (Right)	50
IV-4	Sample Preparation Accessories: Stainless Steel 1/2 Inch Diameter Trimmer (Bottom), and Sample Extruder (Top)	52
IV-5	Details of Critical Region Drying Equipment. . .	54
IV-6	Details of Critical Region Drying Equipment. . .	55
IV-7	Schematic of Critical Region Drying Equipment. .	56
IV-8	Pressure-Specific Volume Isotherms for Water and Water Vapor.	60
IV-9	Isobars of Specific Volume-Temperature for Water and Water Vapor (After Nowak [1962])	61
IV-10	Boiling Phase Line	62
IV-11	Typical Pressure and Temperature vs. Time Relationships for Critical Region Run.	64
IV-12	Typical Pressure and Temperature vs. Time Relationships for Critical Region Run (after J. R. Hooper).	65
IV-13	A Soil Sample Assembled for Critical Region Drying. Porous Stones are Clamped on Either Side of the Sample in the Container.	68

Figure		Page
IV-14	Penetrometer: (From Front to Back) Disassembled, Assembled with Sample, and Filled with Mercury (After Winslow [1969])	74
IV-15	Filling Device (After Winslow [1969])	75
IV-16	Mercury Intrusion Equipment Showing (From Left to Right) Manometer, Vacuum Manifold, Filling Device, and Porosimeter (After Winslow [1969]) .	76
V-1	Soil Aggregation Size Distribution Curves for Edgar Plastic Kaolin	86
V-2	Variation of the Soil Aggregation Sizes d_{10} and d_{50} with the Mixing Water Content for Edgar Plastic Kaolin	88
V-3	Compaction Curves for Edgar Plastic Kaolin, Grundite, Reddish-Brown Limestone Residual Clay, Boston Blue Clay, Crosby Silty Clay, and Volclay Bentonite.	91
V-4	Infra-Red Spectrographs of Oven Dried and Critical Region Dried Boston Blue Clay	98
V-5	Infra-Red Spectrographs of Compacted and Critical Region Dried Edgar Plastic Kaolin	99
V-6	Infra-Red Spectrographs of Oven Dried, Critical Region Dried and 730°F Heated Grundite	100
V-7	X-Ray Diffractograms of Oven Dried and Critical Region Dried Grundite.	102
V-8	X-Ray Diffractograms of Air Dried and Critical Region Dried Volclay Bentonite	103
V-9	Cumulative Intrusion Curves for the Processed and the Unprocessed Crosby Silty Clay Compacted at the Mixing and the Natural Water Contents of 22.2% and 24.4%, Respectively, by the Standard Proctor Method	106
V-10	Cumulative Intrusion Curves for Edgar Plastic Kaolin Aggregations Formed at the Mixing Water Contents of 26.9%, 29.1%, and 34.6%.	109
V-11	Cumulative Intrusion Curves for Grundite Aggregations Formed at the Mixing Water Contents of 19.4% and 23.0%	110

Figure		
V-12	Cumulative Intrusion Curves for Edgar Plastic Kaolin Compacted at Different Water Contents by the Standard Proctor Method	113
V-13	Cumulative Intrusion Curves for Edgar Plastic Kaolin Compacted at Different Water Contents by the Standard Proctor Method	114
V-14	Cumulative Intrusion Curves for Crosby Silty Clay Compacted at Different Water Contents by the Standard Proctor Method.	117
V-15	Cumulative Intrusion Curves for Crosby Silty Clay Compacted at Different Water Contents by the Standard Proctor Method.	118
V-16	Cumulative Intrusion Curves for Boston Blue Clay Compacted at Different Water Contents by the Standard Proctor Method.	121
V-17	Cumulative Intrusion Curves for Grundite Compacted at Different Water Contents by the Standard Proctor Method.	123
V-18	Cumulative Intrusion Curves for Grundite Compacted at Different Water Contents by the Standard Proctor Method.	124
V-19	Cumulative Intrusion Curves for Reddish-Brown Limestone Residual Clay Compacted at Different Water Contents by the Standard Proctor Method.	127
V-20	Cumulative Intrusion Curves for Reddish-Brown Limestone Residual Clay, Crosby Silty Clay, and Grundite Compacted by the Standard Proctor Method at the Water Contents Dry of the Optimum	129
V-21	Cumulative Intrusion Curves for Edgar Plastic Kaolin and Boston Blue Clay Compacted by the Standard Proctor Method to an Approximate Void Ratio of 1.03 at the Moisture Contents Dry of the Optimum	130
V-22	Cumulative Intrusion Curves for Boston Blue Clay, Reddish-Brown Limestone Residual Clay, and Grundite Compacted by the Standard Proctor Method at the Water Contents Near the Optimum.	132
V-23	Cumulative Intrusion Curves for Grundite, Boston Blue Clay, and Crosby Silty Clay Compacted at the Water Contents Wet of the Optimum by the Standard Proctor Method	133

Figure		Page
V-24	Cumulative Intrusion Curves for Edgar Plastic Kaolin Compacted at Different Water Contents by the Modified Proctor Compaction Method. . .	135
V-25	Cumulative Intrusion Curves for Edgar Plastic Kaolin Compacted at Different Water Contents by the Modified Proctor Compaction Method. . .	136
V-26	Cumulative Intrusion Curves for Edgar Plastic Kaolin Compacted at Different Water Contents by Impact Compaction with 10 lb. Hammer, 18" Fall and 12 Blows/Layer on 5 Layers. . . .	137
V-27	Cumulative Intrusion Curves for Edgar Plastic Kaolin Compacted at Different Water Contents by Impact Compaction Method with 10 lb. Hammer, 18" Fall and 6 Blows/Layer on 5 Layers	138
V-28	Cumulative Intrusion Curves for Edgar Plastic Kaolin Compacted at Different Water Contents by the Standard Proctor Method, and Soaked Under a Surcharge Pressure of 3/4 psi.	143
V-29	Cumulative Intrusion Curves for Edgar Plastic Kaolin Compacted at Different Water Contents by the Impact Compaction Method Using 10 lb. Hammer, 18" Fall, 6 Blows/Layer on 5 Layers, and Soaked Under a Surcharge Pressure of 3/4 psi.	144
V-30	Cumulative Intrusion Curve for Edgar Plastic Kaolin Compacted at a Water Content of 23.2% by the Impact Compaction Method Using 10 lb. Hammer, 18" Fall, 12 Blows/Layer on 5 Layers, and Soaked Under a Surcharge Pressure of 3/16 psi	145
V-31	Cumulative Intrusion Curves for Edgar Plastic Kaolin Compacted at Different Water Contents by the Impact Compaction Method Using 10 lb. Hammer, 18" Fall, 12 Blows/Layer on 5 Layers, and Soaked Under a Surcharge Pressure of 3/4 psi .	146
V-32	Cumulative Intrusion Curves for Edgar Plastic Kaolin Compacted at a Water Content of 23.5% by the Modified Proctor Method, and Soaked Under a Surcharge Pressure of 3/16 psi	147
V-33	Cumulative Intrusion Curves for Edgar Plastic Kaolin Compacted at Different Water Contents by the Modified Proctor Method, and Soaked Under a Surcharge Pressure of 3/4 psi	148

Figure		Page
V-34	Cumulative Intrusion Curves for Grundite Compacted at Different Water Contents by the Standard Proctor Method, and Soaked Under a Surcharge Pressure of 3/4 or 3/16 psi.	149
VI-1	Cumulative Intrusion Curves for Edgar Plastic Kaolin Compacted at a Water Content of 31.2% by the Standard Proctor Method, and Trimmed to Different Dimensions for Critical Region Drying	161

LIST OF ABBREVIATIONS

ASCE	American Society of Civil Engineers
ASTM	American Society for Testing and Materials
Å	Angstrom (10^{-8} cm)
C	Centigrade
cm	Centimeter
°	Degree
d ₅₀	Aggregation size with 50 percent by weight of the aggregations finer than this size
F	Fahrenheit
gm	Gram
Hg	Mercury
"	Inch
lb	Pound
μm	Micrometer (10^{-4} cm)
ml.	Milliliter (1 cm^3)
mm	Millimeter (10^{-1} cm)
%	Percent
pcf	Pound/cubic foot
psi	Pound/square inch
U.S.	United States

ABSTRACT

Bhasin, Rakhishwar Nath. Ph.D., Purdue University, May 1975.
Pore Size Distribution of Compacted Soils After Critical
Region Drying. Major Professor: C. W. Lovell.

The major objective of this research was to develop an improved insight into the soil compaction process in terms of the pore size distribution resulting from variations of the soil compaction variables, and of the changes in this parameter arising as a result of exposing compacted soils to soaking under a moderate surcharge, thus partly simulating service conditions.

A number of naturally occurring soils were utilized, but the two soils investigated in greatest detail were Edgar Plastic kaolin and grundite. All these soils were compacted at a number of water contents by the Standard Proctor method and by 3 levels of compactive effort in the Modified Proctor method.

Pore size distributions were obtained on dried specimens of soil aggregations, compacted soils, and compacted soils after soaking. The mercury intrusion technique, consisting of injection under pressure of mercury into the evacuated pores, was used to measure the pore space. Pore size distributions were computed from the intrusion versus pressure data using the Washburn equation.

The samples needed for the pore size distribution study were dried by transforming soil water to water vapor in the critical region. This transformation permits removal of water without formation of menisci of progressively reducing radii, which cause the shrinkage associated with other forms of drying such as air and oven drying. In the absence of shrinkage, the original porosity and probably the size distribution of pores were retained throughout the drying process.

Based on the extensive series of pore size distributions measured in this study it was concluded that:

1. The techniques used in this study for measuring pore size distributions, and involving critical region drying and mercury intrusion, are reliable.
2. Different soils, compacted to a given percentage compaction (e.g., 95% of Standard Proctor maximum dry density) on the dry side of Standard Proctor optimum moisture content, have different total porosities. Furthermore, the pore size distributions of the various soils compacted in this manner are significantly different from each other.
3. Soils compacted at Standard Proctor optimum moisture contents varied considerably in total porosity, but had pore size distributions similar to each other in many respects. All pore sizes intruded were smaller than $0.4\ \mu\text{m}$. Between 0.1 and $0.4\ \mu\text{m}$, all the soils had a characteristic size distribution of pores. Below $0.1\ \mu\text{m}$, the content of pores varied with the clay fraction, and to some extent the type of soil.
4. Increase in compactive effort on the dry side of optimum moisture values decreased the total porosity and diminished the quantity of pores at the larger pore size end of the distribution. The largest pores present were about $6.5\ \mu\text{m}$ for Standard Proctor compaction but were only about $0.4\ \mu\text{m}$ for Modified Proctor compaction. Thus the increased energy applied resulted in a reduced maximum pore size and a finer pore size distribution.
5. Increasing the compactive effort on the wet side of optimum moisture values had little effect on either the total porosity or the distribution of pore sizes.

6. Compaction at optimum moisture content using the Modified Proctor method (or the Modified Proctor - based method using 12 blows/layer) resulted in a smaller maximum pore size and reduced porosity as compared with compaction at optimum moisture content using the Standard Proctor method.

The effect of soaking under a nominal surcharge pressure on soils compacted at about optimum moisture content by the Modified Proctor method (or the Modified Proctor-base method using 12 blows/layer) was less than that undergone by corresponding soils compacted at about optimum moisture content by the Standard Proctor method. The former underwent a smaller increase in both the total porosity and maximum pore size than the latter.

7. After soaking under a nominal surcharge pressure, soils compacted on the dry side of optimum moisture values exhibited a higher porosity and a coarser pore size distribution than the soils compacted on the wet side of the optimum values.
8. The relative distributions of pore sizes effected by variables of moisture content, compactive effort, and soaking tend to agree with previous postulations, e.g., Lambe (1958) and Hodek (1972), with respect to compacted soil fabric.
9. The gross differences in pore size distributions occurring at the same percentage compactions, for different soils and compactive efforts, emphasize the lack of control over the compacted product exercised by most end result compaction specifications.

CHAPTER I

INTRODUCTION

Compacted clayey soils are used extensively in highway construction. The physical response of these clayey soils to the compaction process is not completely understood, because it involves interactions between a number of soil and compaction variables. Variations in soil properties such as permeability, compressibility, and strength are often explained in terms of differences in soil structure brought about by different kinds and extents of compaction employing different levels of energy at different levels of soil variables. The resulting soil structures are generally discussed in qualitative terms, quantitative characterization being difficult and time consuming. Because the differences in soil structure include significant differences in the distribution of total porosity in terms of pore sizes, it would be useful to investigate the pore size distributions of the compacted soils by some direct method. To date, comparatively few studies have been reported on the pore size distributions of soils in their as-compacted and in-service conditions.

The main objective of the present study was to investigate the pore size distributions of a variety of natural

clayey soils (a) after compaction of the soils at different levels of the soil and compaction variables, and (b) after exposing the compacted soils to soaking under a nominal surcharge pressure designed to partly simulate the influence of the service environment on the compacted condition. Soil variables such as soil type and molding water content; compaction variables such as the compactive effort in the Proctor compaction method; and in-service variables such as soaking the compacted soil under nominal surcharge pressures ($\frac{3}{16}$ or $\frac{3}{4}$ psi) were considered in this work.

The various steps involved in determining a pore size distribution include securing of a representative small soil specimen, drying it without effecting a significant change in its total porosity and in the size distribution of the pores using the critical region drying method, evacuating the pores, injecting a non-wetting liquid such as mercury in them, and computing pore size distribution using the intrusion versus pressure data.

The range of pore sizes covered in this investigation extended from 160 \AA to 600 micrometers, which was found to be adequate for the soils used in this study. Pore sizes smaller than 160 \AA might belong to the intradomainal porosity. This study showed that for at least these specific soils the portion of porosity encountered in pore sizes smaller than 160 \AA is not modified by the compaction process.

The study intends to develop basic insight into the soil compaction process in terms of pore size distribution, and the changes in this parameter as a result of exposing compacted soils to a partly-simulated service environment.

re-expressed Proctor's explanation in a more detailed form, considering that the increase in density with increasing molding water contents resulted from thicker but less viscous water films around soil grains. Lambe (1958a) discussed the compaction process in terms of the double layer concepts. These concepts were interpreted by him to imply that the clay particles were flocculated randomly with respect to each other at compaction water contents dry of the optimum moisture content, and were oriented in a face to face fashion, but dispersed, at compaction water contents wet of the optimum moisture content. They did not, however, explain the influence of different compaction methods on the resulting soil structure. Seed and Chan (1959) incorporated the influence of shear strains associated with different compaction methods in the Lambe explanation of compacted clay structure. Experimental data supporting the Lambe explanation were generated by Pacey (1956) and by Seed and Chan (1959). These workers compacted Boston blue clay and Peerless #2 kaolin at a number of water contents by the kneading method and studied thin sections of the resulting soils using a polarizing microscope. For increasing molding water contents, greater orientations were observed by them over regions larger than 10 micrometers, the limit of resolution of the polarizing microscope.

CHAPTER II

LITERATURE REVIEW

The literature review will provide background information for a better understanding of this study, and will focus on specifics such as soil compaction, compaction process details, critical region drying, pore size distribution, and soaking under a nominal surcharge pressure, in the order mentioned.

Soil Compaction

General

One of the objectives of this study is to examine the response of a number of natural soils to the compaction process in terms of pore size distribution. It is pertinent, therefore, to review some of the theories which have been advanced in the recent past to explain the compaction process. Proctor (1933)¹ made a pioneering attempt to explain the usual compaction curve trend observed with most clayey soils. He attributed the increase in density with increasing molding water contents up to the optimum moisture content to increased lubrication of soil grains and to reduction in the capillary pressures. Hogentogler (1936)

¹References are listed alphabetically in the List of References, page 189.

Introduction

1. Background

The purpose of this study is to investigate the effects of various factors on the performance of a system. The study is divided into two main parts: a theoretical analysis and an experimental investigation. The theoretical analysis focuses on the development of a model that can predict the system's behavior under different conditions. The experimental investigation involves the design and execution of a series of tests to validate the model and to determine the range of conditions over which it is applicable. The results of the study are presented in the form of a series of graphs and tables, which show the relationship between the various factors and the system's performance. The study is intended to provide a comprehensive overview of the system's behavior and to identify the key factors that influence its performance.

2. Methodology

The methodology of this study is based on a combination of theoretical and experimental approaches. The theoretical analysis is carried out using a series of mathematical models that describe the system's behavior. These models are developed based on a series of assumptions and are used to predict the system's performance under different conditions. The experimental investigation is carried out using a series of tests that are designed to validate the model and to determine the range of conditions over which it is applicable. The tests are carried out using a series of different input parameters and the results are compared with the predictions of the model. The methodology is intended to provide a comprehensive overview of the system's behavior and to identify the key factors that influence its performance.

3. Results

The results of the study are presented in the form of a series of graphs and tables. The graphs show the relationship between the various factors and the system's performance. The tables provide a summary of the results of the tests and show the range of conditions over which the model is applicable. The results are intended to provide a comprehensive overview of the system's behavior and to identify the key factors that influence its performance.

Domains in Compacted Soils

The existence of domains of oriented clay particles in a number of compacted kaolinitic and illitic soils has been conclusively demonstrated by Aylmore and Quirk (1960a) and by Sloane and Kell (1966), both of whom used electron microscopic techniques to study carbon replicas of the fractured surfaces. Smalley and Cabrera (1969) and Diamond (1971) came to the same conclusion, using scanning electron microscopic techniques. The domains could be transferred from the processed dry soil to the compacted soil (Michaels [1959]), (Aylmore and Quirk [1960b]), or could be generated in the regions encountering large shear strains during compaction (Trollope and Chan [1960]).

The orientation of domains with respect to each other and changes in these orientations caused by changes in molding water content were studied by Sloane and Kell (1966). These workers observed that the orientation of domains with respect to each other improved with increasing molding water contents for Georgia kaolin Hydrite UF samples, prepared by all of the impact, kneading, and static compaction methods. On the other hand, Diamond (1971), working with Edgar Plastic kaolin, did not obtain what he considered to be significant orientation trends between domains, but observed that the micrometer-sized interdomain voids encountered at molding water contents dry of the optimum moisture content disappeared at water contents wet of the optimum. The intradomain

pore sizes found for Edgar Plastic kaolin by mercury porosimetry ranged from 200 to 800 Å (Diamond [1971]). In contrast, values for intradomain pore sizes ranging from 10 to 30 Å were found for an illitic silty clay by Aylmore and Quirk (1960a), using an indirect method of analysis based on adsorption isotherms. In the present work, it has been found that Edgar Plastic kaolin and other soils show a relatively fixed content of pores smaller than about 1000 Å regardless of how the soil was manipulated. This upper limit corresponds roughly to the upper limit of Diamond's intradomain pore size range. Mercury intrusion measurements do not permit evaluation of pores as fine as 10 to 30 Å. As will be seen later, almost all of the porosity has been intruded by this technique and corresponds to sizes much larger than these sizes.

Role of Soil Aggregations in Soil Compaction

A soil aggregation may be considered as a cluster of domains (Aylmore and Quirk [1960b]). The existence of aggregations, or peds, in natural soils is common knowledge to soil scientists and soil engineers. It was observed by Mitchell, Hooper, and Campanella (1965), Nalenzy and Li (1967), Ahmed (1971), Hodek (1972), and the present author that soil aggregations are also formed during carefully controlled mixing of a dry soil with water.

It has also been recognized for some time that the soil aggregations, rather than the individual soil particles, may

play a dominant role in determining the end product of the compaction process. Day and Holmgren (1952) compacted statically moist soil aggregations, 1 to 2 mm in size, of a number of air dried soils, and studied their thin sections using a polarizing microscope. These workers observed that compaction deformed the aggregations exhibiting water contents below the plastic limit mainly by flattening them against one another at the areas of contact, with the inter-aggregation spaces incompletely closed. On the other hand, compaction plastically deformed the aggregations exhibiting water contents at or above the plastic limit, resulting in progressive closing of the interaggregation spaces with increasing pressure.

Mitchell, Hooper and Campanella (1965), Nalenzy and Li (1967), and Hodek (1972) used the experimentally demonstrated deformability behavior of soil aggregations (Day and Holmgren [1952]) to explain either the details of the compaction process or the observed differences in permeability of samples compacted to the same density on either side of the optimum moisture content.

Compaction Process Details

Use of Air Dried Soil in Laboratory Compaction

Use of air dried soil is a routine matter in the specifications for field compaction control. ASTM Designation; D 698-70 specifies air drying of soil at a temperature not exceeding 140°F.

In the field, the borrow soil is generally compacted at approximately its in-situ moisture content. When it is either too dry or too wet, it is suitably modified by addition of water or by air drying. The desirable range of field compaction moisture content is best ascertained from a compaction curve which should perhaps be generated using the natural soil sampled at a number of field moisture contents. Such a procedure would be exceedingly time consuming and cumbersome, and would be unacceptable for normal use. The other alternatives available are to use the natural soil either as-sampled or else after air drying, and to add or remove moisture as required to obtain the desired range of moisture contents. The former alternative is not practicable for clayey soils, because it is difficult to obtain uniform moisture distribution in moist soils after incorporating additional water in them (Casagrande [1932]) or after partial drying (Ladd [1957]). As a consequence, the use of air dried soil adjusted to a range of moisture contents is almost universally employed.

Though air drying causes a slight drop in the liquid and plastic limits of most inorganic clays, the compaction curves obtained using air dried soils are not significantly different from those obtained using the same natural soils without air drying. The above conclusion was reached by Ladd (1957) and by Holtz (1968) working respectively with clayey soils having plasticity indices of 38% and 14%. Some work has,

however, been reported where air drying caused irreversible changes, e.g., with certain montmorillonitic soils (Willis [1946]), (Grady [1949]), soils containing halloysite clay mineral (Matyas [1967]), and organic soils (Casagrande [1932]).

Soil Mixing

The importance of uniform mixing of soil and water could hardly be overemphasized in a soil study. Uniform mixing is generally considered to be promoted when a continually changing array of soil solid surfaces are exposed by some means to a very fine mist of water. That such a technique would probably not produce a completely uniform mixing of clays with water is indicated by the facts that firstly the clays exhibit a high affinity for water (especially when dry), and secondly their particle sizes are smaller than the smallest drops of water which could be generated in a fine mist. It is therefore likely that each water drop will form a small lump of wet clay. Subsequent rolling and sliding of these balled up clay units (called "aggregations") would result in progressively larger aggregations on continued addition of water. This process continues until a relatively high water content is reached when the aggregations turn into a plastic mass. As previously indicated, the formation of soil aggregations during carefully controlled mixing of a dry soil with water were noted by Mitchell, Hooper, and Campanella (1965), Nalenzy and Li (1967),

Ahmed (1971), and Hodek (1972). Hodek also studied the dependence of size distribution of these soil aggregations on mixing water content, and found that the soil aggregations became coarser in size with increasing mixing water contents in the range of water contents used by him.

Curing of Mixed Soil

The inhomogeneity in moisture content distribution of a mixed soil as a consequence of the mixing-induced aggregation is likely to be obviated by curing (Rubin [1949]), (Leonards [1952]). Adequate curing is needed to achieve an even distribution of moisture, which can be recognized by the change in appearance, from mottled to fairly uniform, of the mixed soil (Ladd [1957]). ASTM Designation: D 698-70 specifies a minimum curing period of 12 hours for highly cohesive materials.

The differences in the compaction response of cured and uncured soils have been extensively investigated, but no consistent relationships have been reported between the densities obtained after compaction of the cured and uncured batches of the same soil. Lambe (1951) using the data of Sowers and Nelson (1949), Turnbull (1960), and Lee and Suedkamp (1972) reported higher densities with the cured soils. On the other hand, Ray and Chapman (1954), Tamez (1957), and Rallings (1971) obtained lower densities with the cured soils, due possibly to the elimination of the added lubrication effect of excess surface water on soil

aggregations. Since soils in the field generally represent an equilibrated moisture condition, it would be appropriate to use the cured soils for meaningful laboratory studies. It is likely that such soils exhibit a closer agreement with their response under the field conditions (Turnbull [1960]).

Uniformity in Laboratory Impact Compacted Samples

The uniformity of a soil compacted by the Proctor impact methods is dependent on a number of factors relating both to the soil and to the compaction process. The soil factors include placement of a representative sample of loose soil in the compaction mold (without unavoidable segregation of coarse and fine aggregations), and of the desired quantity of soil to form a compacted layer of predetermined thickness. The factors relating to compaction include a support of sufficient rigidity for the mold, a reproducible free fall of the drop hammer, and manual manipulation of the drop hammer, whose coverage is limited to half of the mold diameter, in a specified ramming pattern so as to uniformly compact each layer.

Different investigators have reached different conclusions concerning the density distributions within the molded samples, depending to some extent on the type and precision of the method used to measure local density. The Waterways Experiment Station (1949b) and Dawson (1960) determined variations in density along the depth of the molded sample by careful measurements of dimensions and weights. The Waterways

Experiment Station reported that the lower half of the molded sample was more uniform in density, and exhibited a density greater than the overall density of the compacted sample. Dawson, however, noted that the computed densities of the lower, middle, and top third layers were respectively greater, equal to, and less than the overall density of the compacted sample. In contrast to these results, Schackel (1969) determined, based on density measurements using the nuclear techniques, that the samples compacted by the Standard Proctor method exhibited a uniform density along their depth, excepting that the density at the base was lower than the overall density of the compacted sample.

Field Compaction versus Laboratory Impact Compaction

Insight into the performance of field compacted soils can be obtained from the study of laboratory compacted soils, if the latter soils exhibit properties similar to those of the field compacted soils. The laboratory compaction techniques such as Proctor compaction have been developed with the intent that the compaction curves obtained by field compaction equipment could be duplicated at least in part by laboratory impact compaction (Proctor [1933b]), (Thompson [1941]), (Waterways Experiment Station [1949a, b]), (Walker and Holtz [1953]), (Hilf [1956]). It has also been reported (Waterways Experiment Station [1949a, b]), (Holtz and Ellis [1963]) that a soil compacted by both the laboratory impact and field methods to identical optimum moisture content and

maximum dry density would exhibit similar shear strengths for the specimens compacted to identical moisture contents and dry densities.

Critical Region Drying

The measurement of pore size distribution requires dry specimens. The removal of water from soil specimens by the conventional methods of drying, such as oven and air drying, involves a water-gas front, which generally causes shrinkage due to progressive reductions in its radii. This shrinkage could be prevented by transforming the water to water vapor in the critical region.

Theory

The critical point of a fluid represents a temperature-pressure combination at which specific volumes of the saturated liquid and the saturated vapor are equal. A fluid at temperature and pressure below the critical point can occur in two coexisting phases exhibiting different specific volumes, depending on the availability status of the latent heat of vaporization. At temperatures and pressures beyond the critical point, however, a fluid can exist only as a single phase exhibiting no latent heat of vaporization and no characteristic changes in properties such as specific volume, enthalpy, internal energy, and entropy which are indicative of a phase change. The "critical region" encompasses all temperature-pressure combinations at and above

the critical point. Within this region, the properties of a fluid entering in the liquid phase change continuously, from those associated with a liquid to those associated with a vapor. This means that on approaching the critical region the specific volume and compressibility of the liquid increase to such proportions as to produce vapor-like behavior.

As pointed out earlier, a fluid can occur in any of several phases below the critical point. The fluid will occur as a compressed liquid when subjected to a pressure in excess of the saturation pressure for a specific temperature. In the compressed liquid region, the specific volume is greatly dependent on temperature, and practically independent of pressure. The fluid could likewise occur as a superheated vapor when exposed to a temperature in excess of the saturation temperature for a specific pressure. In the superheated vapor region, the specific volume is largely dependent on pressure.

Critical region drying of soils or other porous solids containing water consists essentially of the following three steps: (1) raising the pressure and temperature of the soil water such that changes in the specific volume of water are slow in the compressed liquid region; (2) transforming the soil water into vapor within the critical region; and (3) removing the vapor within the superheated vapor region. Since no phase interface occurs within the critical region where the drying takes place, no surface tension forces are

brought into play. Thus, critical region drying could result in drying of soil samples with very minimal disturbance to the soil structure.

Historical Development

The concept of critical region drying has been known to scientists since discovery of the critical point phenomenon. Kistler (1932) working with organic and inorganic hydrogels and Anderson (1950, 1951) working with biological specimens were among the first few investigators who successfully used the concept of critical region drying. Because the specimens were considered unstable at the critical point of water, the water was replaced by a liquid exhibiting a lower critical point. Kistler and Anderson used the successive replacement technique to replace water by ethanol or liquid propane and liquid CO₂ respectively. The specimens suffered insignificant changes in total volume after critical region drying.

The critical region drying of soils was pioneered at Purdue University by Hannigan (1964) and Griffin (1965). Their concern over the stability of the clay minerals other than kaolinite in the water critical region restricted them to the use of a kaolinitic soil. These workers, Sridharan (1968), and Hooper (as reported by Diamond [1970]) successfully critical region dried saturated consolidated, and artificially sedimented flocculated Georgia kaolin. Devenny (as reported by Diamond [1970]) also successfully critical region dried saturated Leda clay containing illite,

montmorillonite, chlorite, and mixed layer clay minerals without change in total porosity. Gillott (1969, 1970) critical region dried a number of sedimentary deposits such as limestone, shale, mudstone, and Leda clay after replacing water in the materials with ethanol, which exhibits a somewhat lower critical point than that of water. Gillott did not investigate the changes in porosity caused by the drying process, though he studied the relative differences in fabric orientations obtained on these samples after drying by a number of methods. These latter results were, however, inconclusive in terms of the effect of critical region drying on the initial sample condition.

The above review indicates that the critical region drying technique has proven effective as a technique for relatively undisturbed drying of essentially saturated soils. The critical region drying of partially saturated soils with the clay mineral composition ranging from that of kaolinite to montmorillonite has not yet been investigated. One of the objectives of this study is to develop the critical region drying method as a general technique for use on a wide variety of soils in their as-compacted and in-service conditions.

Thermal Stability of Clay Minerals

In this study, critical region drying subjects the clay minerals in a soil-water system to a maximum temperature of 388°C and a maximum pressure of 3800 psi under hydrothermal

conditions during the entire process. These conditions are not likely to result in the thermal instability of clay minerals due to dehydroxylation of the mineral lattice. This is supported by the findings of a number of investigators such as Warshaw, Rosenberg, and Roy (1960), who stated that the clay minerals could be heated under hydrothermal conditions a few hundred degrees above their stability temperature in air. Most of the thermal stability investigations have been conducted by heating the clay minerals to a constant weight in air, at certain predetermined temperature intervals. Under these conditions, kaolinite was found to dehydroxylate beyond 400°C (Ross and Kerr [1931]), illite between about 350° or 400° and 600°C (Grim and Bradley [1940]), and montmorillonite beyond 500°C (Grim and Bradley [1940]). Grim (1962), however, indicated in a later publication that the dehydroxylation of kaolinite, illite, and montmorillonite occurred beyond 450°C. Nutting (1943) demonstrated that kaolinite, montmorillonite, and chlorite dehydroxylate at temperatures beyond 500°C when a partial vapor pressure of water of almost 15mm of Hg was maintained in the air enveloping the minerals.

Though the work cited above indicates that the clay minerals are likely to be stable under the conditions encountered in the critical region, their structure before and after critical region drying will still be investigated in this study using the infra-red spectroscopic and X-ray diffraction techniques.

Thermal Expansion of Clay Minerals

The thermal expansion characteristics of the non-expanding clay minerals such as kaolinite and illite have been studied by a number of investigators including Rieke and Mauve (1942) and McKinstry (1965). These studies indicate that such clay minerals suffer reversible thermal expansion on being exposed to a heating and cooling cycle in air. McKinstry used a high temperature X-ray diffraction technique to compute the thermal expansion coefficients of the clay minerals in the temperature range of 25° to 700°C. The values ranged from 9.0 to 18.6×10^{-6} / °C and from 5.2 to 11.1×10^{-6} / °C in the directions perpendicular and parallel to the silicate layer, respectively. Such an order of magnitude of thermal expansion coefficient, applied over the temperature range used in critical region drying, would yield only a very small reversible dimensional change.

The expanding clay minerals such as montmorillonite suffer an irreversible collapse of the clay lattice on heating in air, due to removal of the interlayer water. It is likely that such a collapse of the clay lattice would also occur in the process of critical region drying. A number of soils including Volclay bentonite will be investigated for changes in the basal spacings caused by critical region drying, using X-ray diffraction. Such a study would establish the applicability range of the critical region technique for drying soils without an appreciable change in their original porosity.

Constant Volume Soaking of Compacted Soils

Soaking at constant volume of a compacted soil can eliminate its negative pore water pressures. This causes the soil container to apply a restraining stress to the soil numerically equal to the initial negative pore water pressure. The magnitude of this restraining stress depends on a number of factors such as type of soil, kind and level of compaction, and molding water content (Ladd [1957]), (Mishu [1963]). It is usually presumed (Lambe [1958]), (Seed and Chan [1959]) that soaking at constant volume does not change the particle orientations in a compacted soil. The only indirect evidence in support of identical particle orientations in a compacted soil before and after soaking at constant volume is indirect evidence from the work of Seed and Chan (1959). These workers observed that the axial shrinkages obtained with both the silty clay samples compacted by impact compaction at a number of moisture contents, and soaked at constant volume after compaction, were identical for each compaction water content. It will be presumed in this study that the soaking of compacted soils at constant volume does not change the distribution of pores present in the compacted soils. Soaking at constant volume usually raises the degrees of saturation of the samples to more than 95%. This means that an insignificant amount of air would usually be present at the start of a critical region drying run, and hence the initial pressurization required to bring

the remaining air into solution should not cause a significant distortion to the soil structure.

Solubility of Air in Water

It was mentioned in the previous section that a small amount of air is brought in solution by pressurization in the early part of a critical region drying run. The temperature-pressure-time relationship followed in a run should ensure that the air remains in solution until the critical region is approached. Data regarding the solubility of nitrogen and oxygen in water at high temperatures and pressures were generated by a number of investigators such as Wiebe, Gaddy, and Heins (1933), Saddington, and Krase (1934), and Pray, Schweickert, and Minnich (1952). These investigators found that the solubility of nitrogen and oxygen in water increases with pressure roughly in accordance with Henry's Law. At a constant pressure, however, the solubility decreases to a minimum at a temperature of about 70° to 80°C. Beyond this temperature, the solubility of nitrogen and oxygen in water increases slowly until the gases and water become miscible in all proportions at the critical point of water.

Pore Size Distribution

Significance of Pore Size Distribution

Values of the total pore volume, and information on its distribution with respect to pore sizes may effectively

characterize a porous material such as a soil. Use of these parameters could lead to a better understanding of the engineering properties of a compacted soil such as strength, compressibility, and permeability, which are likely to be directly influenced or controlled by the total pore volume and the relative amounts of different sizes of the pores. It has been recognized for some time by soil engineers that soils with an appreciable proportion of pore volume distributed in a few large pores, rather than in many small pores, will have significantly increased permeability (Lambe [1958]), (Mitchell, Hooper, and Campanella [1965]).

The pore size distribution of a compacted soil also determines the total solid-liquid or solid-gas interfacial area available within the soil for possible reaction with changes in the environment. Knowledge of this could enable the prediction of changes likely to occur in a compacted soil because of changes in the ambient environment.

Methods to Determine Pore Size Distributions

The significance of the pore size distributions in interpreting the behavior of porous media has led to the development of a number of methods for the determination of pore size distributions in such media. While many of these methods are applicable only to a limited pore size range, they represent the practical efforts made by investigators in such varied disciplines as chemical engineering, materials engineering, soil science, and soil engineering to their

particular problems in characterizing porous materials.

Among the methods applicable for soils in a limited pore size range are the techniques described below:

1. Optical and Electron Microscopy
2. Capillary Condensation
3. Capillary Suction
4. Mercury Intrusion

Optical and Electron Microscopy

The distribution of pore sizes can be determined by optical and electron microscopic techniques, using thin sections of soil. The numbers and characteristic shapes of pores, larger than the limit of resolution of the microscope, can be directly observed and pore sizes directly measured, and areas planimetered. Examination of a number of thin sections could give a three-dimensional picture of the pore volume. Though this method is difficult and time consuming, it could be used to obtain a direct measure of the distribution of at least the larger pore sizes. Swanson and Peterson (1942) obtained pore size distributions of undisturbed and cultivated surface horizons of a silty clay using a petrographic microscope, the minimum pore size resolved being 11.7 micrometers. These pore size distributions were in agreement with those obtained by the capillary suction technique. Pusch (1966, 1972) studied thin sections of a number of natural clays using an electron microscope, and could resolve the pores down to a minimum size of 0.05

micrometers. The pore sizes obtained by him for a kaolinitic clay were found to lie within the range obtained by the mercury intrusion technique for a statically compacted Georgia kaolin by Sridharan, Altschaeffl, and Diamond (1971).

Unfortunately, microscopic techniques are subject to possible distortion of the soil structure during preparation of thin sections of soils, especially those containing silt and sand, and are of limited usefulness when significant amounts of fine pores smaller than the resolving power of the microscope are present.

Capillary Condensation

The pore size distributions of porous solids can also be determined by methods based on the phenomenon of capillary condensation. The adsorption and desorption isotherms are experimentally obtained using the nitrogen gas at its boiling point. The Kelvin equation is used to enable computation of the pore size distributions from either the adsorption or desorption isotherm, with appropriate correction for the varying thickness of the adsorbed layer. This technique enables the determination of pore sizes to a maximum value of 1000 \AA (Diamond [1970]). Aylmore and Quirk (1960a, 1960b, 1967) used the capillary condensation technique to determine pore size distributions below 100 \AA for uncompacted and statically compacted soil aggregates of a number of soils. Capillary condensation techniques are applicable

only in a limited way to most engineering soils, even those that are largely clayey, since a significant proportion of the porosity must be in pore sizes larger than 1000 \AA .

Capillary Suction

In this method, increasing increments of suction are applied to water in a saturated soil via a finely porous saturated diaphragm, and the volume of water withdrawn at each successive increment of suction is measured. Since the suction applied counters the capillary pressure at the air-water interface, the equivalent radius of the smallest pore emptied by any suction is computed from the formula for the height of rise of liquids in a capillary tube. Such a system provides a simple method of determining the distribution of pore sizes. Since entry of air into the diaphragm must be prevented, the magnitude of suction used in this method is restricted to one atmosphere. Correspondingly, the minimum pore size measured by this technique is 3 micrometers (Bradfield and Jamison [1938]). Baver (1938), Bradfield and Jamison (1938), Leamer and Lutz (1940), and Russell (1942) successfully used the capillary suction technique to determine pore size distributions of fine and coarse sand and silt fractions of soils. These workers could obtain only incomplete pore size distributions for a number of natural surface and "B" horizon soils. Baver (1938) and Rubin (1949) used the capillary suction technique to show that the static compaction of soil aggregates and

natural soils caused a decrease in the amount and size of the pores larger than 30 micrometers. This technique is not well adapted for use with most engineering soils since it covers only a narrow spectrum of pore sizes, it requires initially saturated specimens whose structure is subject to distortion due to shrinkage generally associated with the suction application, and it is very time consuming.

Mercury Intrusion

None of the above methods is capable by itself of measuring the whole range of pore sizes encountered in a compacted soil, which exhibits pore sizes normally extending over five orders of magnitude. The commercial mercury intrusion equipment available for this study, with a pressuring capacity of 15,000 psi, could intrude pores of sizes ranging from 160 \AA to $600 \text{ }\mu\text{m}$. The lower pore size limit could, however, be extended down to 40 \AA with commercial equipment of 60,000 psi pressure generating capacity. The intrusion technique is based on the premise that the opposition to the entrance of a non-wetting liquid (one exhibiting a contact angle greater than 90° with a given solid) into the empty pores, accessible to the surface of a solid, can be overcome by an applied pressure, and that the applied pressure required to intrude a given increment of pore volume is a measure of the sizes of the pores intruded. Mercury is almost always used as a non-wetting liquid because of its large contact angle with most kinds of solid surfaces, low

vapor pressure, and relative inertness in terms of its chemical reactivity to most solids. The mercury intrusion technique consists essentially of enveloping with mercury a porous dry solid exhibiting an evacuated pore space accessible to the surface, increasing pressure on it in small steps, and noting the volume intruded at each step. The use of this technique to study the pore size distributions of porous materials was first suggested by Washburn (1921), who indicated that the absolute pressure, p , required to intrude a cylindrical pore of diameter, d , was given by

$$p = - \frac{4 \sigma \cos \theta}{d} \quad (V-1)$$

where, σ = surface tension of mercury; and

θ = contact angle between mercury and the pore wall.

Ritter and Drake (1945) successfully used the mercury intrusion technique as proposed by Washburn, and obtained pore size distributions of a wide variety of materials in the pore size range of about 8 μm to about 200 \AA , using a contact angle of 140° and a surface tension value of 480 dynes/cm. Drake (1949) extended the lower pore size limit down to a diameter of 36 \AA , which is 11.5 times the diameter of a mercury atom (3.14 \AA). Drake expressed the opinion that the mercury meniscus in a pore of 36 \AA diameter still appeared to behave as would a much larger meniscus, and that 36 \AA size did not appear to constitute a limiting pore size obtainable by the mercury intrusion technique. Winslow and Shapiro

(1959) subsequently developed a compact instrument to measure the pore sizes between 10.0 and 0.3 μm , using a contact angle of 130° and a surface tension value of 473 dynes/cm. These values of contact angle and surface tension were assumed to remain constant over the range of pressure used in their work. Their instrument subsequently evolved into the porosimeter of the American Instrument Company, Silver Spring, Maryland, which was used with some modifications in this study.

A number of surface tension values of pure mercury have been reported by different investigators (Harkins and Ewing [1920]), (Roberts [1964]). A surface tension value of 484 dynes/cm at 25°C (Kemball [1946]) was selected as the best available value for use in this study. Rootare (1968), however, showed using Equation V-1 that the surface tension value of mercury was not critical in the computation of pore sizes from the pressure data. On the other hand, Rootare (1968) and Orr (1969) showed that the value of contact angle of mercury with different solid surfaces was critical in the computation of pore sizes from the pressure data. Drake and Ritter (1945), Watson, May, and Butterworth (1957), and Hill (1960) used a contact angle of 140° for mercury on a number of fired clay products. Diamond (1970) experimentally determined the contact angle of mercury to lie within a degree of an average value of 147° for kaolinitic and illitic soils tested, and within a degree of

an average value of 139° for several montmorillonitic soils. These values obtained with the oven dried soils were considered more appropriate for use in the computation of pore sizes in the present study. It is presumed in this study that the surface tension and contact angle values of mercury do not change with the applied pressure during a porosimeter run. The deviations between the actual and selected values of surface tension and contact angle for use in the pore size computations would not affect the shapes of the pore size distribution curves and the order of magnitude of the computed pore radii, but would only affect their absolute values.

The assumption of cylindricity of the pore space in the mercury intrusion technique, as in the case of other pore size distribution determination techniques such as capillary condensation and capillary suction, is analogous to the assumption of the spherical model for grain size distribution determinations. The assumption of the circular shape of the pores appears in Equation V-1 as the ratio of perimeter to area, which value is $\frac{4}{d}$, where d is the diameter of such pores. For non-circular pores it would be instructive to compute the values of $\left(\frac{\text{pore perimeter}}{\text{pore area}}\right)$, which would determine the influence of such shapes on the pore sizes. These values are respectively $\frac{4}{d_1}$ and $\frac{7}{d_2}$ for square and equal sided triangular pores with side dimensions of d_1 and d_2 , respectively. For pores of other shapes such as rectangular and elliptical pores, these values are given by $\frac{c}{d_3}$, where c

is smaller than 4 but not by a big factor and d_3 represents the least dimension of the pore. This shows that the pore size distributions obtained on the assumption of a cylindrical pore shape model would be similar in shape and order of magnitude of the pore sizes to those obtained by using other models, but would exhibit slightly different absolute pore sizes. Such a variation in the absolute pore sizes is insignificant when it is considered that the pore size range of the compacted soils normally extends over 5 orders of magnitude.

Efforts to show that the mercury intrusion technique yields pore size distributions similar to those obtained by other techniques have been reported by a number of investigators. The data of Purcell (1949) show that the pore size distributions of sandstone and limestone specimens obtained by the capillary suction and mercury intrusion methods down to the pore sizes of 1400 \AA are identical. Joyner, Barrett, and Skold (1951), Cochran and Cosgrove (1957), and Caro and Freeman (1961) showed similarity of the pore size distributions in the regions of overlap of 33 to 300, 30 to 500, and 20 to 600 \AA respectively for the methods of capillary condensation and mercury intrusion, using different materials such as charcoal, porous alumina, and phosphate fertilizers. Winslow (1969) also obtained such a trend for relatively open structured cement pastes.

Few data are available regarding the pore size distributions of compacted soils obtained by the mercury intrusion technique. Hill (1960a) used this technique to obtain pore size distributions of Victoria kaolin and grundite, which were statically compacted in a cylindrical shape (1/2 inch diameter, 1 inch long) at a water content of 7 percent to a void ratio of approximately 0.7, and fired to respective temperatures of 600°C and 700°C. The partly fired kaolin exhibited most of its porosity in a narrow pore size range of 0.02 to 0.2 micrometers. On the other hand, most of the porosity of the partly fired grundite was evenly distributed in pore sizes ranging from 0.01 to 10 μ m. Sridharan (1968), Diamond (1970, 1971), and Ahmed (1971) obtained similar pore size ranges respectively for oven dried Georgia kaolin and grundite, oven dried Edgar Plastic kaolin and grundite, and freeze dried grundite.

It often appears that the compaction process does not modify the proportion of total porosity present in the fine pores of compacted soils. Experimental evidence in support of this concept came from Rubin (1949), Sridharan (1968), and Diamond (1971). Rubin used capillary suction while the other two authors used mercury intrusion technique to measure the pore size distributions of compacted soils. Rubin and Sridharan reported that the compaction of soils with progressively increasing static compaction efforts did not modify the content of pores present in pore sizes smaller

than about $0.2\ \mu\text{m}$, but gradually reduced the proportion of porosity present in the large pores. Rubin explained the persistence of the fine pores in a number of ways: (a) the fine pores, being filled with water, might resist removal, (b) the destroyed fine pores of a given size might be replaced by others resulting from the diminution of pores of larger sizes, and (c) the fine pores might be present in the most stable particle arrangements. Diamond (1971) indicated that the finer pores in his kaolinite (of diameters between 0.08 and $0.02\ \mu\text{m}$) were intradomain spaces between individual clay plates within compaction-resistant domains or clusters.

It might be expected that out of two samples of a soil compacted at different moisture contents but to the same density, the sample compacted at the lower moisture content will exhibit more large pores. Diamond (1970), Sridharan, Altschaeffl, and Diamond (1971), and Ahmed (1971) provided experimental evidence in support of this expectation, working respectively with impact compacted Edgar Plastic kaolin, statically compacted Georgia kaolin, and grundite compacted by a number of laboratory methods.

Different soils on compaction might yield widely varying distributions of pore space, depending on the differences in the nature and proportion of their soil constituents, differences in stiffness of the individual particles, differences in particle shapes, and differences in domain or other

microstructural aggregations. Sridharan, Altschaeffl, and Diamond (1971) obtained radical differences in the measured pore size distributions for oven dried specimens of statically compacted Georgia kaolin, grundite, and Boston blue clay, and explained such differences in these terms.

The mercury intrusion data presented above were obtained on either oven dried or freeze dried samples, which did suffer some (or in some cases negligible) change in porosity as a result of the drying processes. The pore size distribution determinations performed in the present investigation on critical region dried samples would be useful in investigating the applicability of the reviewed compaction trends to a number of soils prepared by the Proctor compaction methods.

Total Porosity Determinations Using the Mercury Intrusion Equipment

The reliability of the determination of total porosity of a small sample using a mercury intrusion equipment has been studied by a number of investigators including Ulmer and Smothers (1967), working with brick samples. These workers determined the total porosities of a number of small samples in the filling device of a porosimeter at a filling pressure of 90.5 mm Hg, and also by an ASTM procedure (ASTM Designation: C20-70), in which the quantity of water required to saturate bricks after thorough boiling under water is used to compute the total porosity. The porosities obtained by

the two procedures were found to be within $\pm 1\%$ of each other. Though the reported data relate to the brick samples, the present writer has some data indicating that these conclusions regarding the reliability of total porosity obtained using the filling device are valid also for the dried soils.

Soaking Under a Nominal Surcharge Pressure

Changes effected in the total porosity of a compacted soil as a result of soaking under a small surcharge pressure have been of interest to a number of investigators, who simulated such conditions by conducting a one-dimensional volume change test in a consolidometer under loadings of 1 psi (Gibbs and Holtz [1956]), and 1.4 psi (Ladd [1960]), (Seed, Mitchell, and Chan [1962]), or by allowing a soil to swell in a flexible membrane under a surcharge pressure of about 1 psi in a manner approximating closely the free swell test (Liu and Parcher [1965]), (Kayyal [1965]). It was noted by Loxton, Beavis, and McNicholl (1948), and DuBose (1956), and also by the present writer that the restraint imposed in a one-dimensional volume change test makes it difficult to achieve uniform moisture contents and dry densities along the depth of a sample.

The differences in the response to soaking under a small confining pressure of a soil compacted on the dry and wet sides of an optimum moisture content have been studied

by Ladd (1960), Seed, Mitchell, and Chan (1962), and Kayyal (1965). It was observed that a dry-side compacted sample exhibited a greater volume increase for a given water content increase (due to soaking) as compared to that of a wet-side sample, though the volume increase was always smaller than the water content increase. It was also noted that the samples compacted at the same molding water content on the dry side of an optimum moisture content, but with higher compactive efforts, encountered greater increases in volume for a given water content increase due to soaking.

The nature of the changes effected in the distribution of pore space of a compacted soil as a result of soaking under a small surcharge pressure have not yet been reported. Such changes were monitored and will be reported later in this study.

CHAPTER III

SOILS STUDIED

General

A number of naturally occurring soils were used in this study, but the two major soil materials investigated in greatest detail were Edgar Plastic kaolin and grundite. The latter are commercial clays mined and processed by the Edgar Plastic Kaolin Company, Edgar, Florida and the Illinois Clay Products Company, Grundy County, Illinois, respectively. They were employed because of their ready availability in large batches, which did not differ significantly from one another, and because of their content of common clay minerals. Finally, there was considerable evidence (Perloff [1966]) that the compaction behavior of these soils was similar to those of many naturally occurring silty clays. Other soils studied to a limited extent included reddish-brown limestone residual clay, Boston blue clay, Crosby silty clay, and Volclay bentonite. Their use was intended generally to confirm the trends observed in the study of the commercially available soils.

The results of identification and classification tests on the soils are summarized in Table III-1, and their grain size distributions are given in Figure III-1. Table III-1

TABLE III-1
Classification Properties of Soils Studied

	Volclay Bentonite	Edgar Plastic Kaolin	Grundite	Reddish-Brown Limestone Residual Clay	Boston Blue Clay	Crosby Silty Clay
Liquid Limit (%)	521	59	56	53	44	38
Plastic Limit (%)	473	37	32	31	24	22
Plasticity Index (%)	48	22	24	22	20	16
Specific Gravity of Solids	2.80	2.65	2.79	2.81	2.80	2.69
Clay Fraction (% < 2 μ m)	92.0	76.0	67.0	45.5	33.5	18.5

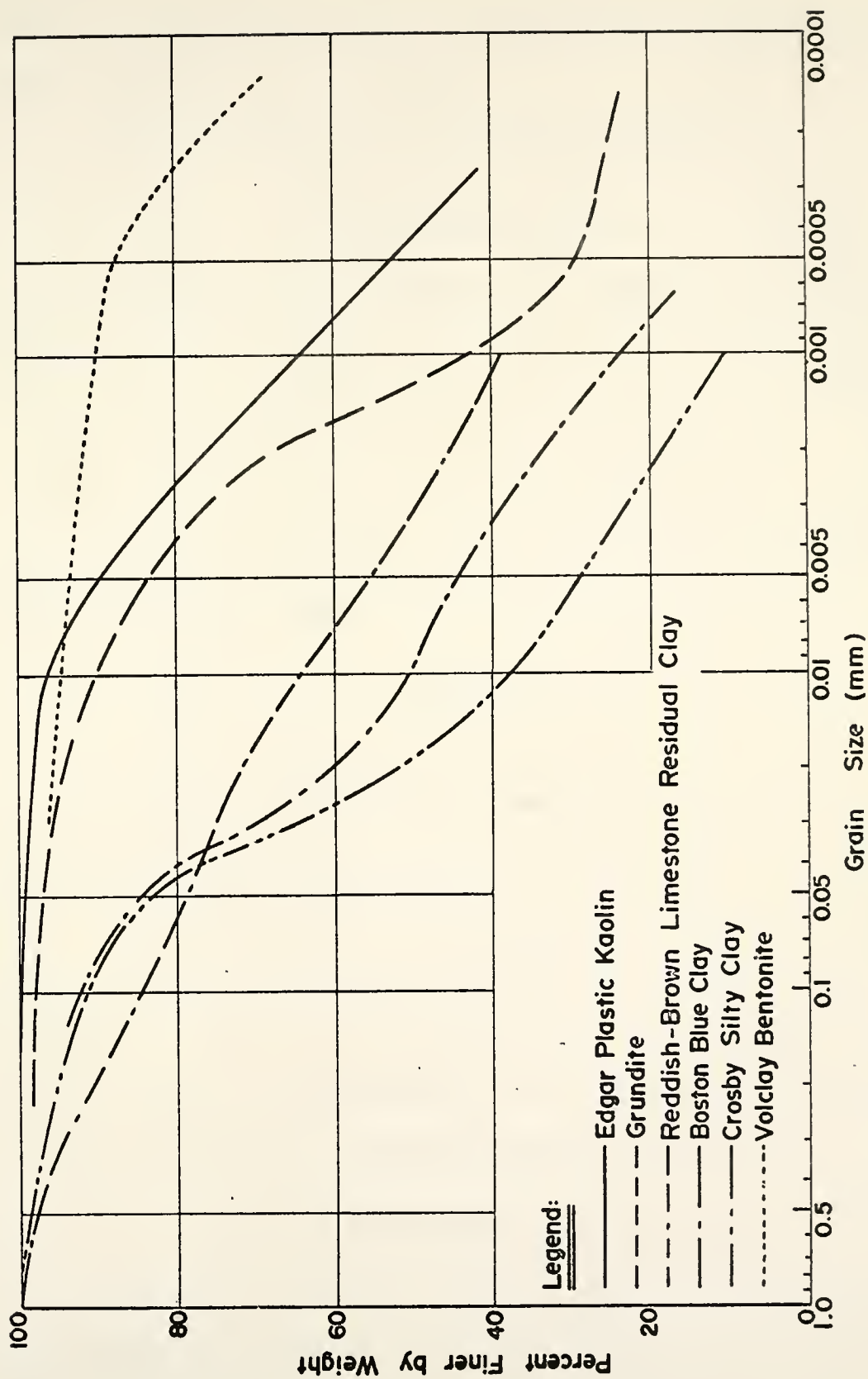


FIGURE III-1 - GRAIN SIZE DISTRIBUTION FOR SOILS STUDIED.

shows that the soils contain clay-sized particles in percentages ranging from 92.0 to 18.5.

A brief description of the soils follows.

Edgar Plastic Kaolin

This mined clay is commercially processed to remove material coarser than 40 micrometers in size, dried in a tunnel dryer at temperatures ranging from 300° to 450°F, and then pulverized. According to the manufacturer, the clay mineral composition of this moderately well crystallized kaolin is 99.5% kaolinite, with the remainder as micro-sized alpha quartz and mica.

Grundite

The mined clay is commercially dried at about 300°F in a rotary dryer and then pulverized and screened to remove material coarser than the No. 40 U. S. Standard sieve size, i.e., 420 micrometers. The mineralogical composition of the clay fraction ($< 2\mu\text{m}$) is 95% illite and 5% quartz (Olson and Langfelder [1965]). On the other hand, Hill (1960a) reported grundite to be composed of 50 to 60% illite, 20% chlorite, 7% pyrite, and some haematite and quartz.

Reddish-Brown Limestone Residual Clay

This soil is a reddish-brown residual clay (pedologically classed as Frederick) derived from limestone of Mississippian age and obtained from a location near Bedford in southern

Indiana. The clay was available in a processed form in the Soil Mechanics Laboratory of Purdue University. The processing presumably consisted of air drying, crushing, and removing of material coarser than the No. 40 U. S. Standard sieve size. The clay mineral composition of the soil is 50% vermiculite (possibly interstratified with some montmorillonite), 40% halloysite, and 10% illite (Girault [1960]).

Boston Blue Clay

This clay is generally found in thick deposits underlying the Greater Boston area, and was obtained in a processed form from Cambridge, Massachusetts. Its predominant clay minerals are illite and chlorite (MIT [1961]).

Crosby Silty Clay

This soil was obtained from a location near Lafayette, Indiana. It is a brown glacial silty clay from the pedological "B" horizon. The clay was air dried, pulverized in a mortar with a rubber-tipped pestle, and processed through the No. 40 U. S. Standard sieve. The predominant minerals in the soil are illite and quartz (Andersland [1960]).

Volclay Bentonite

This soil is mined and processed commercially in the Black Hills of South Dakota by the American Colloid Company, Skokie, Illinois. The processing of the mined soil consists

of first reducing the moisture content to about 4 to 9% by heating in a rotary kiln at a temperature slightly less than 400°F. The dried material is then reduced in size by a combination of crushers, impact mills and screens. According to the manufacturer, the mineralogical composition of Volclay bentonite is 90% montmorillonite and 10% feldspar and quartz.

Efforts were made to achieve uniform conditions in each of the processed soils. The entire quantity of processed soil was thoroughly mixed and stored in plastic garbage can liners.

CHAPTER IV

APPARATUS AND EXPERIMENTAL PROCEDURES

Mixing and Curing

Mixing

The soils were brought to the desired moisture contents mechanically with the use of a twin-shell liquid-solids blender manufactured by the Patterson-Kelley Company of East Stroudsburg, Pennsylvania. The blender, shown in Figure IV-1(a), consists of two cylinders placed at an angle to form a "V". The "V" shape provides a non-symmetrical shape about the rotation axis, which encourages an effective mixing action of the constituents within the slowly rotating shell. The rotating shell keeps the soil in continual motion. De-ionized water is introduced into a high speed liquid dispersion bar provided with dispersion blades. The water spray issues radially in a finely divided droplet form through a minute crack around the entire periphery of the dispersion bar. The dispersion blades aerate and suspend solids in the area of the spray band, as shown in Figure IV-1(b). Thus the water spray strikes soil particles rather than the vessel walls.

Extensive experimentation showed that the use of a maximum of 4000 grams of soil (which is just sufficient to

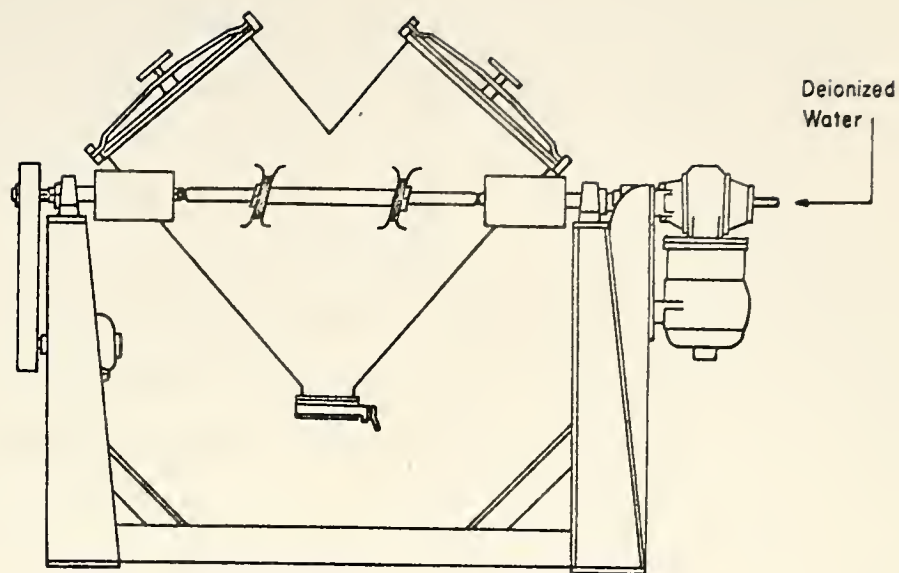


FIGURE IV-1(a)-LIQUID-SOLIDS TWIN-SHELL BLENDER.

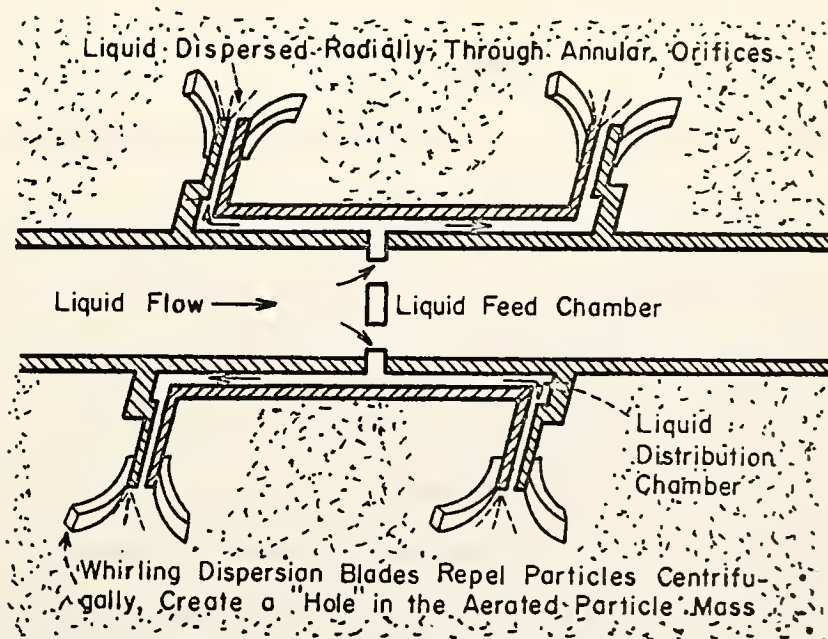


FIGURE IV-1(b)-MIXING OPERATION DETAILS OF DISPERSION BLADES.

occupy the portion of the "V" below the rotation axis), together with a water addition rate of 50 milliliters per minute and a mixing time of 30 minutes, yielded a uniform soil-water mix.

Curing

The mixed soil was placed in airtight double plastic bags to prevent loss of moisture due to evaporation. The first bag was tied with a thin metal wire, and the second bag was then heat sealed. The identification mark of the mixed soil was placed between the plastic bags. The bagged samples were stored in an atmosphere of nearly 100% relative humidity and at a constant temperature of approximately 21°C for at least a week, in order to secure an improved distribution of soil moisture through the process of vapor diffusion.

Preparation and Protection of Compacted Samples

Impact compaction was used for most of this study. The major level of impact compaction was Standard Proctor compaction in accordance with ASTM Designation: D698-70. This compaction technique consisted of compacting cured soil in three equal layers in a 1/30 cubic foot capacity mold, by applying 25 evenly distributed blows of a 5.5 pound hammer having a foot diameter of 2 inches (half of the mold diameter), dropping through a height of 1 foot. The mold was split vertically along the side, and held closed by two bolts and wing nuts. The release of the tension in the bolts of

the mold, plus lubrication of the mold, collar and base with silicone oil, facilitated removal of the compacted sample from the mold assembly.

The amount of soil to be used for each layer was predetermined by trials. The top of each layer was scarified before the succeeding layer was compacted to partly eliminate the "smeared" zone created at the surface. It is likely that the "smeared" zone may not have had the same properties as the soil compacted under grain to grain contact. After compacting the last layer, the top collar was gradually rotated and removed. The surface of soil, which might be slightly above the top rim of the mold (not exceeding 1/8 inches), was carefully trimmed using a straightedge. Trimming was done from the center to the edge of the mold.

After being extruded from the mold, the sample was encased in an airtight double plastic bag or sealed in a mixture of paraffin wax and petrolatum to prevent loss of moisture. The sealed compacted sample was stored in an atmosphere of nearly 100% relative humidity, and a constant temperature of approximately 21°C to decrease the possibility of drying, and to achieve equilibration of moisture in the compacted sample. The compacted sample was cured for at least a week.

A fresh batch of soil was used for each compaction test. This eliminated any of the residual fabric effects which can arise from the reuse of compacted material from one water content to another.

Impact compaction was varied as to the type of hammer, number of blows per layer and the number of layers, to produce energy levels ranging from that of the Standard Proctor method to that of the Modified Proctor method (ASTM Designation: D 1557-70) for a limited part of the study. Static compaction was also used for a very limited portion of the work.

Soaking and Swelling of Compacted Samples

Compacted samples were given access to water and were allowed to swell generally under a light surcharge pressure of $3/4$ psi. The equipment initially used to give controlled access to water consisted of a polished and teflon-tape-lined stainless steel container of $5/8$ inch diameter and $1-1/4$ inch height, with one saturated porous stone fixed on one end and the other free to move in the container. The container was split longitudinally into two halves. The halves were held together with stainless steel connectors, which facilitated removal of the sample after swelling.

The assembled container was sprayed with a silicone spray lubricant, and a sample $5/8$ inches in diameter and $5/8$ inches in height was placed in it. The sample was subjected to a dead load surcharge pressure of $3/4$ psi and was initially allowed to imbibe moisture by capillary action from the bottom so as to let the air from the sample escape from the top. The sample was subsequently given access to

water through saturated porous stones both from the bottom and the top. Extensive experimentation showed that such a system did not produce uniformity of moisture and density conditions along the sample length after swelling, even when the system was given an opportunity to equilibrate for more than a month.

Another technique, which was more successful, consisted of enclosing a soil sample 1.31 inches in diameter and 2.62 inches in height in a latex membrane of 0.006 centimeter thickness, using a special former. The soil sample was given access to water through saturated porous stones fastened to the ends of the membrane with stainless steel connectors. The assembled soil sample ready for soaking is shown in Figure IV-2. The surcharge pressure was controlled by the depth of water over the sample. Such a system gave uniform moisture and density conditions along the sample length in a week, and was adopted for this study. This occurred despite the unknown but small restraint offered by the membrane in both directions.

After soaking, and swelling, the compacted samples were trimmed to the desired size using techniques discussed under the next section.

Preparation of Samples for Critical Region Drying

Compacted Soil

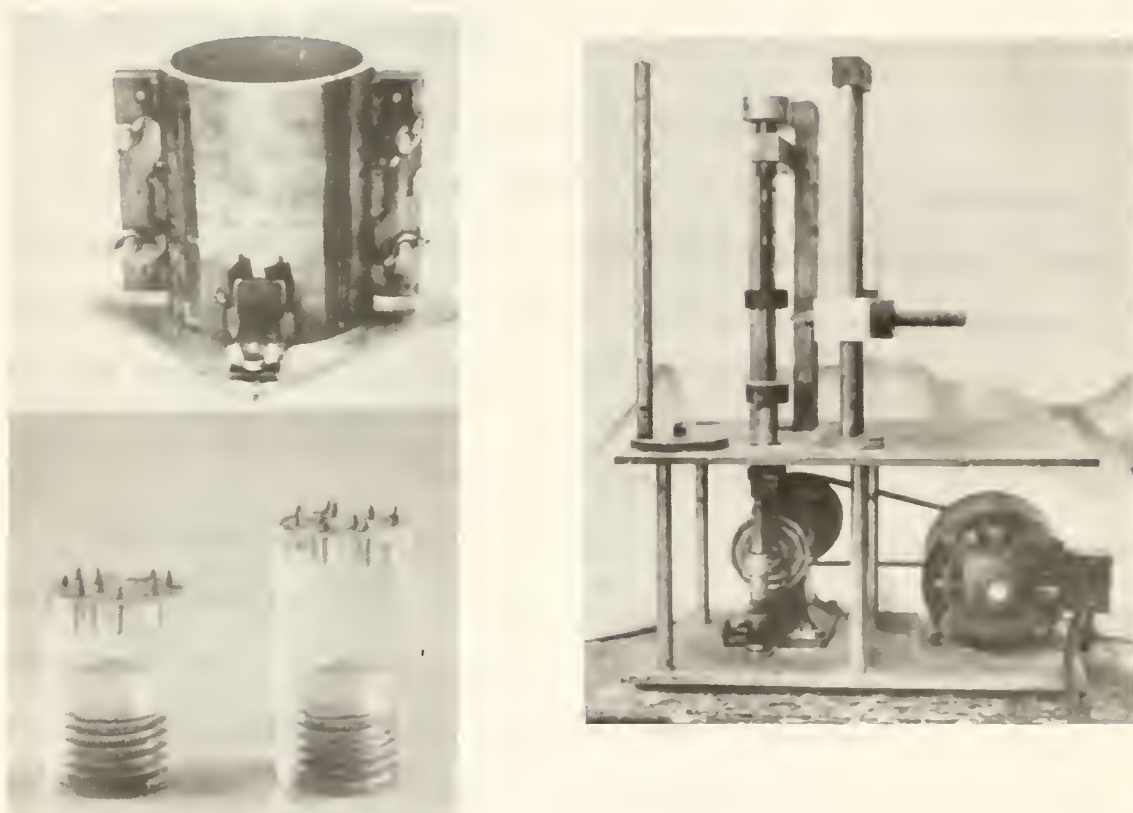
In the initial stages of the experimentation, the compacted soil was sampled using a 0.007 inch thick tool



FIGURE IV-2- A SOIL SAMPLE ASSEMBLED FOR THE SOAKING TEST SHOWING POROUS STONE, LATEX MEMBRANE, AND STAINLESS STEEL CONNECTORS.

steel sampler, having an inside diameter of $3/8$ inches and a height of $7/16$ inches. Though the sampler had an area ratio (Hvorslev [1949]) of only 3.75%, it caused a significant increase in density of the sampled material, presumably due to the pushing into the sampler of the soil displaced by the sampler wall volume. This method of sample preparation was discarded after a few preliminary trials.

Samples were prepared satisfactorily by trimming of the compacted soil. It was desired to critical region dry small samples, and a size of $1/2$ inch diameter and $1/2$ inch height was arbitrarily chosen. The procedure for sample preparation consisted of cutting the compacted soil into four quarters, by continuous one-directional motion of a metal band saw. The metal blade was guided by vertical slots in a specially fabricated steel cylinder, shown in Figure IV-3, which contained the compacted sample. Coarse cutting of the sawed sample was done manually with a sharp straightedge, using a soil lathe also shown in Figure IV-3. The lathe heads were specially fabricated of plexiglass, and were $1/2$ inches in diameter. The sample from the middle third compacted layer and having lateral dimensions roughly on the order of $1/2$ inch was finally trimmed to a $1/2$ inch diameter using a sharp-edged stainless steel trimmer coated with silicone grease. The trimmed sample was extruded from the trimmer. The trimmer and the extruder were connected centrally to loading plates, which were guided via ball



**FIGURE IV-3- SAMPLE PREPARATION ACCESSORIES:
SLOTTED STEEL CYLINDER (LEFT TOP), 1/2 INCH
DIAMETER PLASTIC LATHE HEADS (LEFT
BOTTOM), AND LATHE FOR ROUGH TRIMMING
(RIGHT).**

bushings sliding along vertical machined steel uprights. The trimming system, along with the extruder, is shown in Figure IV-4. The ends of the sample were trimmed to a finished length of 1/2 inches in a lubricated metal miter box and with a sharp blade.

Compacted Soil After Soaking

The soil sample was removed from the latex membrane, and excess surface water was wiped off using a paper towel. The samples for critical region drying were then prepared by the same procedure cited above.

Soil Aggregations

The mixed soil was compacted statically under a nominal pressure of either 15 or 25 psi to a sample size of 1/2 inch diameter and 1/2 inch height. The extrusion assembly described earlier was used for the static compaction setup. The mixed soil was placed in a lubricated stainless steel container provided with a collar, and was compacted by the application of loads to the loading plate for a period of two minutes. The compacted soil aggregations protruded just slightly above the top of the container, and were trimmed flush with the end using a sharp blade.



**FIGURE IV-4-SAMPLE PREPARATION ACCESSORIES:
STAINLESS STEEL 1/2 INCH DIAMETER
TRIMMER (BOTTOM), AND SAMPLE
EXTRUDER (TOP).**

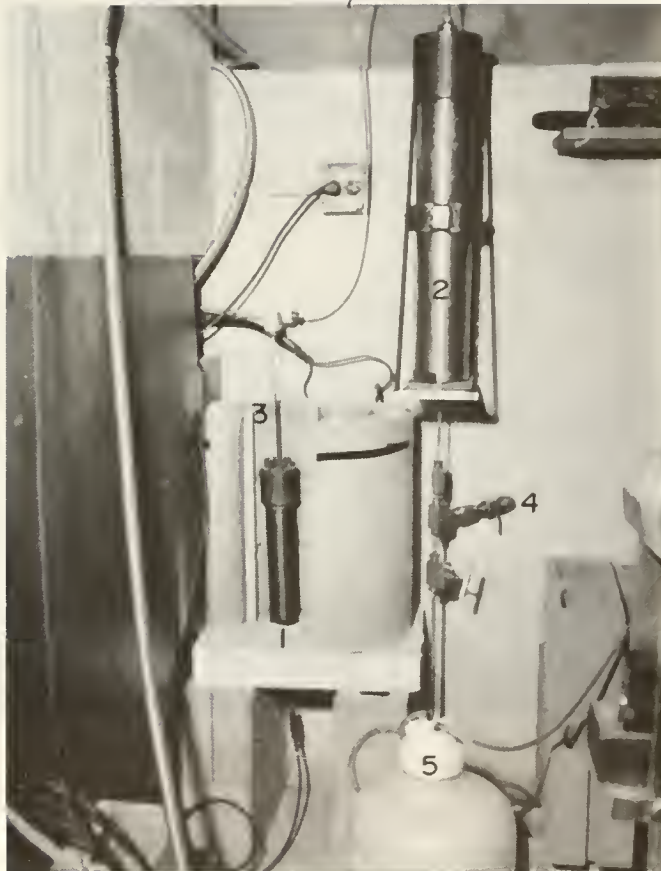
Critical Region Drying

The Apparatus

The apparatus¹ is shown in Figures IV-5 and IV-6 and schematically in Figure IV-7. It consists essentially of a critical region vessel 1-1/2 inches in internal diameter and 10 inches in height, having a pressure connection at the top, and an iron-constantan thermocouple at the bottom. The vessel is made of stainless steel 316, and is designed to withstand a maximum pressure of 6900 psi at 800°F. A seal is provided by compressing a stainless steel gasket against its top, using thrust bolts. The pressure connection at the top of the critical region vessel is in communication with two pressure sources. A high pressure regulator used in conjunction with a nitrogen gas tank provides controlled initial pressure up to a maximum of 2000 psi. A manually operated stainless steel jack having a small volume capacity of 30 milliliters generates pressure in excess of that provided initially by the nitrogen gas and up to a maximum of 15,000 psi. The pressure in the system is registered by a 7500 psi Bourdon pressure gage with a scale sensitivity of 10 psi.

The thermocouple at the bottom of the critical region vessel is arranged with the temperature sensing tip protruding about 1/4 inch into the vessel. It was checked for

¹The critical region drying equipment used in this study was adapted from that originally designed by James R. Hooper, presently employed by McClelland Engineers, Inc. of Houston, Texas.



1. Critical Region Vessel
2. Balance Control Vessel
3. Hollow Cylindrical Heater
4. Safety Blow-Out
5. Water Pump

FIGURE IV-5 - DETAILS OF CRITICAL REGION DRYING EQUIPMENT.



- 6. Manually Operated Pressure Jack
- 7. Pressure Regulator for Nitrogen Gas
- 8. Thermac Temperature Controller
- 9. Data Track Programmer
- 10. Bourdon Pressure Gage

FIGURE IV-6- DETAILS OF CRITICAL REGION DRYING EQUIPMENT.

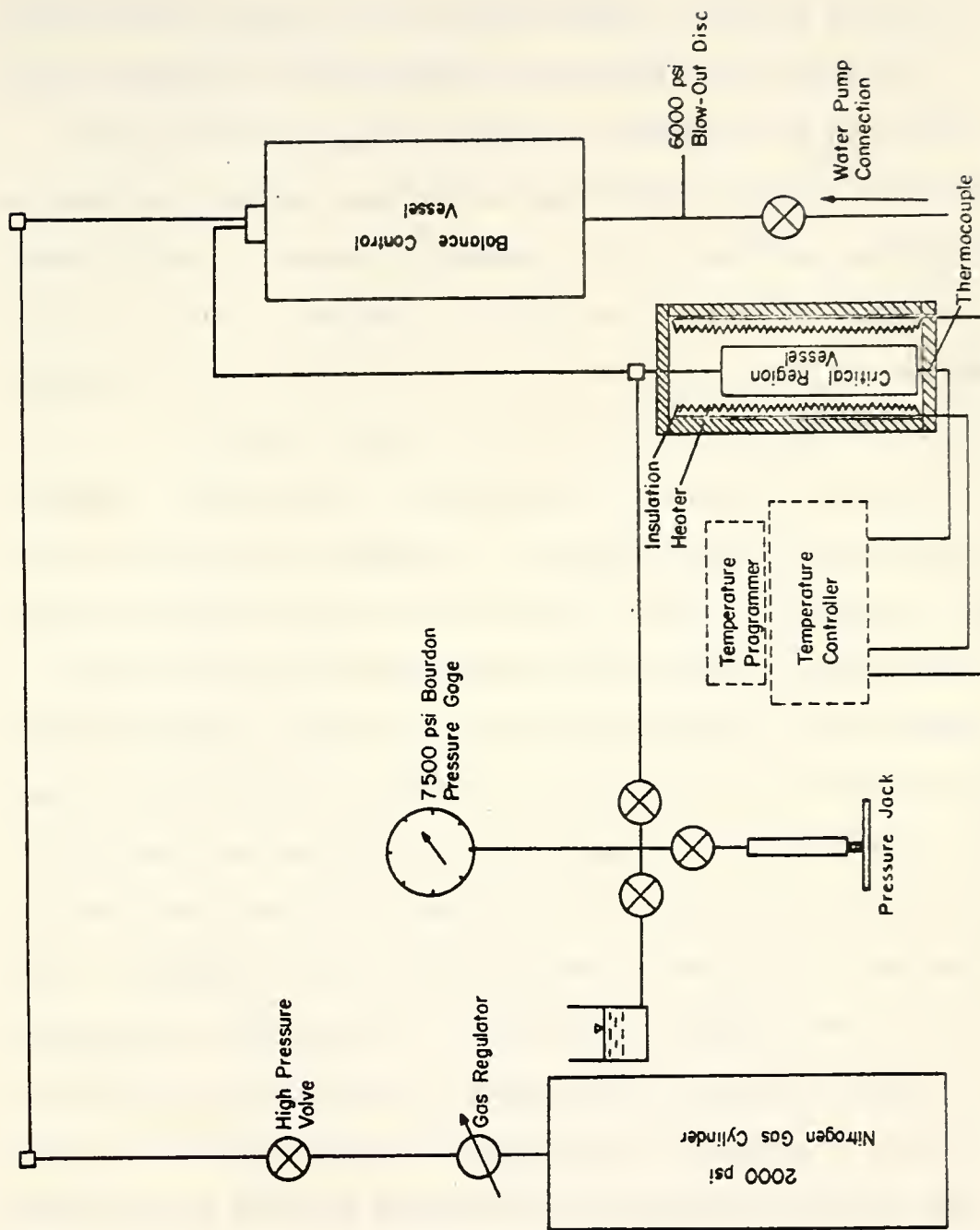


FIGURE IV -7 - SCHEMATIC OF CRITICAL REGION DRYING EQUIPMENT.

calibration using ice and steam baths, and was found to give temperature measurements accurate to within 1°F.

The critical region vessel is heated with a hollow cylindrical heater made of nickel-chrome coiled wires recessed within undercut grooves in a cylindrical refractory. The heater has a wattage of 2000 and reaches a maximum temperature of 1000°C when supplied with a maximum voltage of 230. A Thermac temperature controller manufactured by Research Incorporated, Minneapolis, Minnesota is used to control the rate of change of temperature of the heater. The controller adjusts the voltage fed to the heater so as to reduce the difference between the command temperature and the temperature sensed by the thermocouple. The command temperature could be fed to the controller through the use of program, set point, or manual modes of operation. The program mode could be used only in conjunction with the Data Track Programmer also manufactured by Research Incorporated, Minneapolis, Minnesota. The Thermac temperature controller is provided with bands of proportional control ranging from 270 to 15°F for effective temperature control. The band of proportional control determines the extent to which the heater temperature may deviate below the command temperature before the controller applies the corresponding maximum corrective voltage to the heater.

A balance control vessel made of stainless steel 316, 2.5 inches in internal diameter and 21 inches in height, is

connected to the critical region vessel at the top. At the bottom, it is provided with a blow-out disc and a water pump. The balance control vessel is used to avoid adverse effects on the soil samples, caused by abrupt changes in pressure in the system. The vessel is maintained at ambient room temperature, because heat transferred along the long length of pipe connecting it to the critical region vessel is nearly dissipated. Pressure change in the system due to specific volume change of water in the critical region vessel is much smaller than when the balance control vessel is not used. Furthermore, nitrogen gas under pressure in the top portion of the balance control vessel acts as a cushion, and the effect of pressure change on soil samples is further reduced. Sealing in the balance control vessel is provided at the top with a Buna N "O" ring, which is stable up to a maximum temperature of 250°F. The blow-out disc provided at the bottom of the vessel serves to maintain a factor of safety against overstressing and ultimate collapse of various parts of the equipment. The disc ruptures under a pressure of 6000 psi at 72°F. The water pump consists of a polyethylene flask in which air over deionized water is pressured by manual manipulation of a rubber balloon, to allow water to rise in the system.

The Technique

Drying of soils using the critical region approach involves arranging a dynamic program of temperature and pressure

so that change of the specific volume of water in the soil sample is slow and does not cause disturbance to the soil. The dynamic program of temperature and pressure used in this study is based on pressure-specific volume isotherms for water and water vapor, and solubility of air in water. These isotherms are shown in Figure IV-8 and are drawn for the most part from the data of Keenan and Keyes (1955). Isotherms in the vicinity of the critical point such as those from 705.5 to 750°F are drawn from the data reported by Nowak (1962). These data are also presented in the form of specific volume-temperature isobars in Figure IV-9. Figure IV-8 shows the saturation line, in addition to significant isotherms. A part of the saturation line is also plotted in Figure IV-10 as the boiling phase line. The region to the left of the boiling phase line shows all combinations of pressure and temperature which do not result in the boiling of water.

Figures IV-8 and IV-9 show that the critical constants of free water are 705.5°F and 3210 psi. The critical constants of pore water are not known, but it is safe to assume that they are higher than those of free water. It is also recognized (Sengers and Sengers [1968]) that unsteady conditions prevail around the critical point. These conditions make it desirable to proceed to temperature and pressure well above the critical constants, and values of 730°F and 3800 psi, well within the critical region, were chosen.

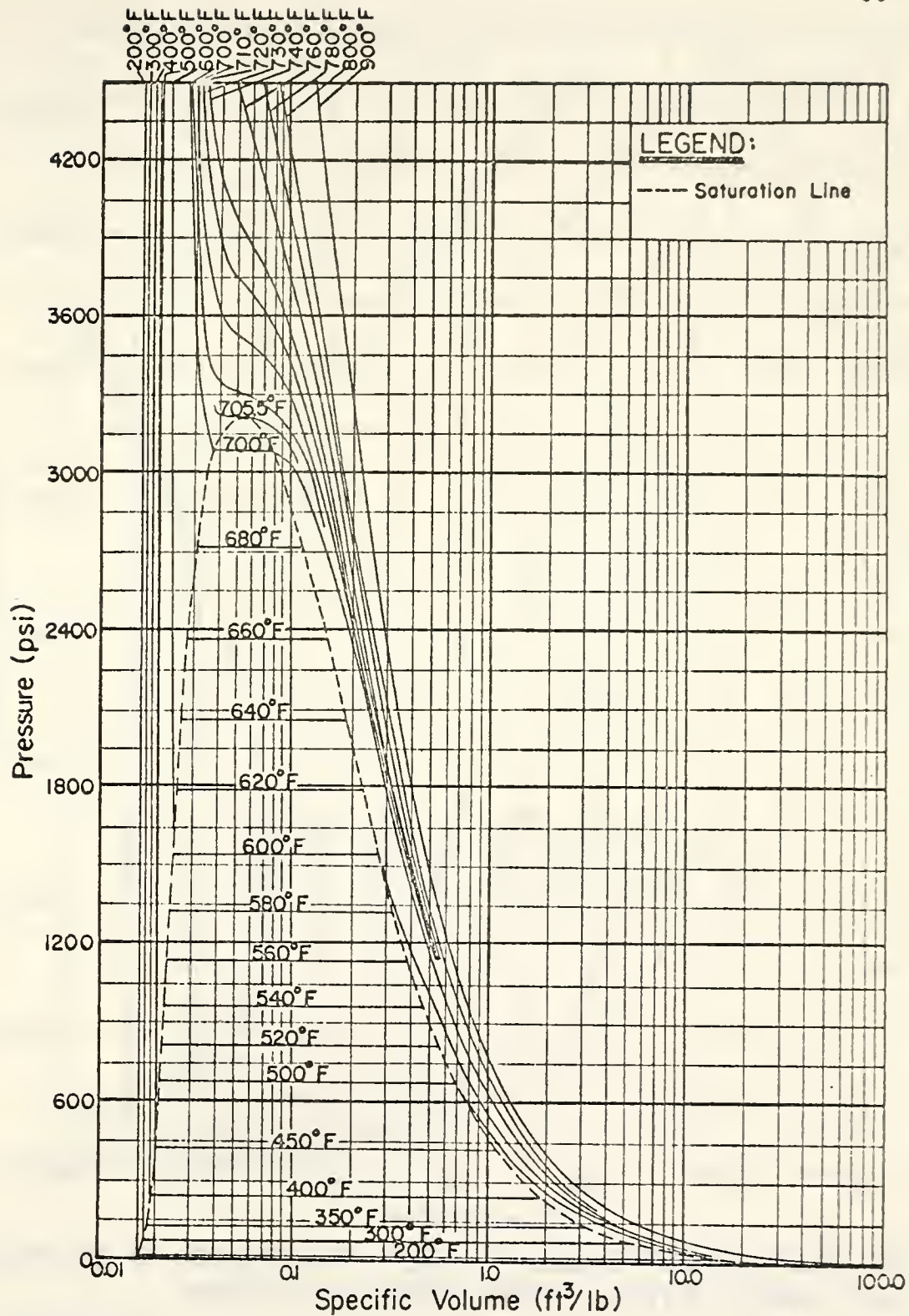


FIGURE IV-8- PRESSURE- SPECIFIC VOLUME ISOTHERMS FOR WATER AND WATER VAPOR.

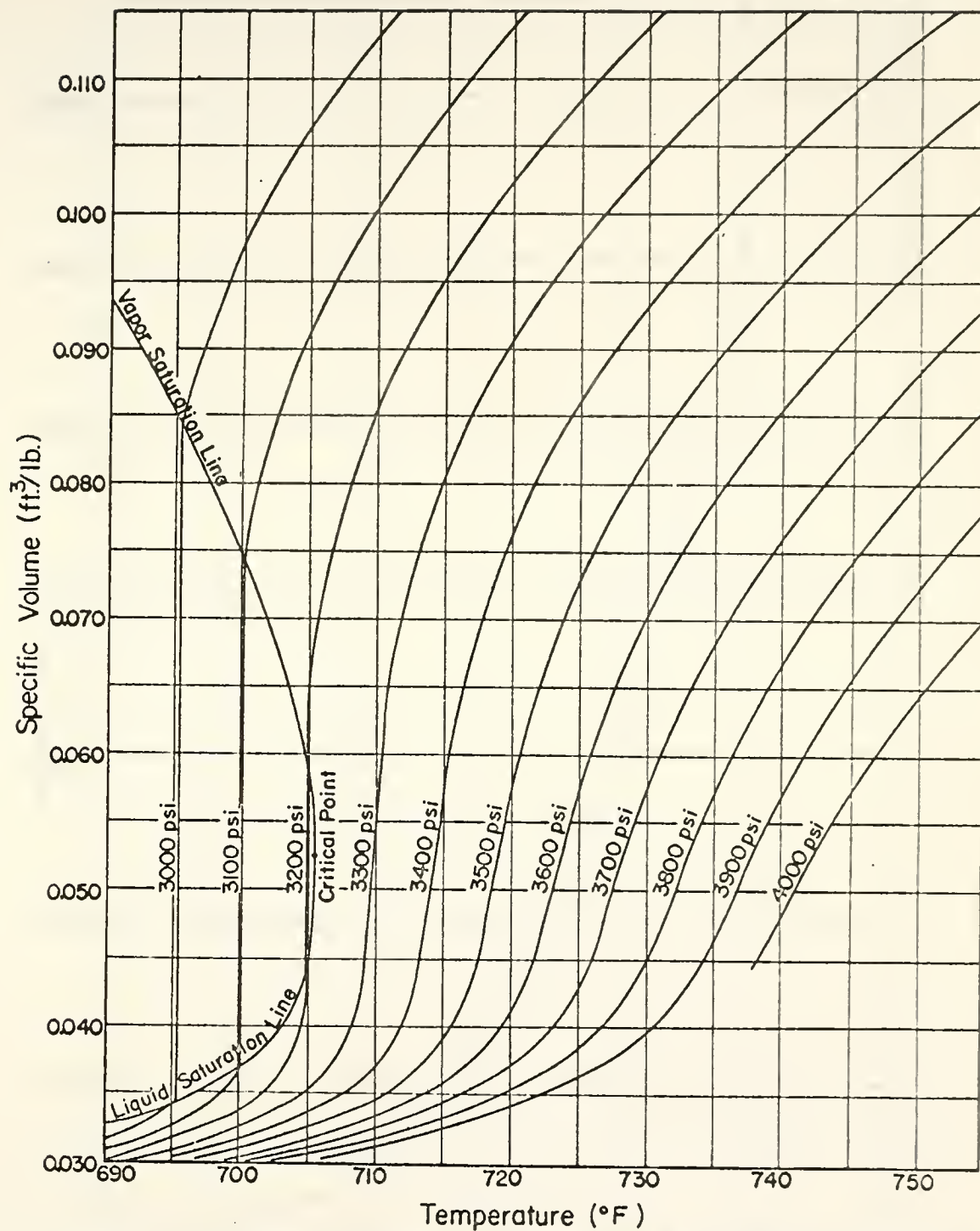


FIGURE IV-9- ISOBARS OF SPECIFIC VOLUME-TEMPERATURE FOR WATER AND WATER VAPOR (AFTER NOWAK, 1962).

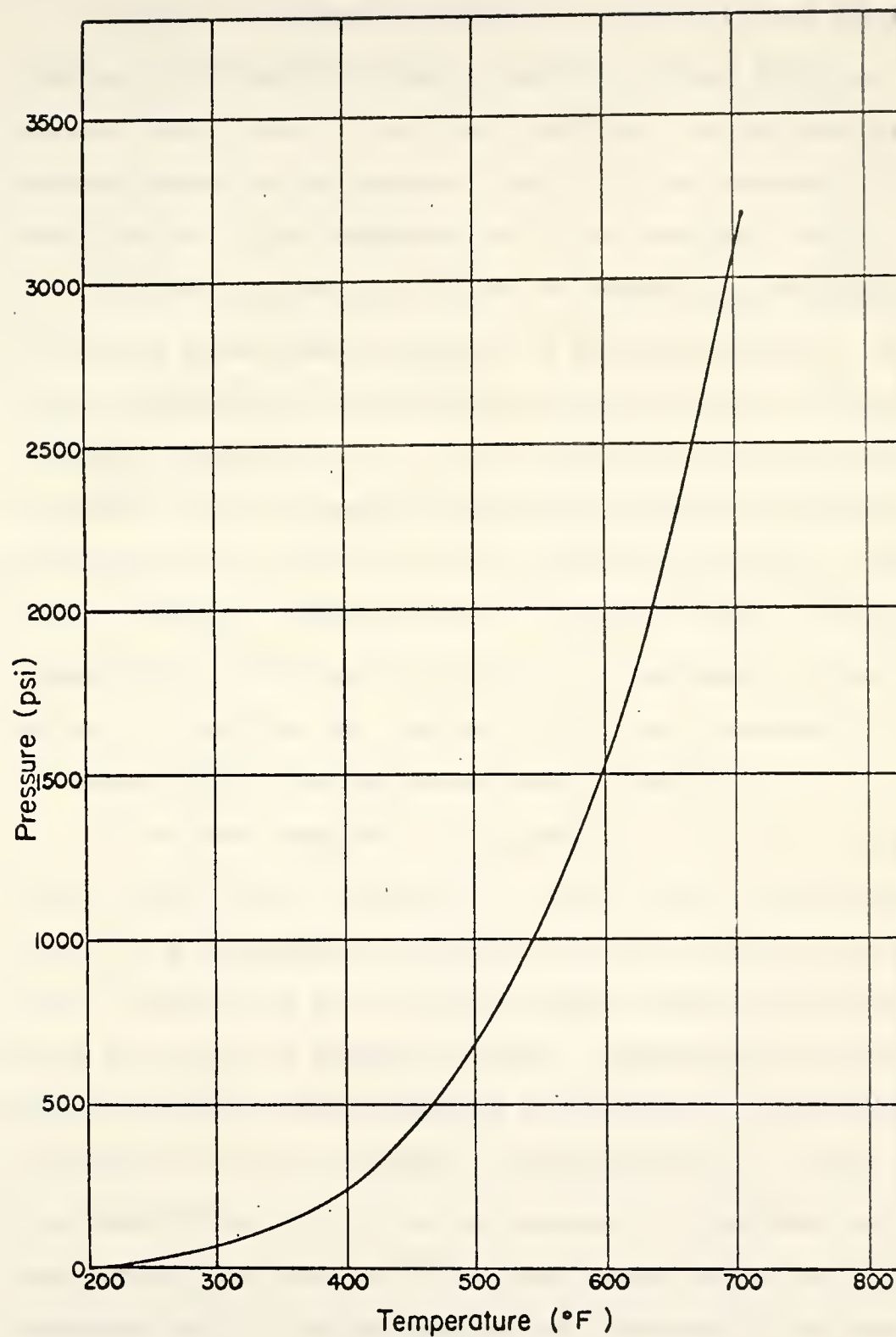


FIGURE IV -10-BOILING PHASE LINE.

A critical region run consists essentially of gradually raising the temperature and pressure of water from the ambient conditions to 730°F and 3800 psi, and releasing the pressure along an isotherm of 730°F. It is desirable to stabilize the fluid temperature in the critical region at 730°F for at least half an hour, to reduce the possibility of boiling conditions occurring on pressure release. A typical temperature and pressure program used in this study is shown in Figure IV-11. It is interesting to note the similarity of the pressure-temperature-time relationship developed by the author to that obtained by another research worker, James R. Hooper (shown in Figure IV-12). Hooper independently developed techniques on equipment of another design (as reported by Diamond [1970]) for successful critical region drying of saturated kaolin samples.

It has been observed that partially saturated soils tend to imbibe water and swell or slake when they are subjected to a negligible restraint and are given access to water. Such soils are critical region dried only after first being saturated at constant volume. Saturation at constant volume results in the container surfaces applying stresses equivalent to those released in the saturation process. It is presumed that saturation at constant volume does not change the distribution of the pore space of the partially saturated soil. The presumption was indirectly and partly validated when compacted soil samples trimmed to different

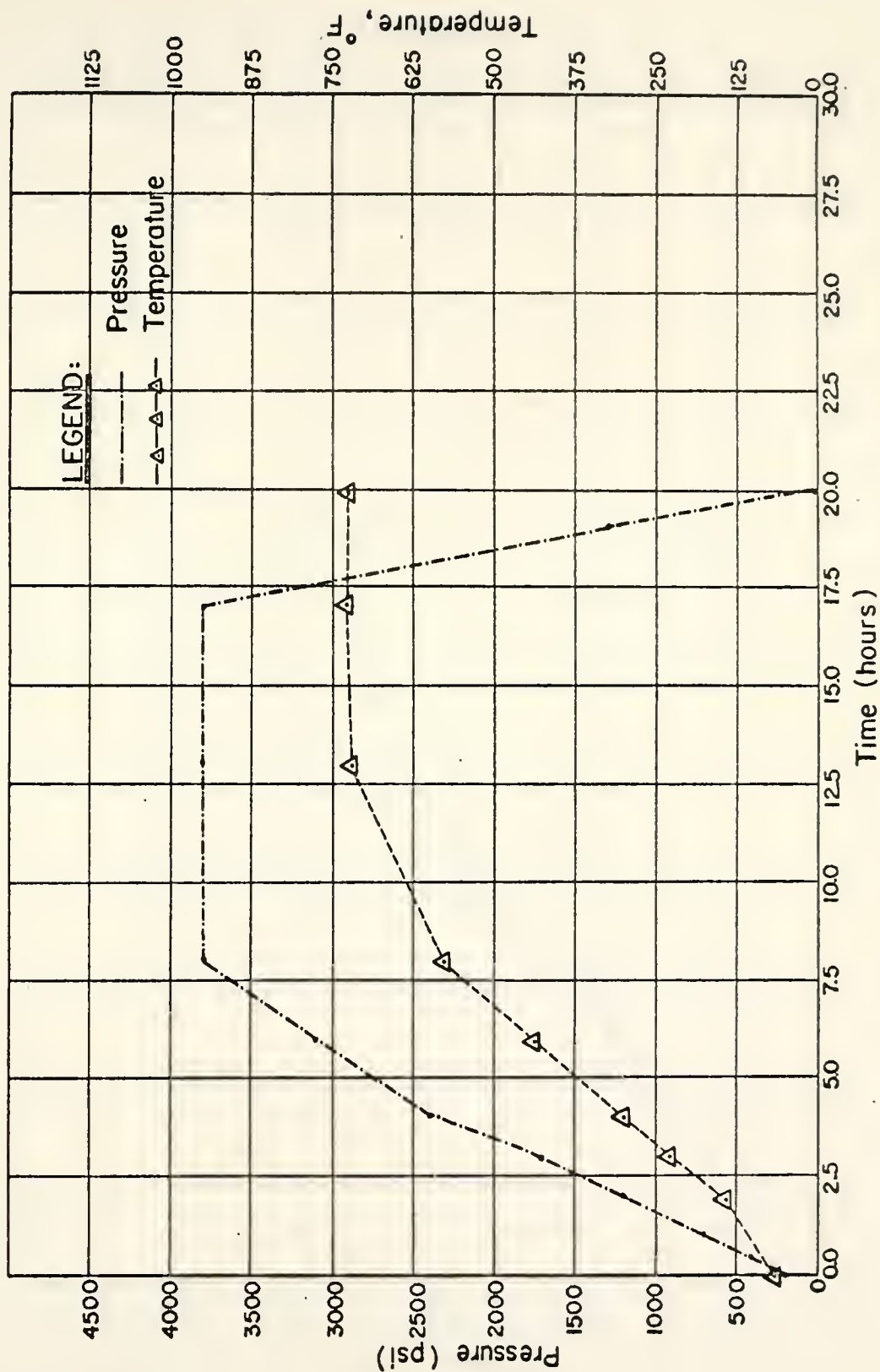


FIGURE IV-II - TYPICAL PRESSURE AND TEMPERATURE VS. TIME RELATIONSHIPS FOR CRITICAL REGION RUN.

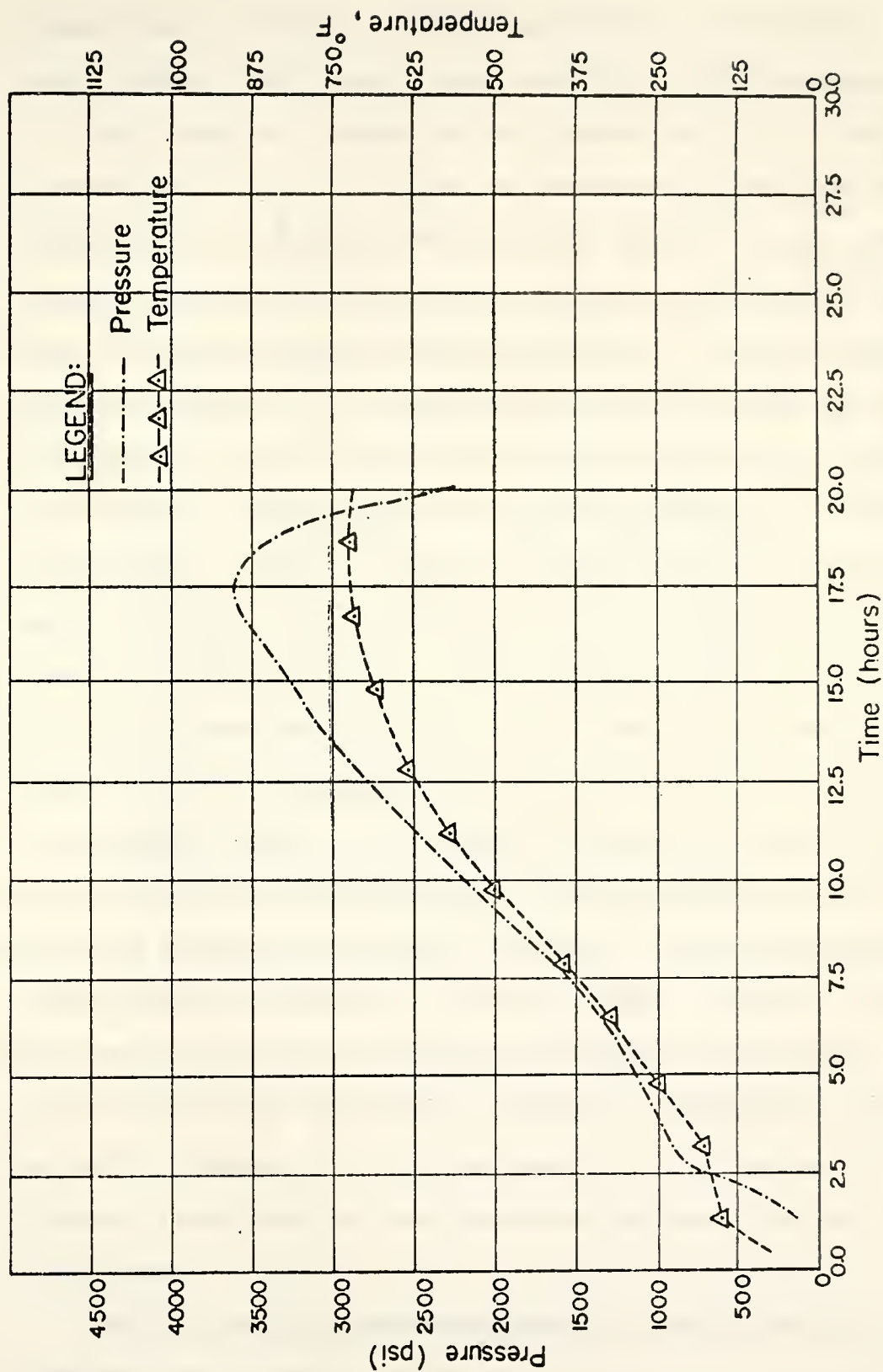


FIGURE IV-12 - TYPICAL PRESSURE AND TEMPERATURE VS. TIME
RELATIONSHIPS FOR CRITICAL REGION RUN.(AFTER J. R. HOOPER).

dimensions, saturated at constant volume, and critical region dried, gave almost identical pore size distributions.

Soil samples trimmed to the dimensions of 1/2 inch diameter and 1/2 inch height, as described under the section "Preparation of Samples for Critical Region Drying", were placed in special close fitting specimen containers. These were fabricated either from fired grade "A" lava or from stainless steel 347. Graphite lubricant was used to enable the specimen to be inserted into the container with minimum disturbance. The graphite lubricant worked well at high temperatures. Lava, a hydrous aluminum silicate, can be easily machined in its raw condition and becomes hard when fired to 1000°C (1832°F). Extensive experimentation showed that fired lava and stainless steel sample containers are highly corrosion resistant and are equally suited for critical region drying. Lava sample containers could not be used for critical region drying of Volclay bentonite, as the swelling pressure exerted by the soil in the saturation process was high enough to fracture them. The soil samples were enclosed in lava or stainless steel containers to protect them from detrimental effects of unsteady conditions prevailing around the critical point, and to maintain the stresses introduced at the container surfaces during saturation.

Low air entry Carborundum porous stones, having a predominant pore diameter of 100 micrometers and a gross thickness of 1/4 inches, were saturated with deionized water

under vacuum, and placed on both ends of the sample in its container. Carborundum porous stones were used in preference to ceramic or sintered bronze porous stones, as they were more resistant to the condition of the tests. The porous stones were clamped to the container by a bolting together of stainless steel 304 discs placed on their outer sides. The assembled container is shown in Figure IV-13. The porous stones were used on both ends of the sample container to ensure that water outside of the container was in complete communication with water in the soil sample, and to allow transfer of pore water from the sample in the critical region drying phase.

After insertion into their containers, the soil samples were initially permitted to imbibe deionized water by capillary action at constant volume, letting air escape from the top. Each sample was then held under a head of one foot of water for at least a week. This resulted in degrees of saturation generally greater than 95 percent. After such saturation, the porous stones were removed. Ottawa sand 50-70 was sparingly sprinkled on both ends of the saturated sample, and the saturated porous stones were again clamped to the container. It was observed that in the absence of the sand, the soil sample stuck to the porous stones after critical region drying, presumably due to seepage forces occurring during the transfer of pore fluid from the sample.

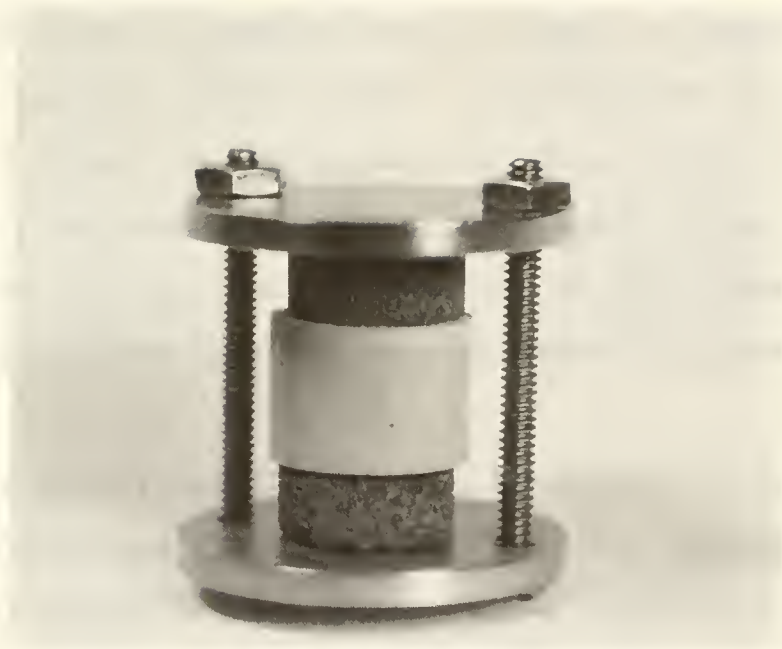


FIGURE IV-13- A SOIL SAMPLE ASSEMBLED FOR CRITICAL REGION DRYING. POROUS STONES ARE CLAMPED ON EITHER SIDE OF THE SAMPLE IN THE CONTAINER.



HERSCHEL

The assembled samples were placed in the critical region vessel. The vessel was filled with deionized water so that at least a shallow cover of water was maintained on top of the upper sample. The dimensions of the vessel allowed a maximum of six samples to be dried in a single run. The filled critical region vessel was connected to the remainder of the system. The system was saturated with deionized water by pumping water through the bottom connection of the balance control vessel. Air escaped through water in a small flask. A small quantity of air remained entrapped in the pipe connecting the balance control vessel to the nitrogen gas cylinder. Saturation of the system reduced the need to use the jack for pumping water for pressure generation.

It was stated earlier that saturation at constant volume resulted in degrees of saturation generally greater than 95 percent. This means that a negligible quantity of air remained entrapped in the soil samples. Some pressurization of water in the system at room temperature was considered desirable to dissolve the remaining air in the water. A pressure of 200 psi was applied gradually using nitrogen gas pressure. The pressures in excess of 200 psi and up to 3800 psi were generated during the heating process by nitrogen gas pressure and use of the jack, in accordance with the pressure-time relationship of Figure IV-9.

In a few preliminary trials the critical region vessel was heated using the program mode of operation of the Thermac controller. It was noticed that synchronization of the command temperature (fed by the program) with the control temperature was difficult, even when different bands of proportional control were used. It should be explained that "control temperature" refers to the temperature of water in the critical region vessel, and "command temperature" refers to the desired temperature as indicated by the temperature-time relationship in Figure IV-11. When narrower bands of proportional control were used, control temperatures invariably exceeded the command temperature and vice versa. When using wider bands of proportional control, additional voltage invariably had to be supplied using manual-reset index control incorporated into the Thermac temperature controller. This reduced and finally eliminated the offset between command and control temperatures.

Use of the program mode was finally discarded in favor of the set point mode. The command temperature was set at 730°F. A small voltage was steadily supplied to the heater at a uniform rate, using a band of proportional control of 200°F. This resulted in a gradual rise of heater temperature. The differences between the control and command temperatures were monitored at frequent intervals. The bands of proportional control were changed to 150°, 100°, 50° and 20°F as the temperature differences reduced to 200°,

THE UNIVERSITY OF CHICAGO PRESS

1215 EAST 58TH STREET, CHICAGO, ILL. 60637

TEL. (312) 707-7000

TELETYPE (312) 707-7000

CABLE CHICAGO 5-5000

POSTMASTER: SEND ADDRESS CHANGES TO THE UNIVERSITY OF CHICAGO PRESS, 1215 EAST 58TH STREET, CHICAGO, ILL. 60637

ALL ORDERS AND INQUIRIES SHOULD BE SENT TO THE UNIVERSITY OF CHICAGO PRESS, 1215 EAST 58TH STREET, CHICAGO, ILL. 60637

THE UNIVERSITY OF CHICAGO PRESS, 1215 EAST 58TH STREET, CHICAGO, ILL. 60637

TELEPHONE (312) 707-7000

TELETYPE (312) 707-7000

CABLE CHICAGO 5-5000

POSTMASTER: SEND ADDRESS CHANGES TO THE UNIVERSITY OF CHICAGO PRESS, 1215 EAST 58TH STREET, CHICAGO, ILL. 60637

ALL ORDERS AND INQUIRIES SHOULD BE SENT TO THE UNIVERSITY OF CHICAGO PRESS, 1215 EAST 58TH STREET, CHICAGO, ILL. 60637

THE UNIVERSITY OF CHICAGO PRESS, 1215 EAST 58TH STREET, CHICAGO, ILL. 60637

TELEPHONE (312) 707-7000

TELETYPE (312) 707-7000

CABLE CHICAGO 5-5000

POSTMASTER: SEND ADDRESS CHANGES TO THE UNIVERSITY OF CHICAGO PRESS, 1215 EAST 58TH STREET, CHICAGO, ILL. 60637

ALL ORDERS AND INQUIRIES SHOULD BE SENT TO THE UNIVERSITY OF CHICAGO PRESS, 1215 EAST 58TH STREET, CHICAGO, ILL. 60637

THE UNIVERSITY OF CHICAGO PRESS, 1215 EAST 58TH STREET, CHICAGO, ILL. 60637

TELEPHONE (312) 707-7000

TELETYPE (312) 707-7000

CABLE CHICAGO 5-5000

150°, 100° and 50°F, respectively. Heating was continued until the difference between command and control temperatures was zero for at least half an hour.

After achievement of the desired pressure-temperature combination within the critical region, the pressure was dropped along the isotherm of 730°F at the rate of 25 psi/minute. During the pressure drop, the fluid density in the soil sample decreases as shown in Fig. IV-9, and a corresponding amount of fluid escapes from the soil sample through the porous stones. When the pressure was reduced to the atmospheric pressure, the critical region vessel was still at a temperature of 730°F. At that instant, the critical region vessel was detached from the system to protect the dried samples from potential sources of moisture in the system, and was allowed to cool overnight to ambient room temperature.

The samples were removed from the sample containers using the extruder described under the section "Preparation of Samples for Critical Region Drying." They were stored in desiccators containing anhydrous magnesium perchlorate for at least a week to remove moisture absorbed from the atmosphere during the cooling of the critical region vessel, and to maintain them in the dry state.

It was observed that the critical region vessel made of stainless steel 316 became corroded at the high temperatures and pressures encountered in the critical region drying process. Corrosion left finely suspended metal particles

floating in the water. These particles could get into the soil samples, if they had dimensions smaller than the predominant pore diameter of the porous stones, i.e., 100 micrometers. It was necessary to prevent the entry of metal particles into the soil samples, and this was achieved by letting the pressure drop from 3800 psi to atmospheric pressure along the isotherm of 730°F. This resulted in a continuous increase of specific volume of fluid in the sample, thus preventing the drawing of outside water into the soil pores. (It is desirable to periodically pressure test the critical region vessel against a pressure of 6000 psi, as there is a likelihood of its weakening due to corrosion and pitting of the walls of the vessel during critical region drying.)

Extensive experimentation showed that, excepting in the case of Volclay bentonite, the dimensions of soil samples remained unchanged, i.e., the total porosity remained unchanged, in the process of critical region drying. X-ray diffraction and infra-red spectral analysis on the soils before and after critical region drying showed no change in the basic characteristics of the clay minerals.

Pore Size Distribution

The Apparatus

The principle that a non-wetting liquid, such as mercury, enters an empty capillary only under pressure, and that the

pressure required to intrude the smaller capillaries is larger, forms the basis of establishing the mathematical pore size distribution in this study.

The apparatus used in pore size distribution determinations consists essentially of three units, i.e., the penetrometer, the filling device, and a modified Aminco porosimeter. The penetrometer, shown in Figure IV-14, is of glass, and has a bulk volume of about 6 ml. It is equipped with a precision bore capillary stem of 1.3 mm diameter. The stem has a total bore volume of 0.200 ml., and is calibrated at 0.002 ml. intervals. The bulb end of the penetrometer contains the dry soil sample, and is closed by means of a steel cap pressing against its lubricated end, kept in contact by means of a teflon retaining device.

The filling device of an advanced design (U. S. Patent No. 3, 438, 245 Prado Laboratory, Inc., Cleveland, Ohio) was used for the initial mercury filling, and for measurement of intrusion volumes at pressures lower than atmospheric. The filling device, shown in Figure IV-15, consists of a two-chambered glass tube having a bullet nose, A, at one end, in which the stem of the penetrometer rests with the mercury surface touching its underside and with a stopcock, B, at the other end. The stopcock connects the filling device with the vacuum manifold, mercury manometer, McLeod gage, and a fine needle valve, shown in Figure IV-16, to admit controlled air increments to the entire system. The

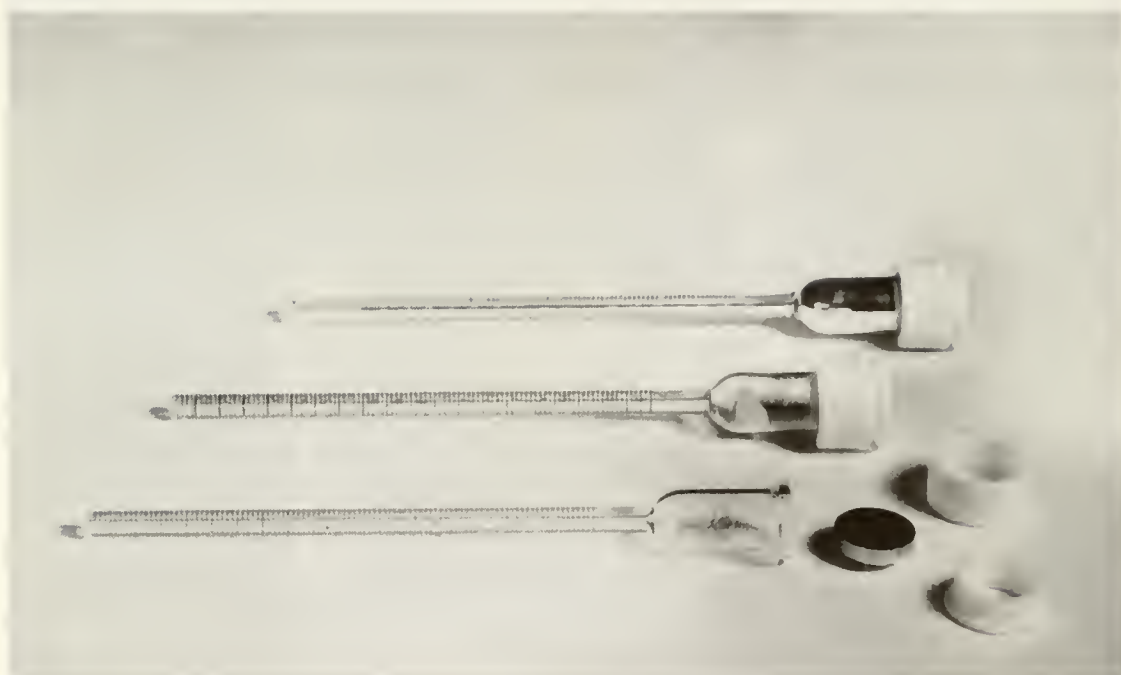


**FIGURE IV-14 - PENETROMETER: (FROM FRONT TO BACK)
DISASSEMBLED, ASSEMBLED WITH SAMPLE,
AND FILLED WITH MERCURY.**

(After Winslow, 1969)

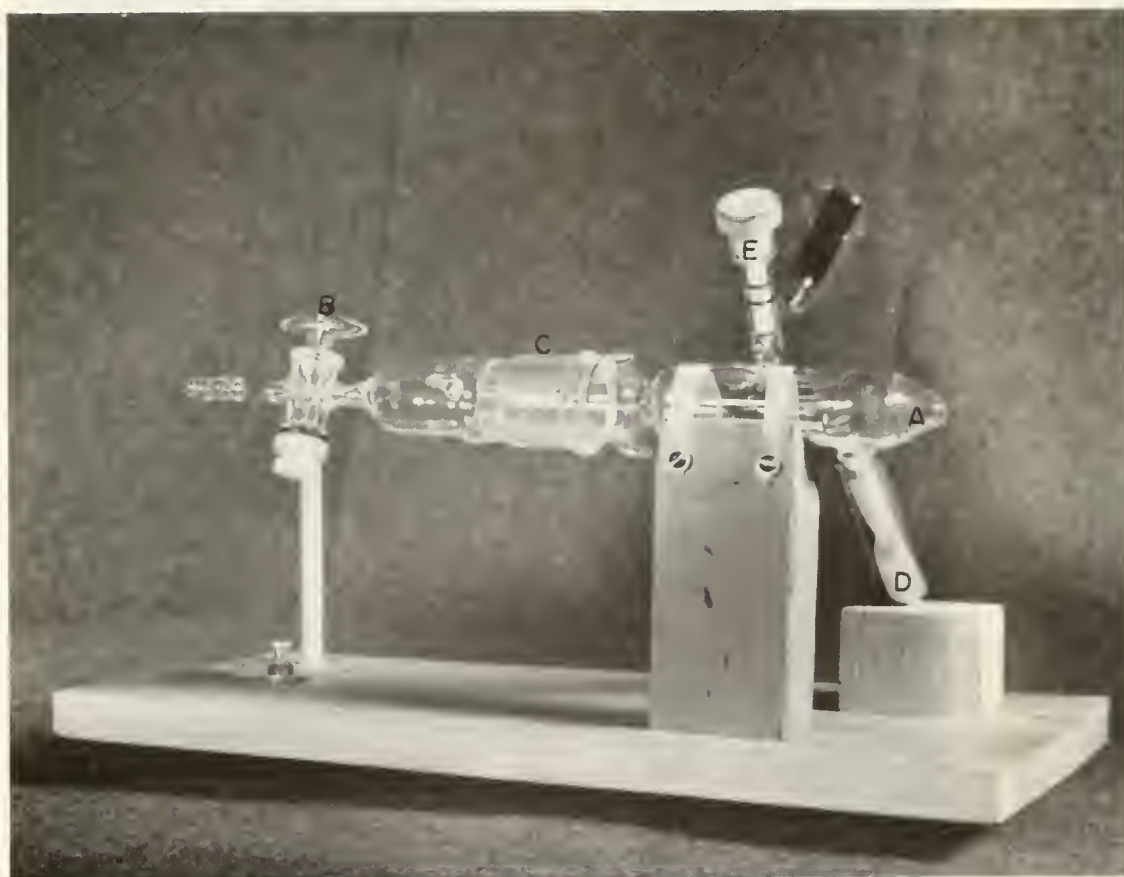


FIGURE IV-15- FILLING DEVICE. (After Winslow, 1969)



FIGURE IX-16- MERCURY INTRUSION EQUIPMENT SHOWING (FROM LEFT TO RIGHT) MANOMETER, VACUUM MANIFOLD, FILLING DEVICE, AND POROSIMETER.
(After Winslow, 1969)

main tube can be separated at the ground glass joint, C, to allow the penetrometer to be positioned within the filling device. The portion of the main tube associated with the ground glass joint contains a wad of glass wool, which presses against the head of the penetrometer. The main chamber is constricted as shown in the Figure. This constriction carries a tapered teflon stopper split longitudinally, which is mounted on the penetrometer stem to hold it in a horizontal position. The split also provides communication for gas between the two chambers of the main tube. A side arm, D, serves as a mercury reservoir, and functions to adjust the level of mercury in the main chamber. An ungreased teflon stopcock, E, is used to introduce additional mercury to the main chamber between tests.

A modified porosimeter, shown in Figure IV-16, was used for measurement of intrusion at pressures higher than atmospheric. Several modifications were effected on the commercially available Aminco porosimeter manufactured by the American Instrument Co., Silver Spring, Maryland (Winslow [1969]). The porosimeter consists of a pressure chamber in which 15,000 psi pressure is generated by an electrically driven hydraulic pump using ethanol; Bourdon pressure gages of 1,000 and 15,000 psi capacities with sensitivities of 5 and 100 psi, respectively; and a means of sensing the intrusion of mercury. Such mercury intrusion is sensed by a stainless steel needle which follows the position of the meniscus of

the mercury in the capillary stem of the penetrometer. As the needle advances, its linear movement is recorded digitally by a mechanical readout device in units of 0.0001 ml.

The Technique

A representative critical region dried sample, having a void volume not exceeding the total volume measuring capacity of the porosimeter of 0.200 ml., was weighed on an analytical balance of 0.0001 gram sensitivity, and was placed in the bulb of the penetrometer. Vacuum grease was applied lightly to the bulb end of the penetrometer. The smooth side of the steel cap was placed on the bulb end and rotated to eliminate entrapped air in the grease layer sandwiched between the steel cap and the bulb end of the penetrometer. The steel cap was held tightly against the bulb end of the penetrometer using a teflon screwing arrangement. The assembled penetrometer was weighed. The tapered teflon stopper, split longitudinally, was slipped over the penetrometer stem.

The filling device was opened at the ground glass joint, C, (Figure IV-15), and the penetrometer inserted into the main chamber. When in position, the open end of the penetrometer stem rested in the bullet nose. The stopper pressed against the constriction and the split in the stopper pointed approximately vertically. The vacuum pump was started, and the system was connected to it by opening the stopcock, B. The side arm, D, was raised to introduce mercury into the

main chamber. The filling device was brought into level. Mercury was introduced through the teflon stopcock, E, until it just touched the underside of the penetrometer stem. Evacuation continued until the residual pressure, measured by a McLeod gage, dropped to a typical value of 0.010 mm Hg. The side arm, D, was raised further such that the level of mercury in the main chamber rose and just blocked the borehole in the penetrometer stem. The system was isolated from the vacuum pump, and pressure was increased to 20 mm Hg via the fine needle valve connecting the system and the atmosphere. Mercury flowed through the stem and filled the space surrounding the sample in the penetrometer bulb. It was observed that, in some cases, the soil sample stuck to the inside glass surface of the penetrometer bulb, and was not completely enveloped at the filling pressure of 20 mm Hg. In such cases, the filling pressure was raised in small increments to a value of 40 to 80 mm Hg so as to completely envelop the soil sample. It was generally observed that the soil samples tested had essentially zero pore volume up to a pressure of 80 mm Hg. Pressures in this range and up to one atmosphere were measured with a mercury manometer.

After the penetrometer was filled with mercury, the side arm, D, (Figure IV-15), was lowered such that the borehole of the penetrometer stem was no longer immersed in mercury, and the mercury column broke near the open end of the stem. The position of mercury on the stem was recorded.

The pressure was increased in steps by manipulation of the fine needle valve and mercury penetration was read on the stem following each pressure increment. This process was repeated until the pressure in the system reached one atmosphere. The filling device was opened at the ground glass joint, C, and the penetrometer removed and weighed to obtain the weight of mercury present. The temperature of mercury in the filling device was recorded. Thus, the volume of mercury in the penetrometer was known.

The assembled penetrometer was placed, stem down, in the pressure chamber of the modified Aminco porosimeter. The top of the pressure chamber was closed with a socket pressing down on a cap. The cap maintains a seal with the chamber sides, using a lubricated Buna N "O" ring embedded in a groove in its periphery. In addition, it incorporates a stainless steel sheet spring maintaining electrical contact with the stainless steel cap of the penetrometer, as well as a small vent for the escape of air from the pressure chamber. The vent was closed when the chamber was completely filled with ethanol. Subsequently, the electric contact with the mercury column was established when the probe was actuated to sense the position of mercury in the penetrometer stem. It may be mentioned here that the placing of the penetrometer with the stem down caused application of pressure less than atmospheric on the soil sample. The initial pressure increment applied to the mercury column brought the pressure on the sample to one atmosphere and the corresponding digital readout

was noted. The difference between penetrometer stem readings, corresponding to a pressure application of one atmosphere in the porosimeter and in the filling device, gave the correction to be applied to the subsequent digital readouts of the porosimeter. The pressure was applied in increments to a maximum value of 15,000 psi, and the intrusion of mercury was registered by the digital readout, after equilibrium was reached at each pressure increment. The equilibrium condition corresponded to no change in volume being registered by the readout in one minute. The number of pressure increments were selected to accurately define the pore size distribution curve.

At the conclusion of the test the probe was returned to its initial position, the digital readout was reset to 0.0000 ml., the pressure was gradually reduced to one atmosphere, and the penetrometer was removed from the pressure chamber. Mercury recovered from the penetrometer was cleaned before being reintroduced into the filling device.

The soil samples were fractured to study the pattern of interconnected capillaries through which mercury might have been forced into them. It was generally observed that most of the mercury extruded from capillaries accessible to the surface during the depressuring process. The soil samples were also examined for the detrimental effects of differential pressuring. It was observed that the soil samples retained their initial volumes, shapes and topographic outlines.

The penetrometer was cleaned and dried in an oven at 105°C for at least 2 hours before being cooled to room temperature for reuse.

Reduction of Data to Pore Size Distributions

The pressure and the mercury intrusion data obtained during a typical run are subjected to a number of corrections. The pressures recorded during the filling operation were absolute pressures, while those recorded during the porosimeter operation were gage pressures. To obtain the absolute pressures on the sample during the latter operation, one atmosphere of pressure must be added. Furthermore, pressure corresponding to a negative head of mercury in the stem must be subtracted from the registered gage pressure to obtain the actual pressure on the sample. The net correction was an addition of 11 psi to the gage pressure.

The volume of intruded mercury is corrected for the compression of residual air entrapped in the penetrometer during the filling operation. This correction was important only at pressures below one atmosphere. At pressures typically in excess of 200 psi, the volume of intruded mercury is corrected at each pressure step for the effective compression of the mercury in the penetrometer. The correction was typically 0.0011 ml. per ml. of mercury in the penetrometer at 15000 psi. No correction was applied for the compressibility of the soil solids and of the soil skeleton, as it was considered negligible.

The reduction of the absolute pressures and the corrected volumes of intruded mercury to pore size distributions requires the assumption of a shape for the pores. Assuming a cylindrical shape, and knowing the values of the contact angle between mercury and soil, and the surface tension of mercury, the absolute pressures can be reduced to cylindrical pore diameters using the Washburn equation (Washburn [1921]). Diamond (1970) measured the contact angles between mercury and soils using the sessile drop method. He found that the contact angles for kaolinitic and illitic soils were within a degree of an average value of 147° , while those for montmorillonitic soils were within a degree of an average value of 139° . The value (Kemball [1946]) for the surface tension of clean mercury of 484 dynes/cm at 25°C was considered appropriate for use in this study.

The major assumption of questionable validity in the pore size distribution measurements is the accessibility of pore space through entryways which are as large as the pores to be intruded. In view of this assumption, the pore sizes will be referred to as "equivalent cylindrical pore sizes."

The data obtained during the filling device operation, such as void ratio, were processed using the Programma, a program desk calculator manufactured by Olivetti-Underwood Corporation. Such data, as well as those obtained during the porosimeter operation, and the corrections became input

for a computer program written in Fortran IV language with a plotting subroutine. The program was used to compute and then plot either the cumulative pore space per gram of dry solids or the cumulative percentage of total pore space as the ordinate and the equivalent cylindrical pore diameter as the abscissa.

CHAPTER V

RESULTS

The results are presented in the following order: variables relating to the soil mixing, and to the soil compaction; effect of the drying procedures; and pore size distribution variations relating to the soil aggregations themselves, to the compacted soils, and to changes induced in the compacted soils after soaking.

Soil Mixing and Aggregation

The mixing of soil with water in the twin-shell liquid-solids blender resulted in extensive formation of soil aggregations over a wide range of water content. Size distributions of the resulting aggregations were obtained by screening them gently through a series of sieves. A typical set of aggregation size distribution curves is shown for Edgar Plastic kaolin in Figure V-1. The data are presented in terms of cumulative percent finer (by weight) as the ordinate and the sieve opening size (on a logarithmic scale) as the abscissa. The curves represent single determinations, which were found to be reproducible for an arbitrarily fixed level of the soil and the mixing process variables. The data show that the aggregation size distributions have a strong dependence on the mixing water content,

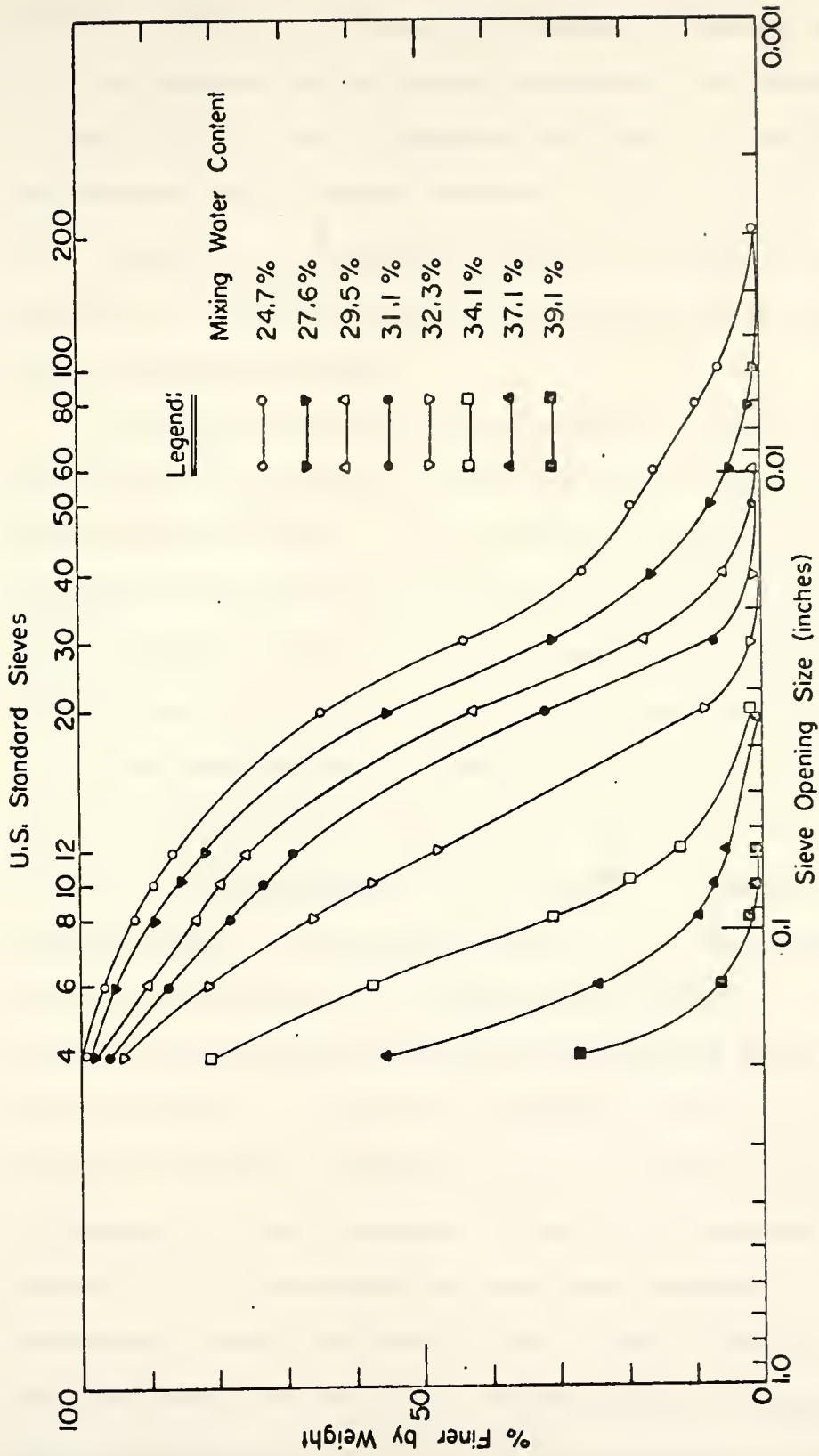


FIGURE Y-1 -SOIL AGGREGATION SIZE DISTRIBUTION CURVES FOR EDGAR PLASTIC KAOLIN.

and that the soil aggregations exhibit greater uniformity with increasing mixing water contents. The uniformity coefficients¹ of the soil aggregations are 4.1 and 2.3 at the respective mixing water contents of 24.7 and 31.1%. The soil aggregations lost their physical identity at moisture contents in excess of 39.1%, and melded into a macroscopically homogeneous mass.

Figure V-2 exhibits the variation of the aggregation index sizes, d_{50} and d_{10} , with the mixing water content for Edgar Plastic kaolin. It is apparent that both of the aggregation size indices increase with increasing mixing water contents. The size increases are, however, most significant for the mixing water contents in excess of 31%.

The demonstrated increase in the soil aggregation sizes with increasing water contents is the result of a "balling up" of the aggregations, as a result of numerous interactions between them in the mixing process. In the absence of shearing effects with the twin-shell blender, these aggregations are not broken down but remain and acquire reasonable strengths. It might be expected that these soil aggregations formed at increasing water contents should exhibit increasing dry unit weights. Table V-1 provides data in support of this expectation, and the degrees of "internal saturation" both for Edgar Plastic kaolin and for grundite aggregations. The dry unit weight data are based on the

mercury-porosimeter porosity determinations of aggregations $\frac{1}{d_{10}} \frac{d_{60}}$, where d_{60} and d_{10} are the aggregation sizes with 60 and 10 percent by weight, respectively, of the aggregations finer than these sizes.

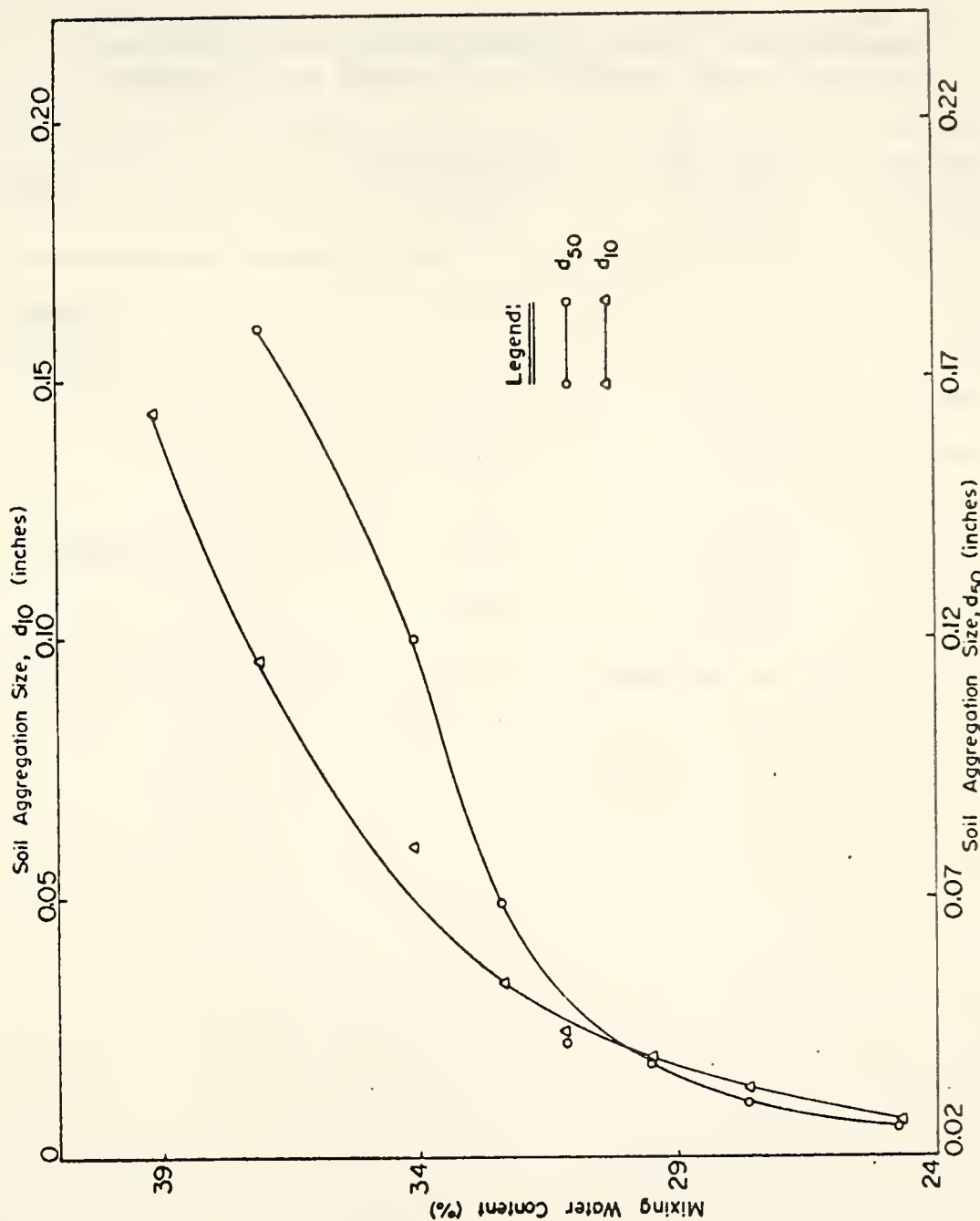


FIGURE Y-2 -VARIATION OF THE SOIL AGGREGATION SIZES d_{10} AND d_{50} WITH THE MIXING WATER CONTENT FOR EDGAR PLASTIC KAOLIN.

TABLE V-1

Variation of the Dry Unit Weight and the Degree of Saturation for Edgar Plastic Kaolin and Grundite Aggregations Formed at Different Water Contents

Soil	Mixing Water Content (%)	Dry Unit Weight (pcf)	Degree of Saturation (%)
Edgar Plastic Kaolin	26.9	72.4	55.5
	29.1	76.7	66.7
	34.6	79.2	84.2
Grundite	19.4	81.2	47.3
	23.0	87.3	64.6

after critical region drying. The porosity values were computed independently in a few cases by determining unit weights of wet soil aggregations that were coated with a mixture of paraffin wax and petrolatum by the ethyl alcohol displacement method. The porosity values obtained by the two procedures were found to be within $\pm 5\%$ of each other.

Compacted Soil

The cured soil-water mixes were compacted to obtain a series of compaction curves as shown in Figure V-3. The optimum moisture contents and the corresponding maximum dry unit weights for the soils are given in Table V-2. The compaction data were generated for laboratory processed soils, excepting for Crosby silty clay at the water content of 24.4%, which was compacted without processing and at the field moisture content. The compaction response of the processed and the unprocessed Crosby silty clay suggests similarity in their compaction behavior.

The compaction data show that the compaction response of Edgar Plastic kaolin is similar to that of Boston blue clay and Crosby silty clay. The higher optimum moisture contents and the lower dry unit weights of Edgar Plastic kaolin are associated with the absence of any coarse soil fraction with this commercial clay.

The compaction response of grundite is similar to that of reddish-brown limestone residual clay. Both soils exhibit a relatively small variation in dry density when

TABLE V-2

The Optimum Moisture Contents and the Maximum Dry Densities of the Compacted Soils

Soil ****	Compaction Type and Level	Optimum Moisture Content (%)	Maximum Dry Density (pcf)
Edgar Plastic Kaolin	Standard Proctor Compaction *	31.8	86.8
	10 lb Hammer, 18" Fall, 5 Layers, 6 Blows/Layer ***	32.6	85.7
	10 lb Hammer, 18" Fall, 5 Layers, 12 Blows/Layer ***	29.5	91.6
	Modified Proctor Compaction **	27.4	93.8
Grundite	Standard Proctor Compaction *	20.6	99.7
Reddish-Brown Lime- stone Residual Clay	Standard Proctor Compaction *	21.7	104.0
Boston Blue Clay	Standard Proctor Compaction *	22.5	103.2
Crosby Silty Clay	Standard Proctor Compaction *	17.1	110.7

* ASTM Designation: D698-70, Method A

** ASTM Designation: D1557-70, Method A

*** ASTM Designation: D1557-70, Method A, with the exception that 6 or 12 blows/layer are used in these cases, instead of the specified number of 25.

**** All soils are free of material coarser than the No. 40 U. S. Standard sieve size. The ASTM Designations: D698-70 and D1557-70, Method A, however, specify the removal of material coarser than the No. 4 U. S. Standard sieve size.

compacted over a wide range of water contents. Volclay bentonite does not show the familiar compaction trend in the range of water contents used in this study.

Effect of Drying Procedures

The drying procedures used in this study included, primarily, critical region drying and, secondarily, freeze drying and oven drying. The critical region drying procedure has been described in detail in Chapter IV. The freeze drying procedure consisted essentially of "quick" freezing of a small soil sample of dimensions of a few mm, in isopentane cooled by liquid nitrogen to -120°C . Subsequently, the ice was sublimed under a vapor pressure gradient maintained across the sample surface. During the sublimation stage, the sample was kept frozen using a partially frozen m-xylene slush bath. The vapor pressure gradient maintained across the sample surface allowed the transfer of water vapor to a condensing tube, cooled to liquid nitrogen temperature through a small evacuated space.

The oven drying procedure consisted of drying a small sample in a forced-draft oven at 105°C for 24 hours.

Because of the high temperature and pressure involved, it was thought that the critical region drying procedure, in particular, might give rise to various changes in the soil system. Such changes might involve the porosity or the pore size distribution, or even the basic structures of the clay

minerals present. A number of investigations were carried out to explore the existence of such possible artifacts in the present study.

The question of changed porosity is crucial to this study, in that the point of developing the rather difficult critical region drying procedure was precisely to avoid such changes. Evidence bearing on this point is provided in Table V-3 which shows data regarding the "as-molded" porosity and the porosity obtained after drying of the small samples, both for grundite and Crosby silty clay. The values for the "as-molded" porosity were calculated from the bulk density (as determined by the total weight of soil in the compaction mold and the volume of the mold), molding water content, and the specific gravity of the soil. The values for the porosity after the drying treatments were calculated using the bulk density of small specimens as determined during each mercury porosimetry run. The data indicate that the porosity of the critical region dried small samples approximates closely the "as-molded" porosity of the compacted samples. Table V-4 exhibits similar data for most of the soils used in this study, in terms of percent variation between the "as-molded" porosity of the compacted samples and the porosity of critical region dried small samples. It is apparent that the variations are generally small in magnitude and random in direction except for Volclay bentonite, which exhibits a more-or-less uniform reduction from the "as-molded" porosity as a result of critical region drying.

TABLE V-3

Comparison of the "As-Molded" Porosity of Grundite and Crosby Silty Clay Compacted at Different Water Contents by the Standard Proctor Method with the Porosities Obtained After Oven Drying, Freeze Drying, and Critical Region Drying of Small Samples

Soil	Molding Water Content (%)	"As-Molded" Porosity (cm^3/gm)	Oven Dried Porosity (cm^3/gm)	Freeze Dried Porosity (cm^3/gm)	Critical Region Dried Porosity (cm^3/gm)
Grundite	9.1	0.296	0.281	0.259	0.294
	16.4	0.282	0.224	0.248	0.276
	21.0	0.259	0.157	0.189	0.247
	23.0	0.273	0.153	0.219	0.262
Crosby Silty Clay	16.3	0.196	0.161	0.159	0.196
	18.2	0.196	0.143	0.158	0.199
	21.2	0.225	-	0.159	0.228

TABLE V-4

Comparison of the "As-Molded" Porosity of Edgar Plastic Kaolin, Grundite, Crosby Silty Clay, Reddish-Brown Limestone Residual Clay, and Volclay Bentonite Compacted at Different Water Contents by the Standard Proctor Method with the Porosity Obtained After Critical Region Drying of Small Samples

Soil	Molding Water Content (%)	"As-Molded" Porosity (cm^3/gm)	Critical Region Dried Porosity (cm^3/gm)	Percent Variation
Edgar Plastic Kaolin	22.7	0.460	0.479	+ 4.1
	27.6	0.413	0.437	+ 5.8
	30.0	0.402	0.382	- 5.0
	31.2	0.343	0.340	- 0.9
	34.6	0.367	0.360	- 1.9
	36.7	0.388	0.387	- 0.3
	39.1	0.413	0.425	+ 2.9
Grundite	9.1	0.296	0.294	- 0.7
	16.4	0.282	0.276	- 2.1
	21.0	0.259	0.247	- 4.6
	23.0	0.273	0.262	- 4.0
	25.0	0.280	0.270	- 3.6
	26.0	0.283	0.273	- 3.5
Crosby Silty Clay	13.4	0.243	0.248	+ 2.0
	15.6	0.200	0.206	+ 3.0
	16.3	0.196	0.196	0.0
	18.2	0.196	0.199	+ 1.5
	21.2	0.225	0.228	+ 1.3
	24.4	0.258	0.253	- 1.9
Reddish-Brown Limestone Residual Clay	16.1	0.278	0.265	- 4.7
	21.8	0.246	0.238	- 3.3
	28.1	0.309	0.309	0.0
Volclay Bentonite	25.4	0.516	0.410	-20.5
	37.6	0.558	0.471	-15.6
	60.9	0.683	0.581	-14.9

Examination of the data of Table V-3 suggests that neither the freeze drying nor oven drying procedures were uniformly successful in dewatering the soils without volume change. Freeze drying reduced the measured porosity by 12 to 18 percent for the dry-side specimens and 20 percent or more for the wetter ones. While reasonably satisfactory with the driest specimens, oven drying yielded measured porosity losses in excess of about 20 percent for the wetter specimens.

Possible changes in the basic structure of the soil minerals caused by critical region drying procedure were investigated using infra-red spectroscopic and X-ray diffraction techniques.

Infra-Red spectroscopic studies were conducted with KBr pellets using a Beckman IR-10 infra-red spectrophotometer. The infra-red spectra for Boston blue clay, Edgar Plastic kaolin and grundite, shown in Figures V-4 through V-6, demonstrate that the oven drying and critical region drying procedures do not cause serious alteration or disappearance of the absorption bands characteristic of various clay minerals present. The only effect observed was a slight broadening of the main Si-O lattice vibration centered near 1000 cm^{-1} for the critical region dried Boston blue clay.

X-Ray diffraction studies were conducted on randomly oriented powdered samples using molybdenum K α radiation. X-Ray diffractograms of Edgar Plastic kaolin and grundite

Legend:
I-Oven Dried
II-Critical Region Dried

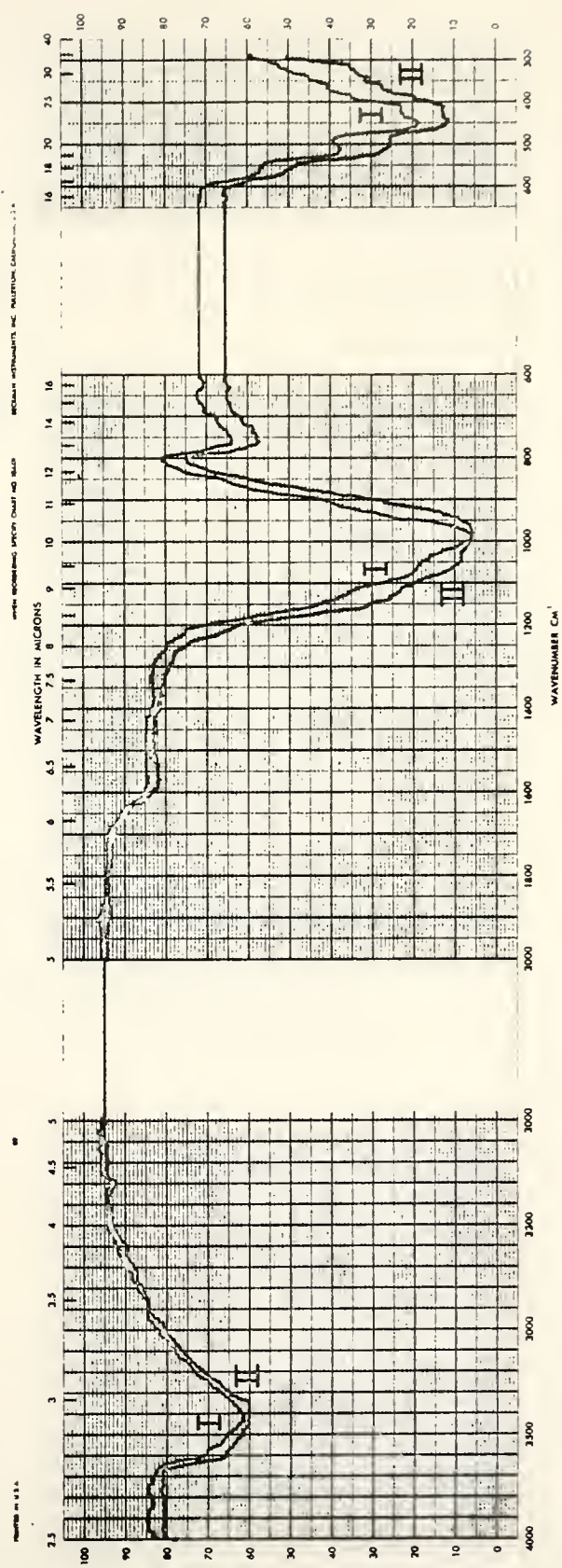


FIGURE V-4 - INFRARED SPECTROGRAPHS OF OVEN DRIED AND CRITICAL REGION DRIED BOSTON BLUE CLAY.

Legend:
 I - Compacted
 II - Critical Region Dried

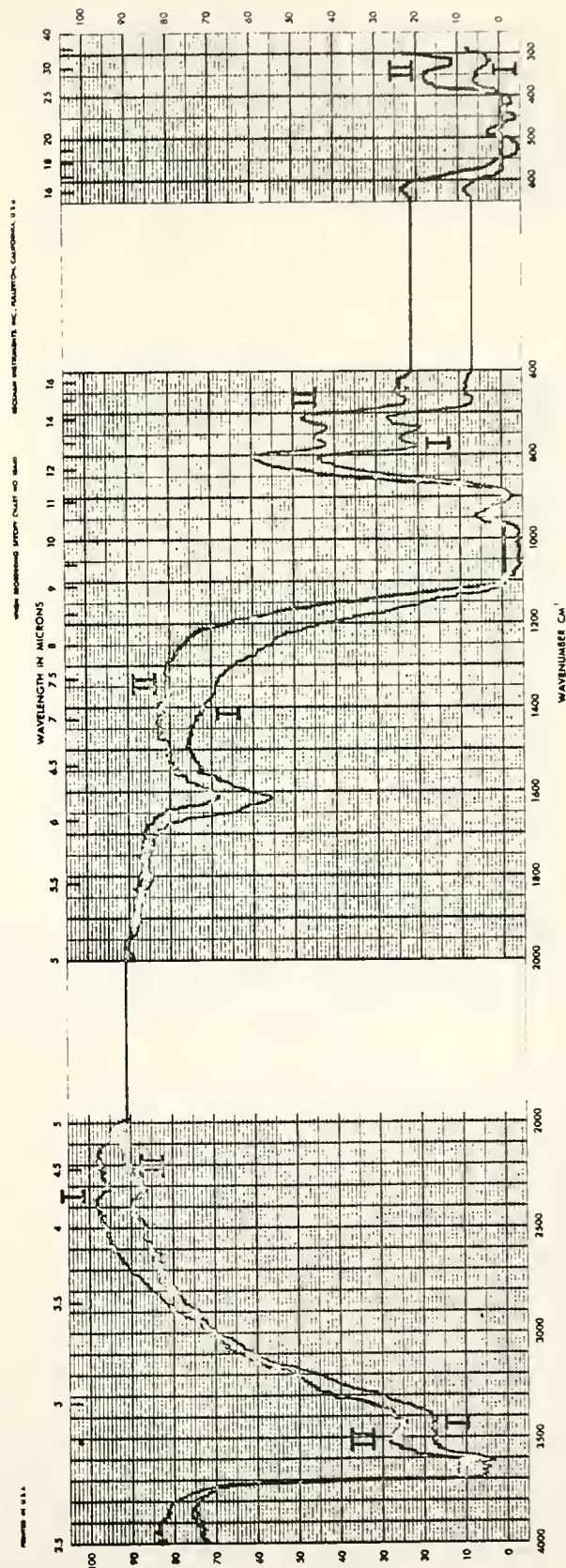


FIGURE V-5- INFRA-RED SPECTROGRAPHS OF COMPACTED AND CRITICAL REGION DRIED EDGAR PLASTIC KAOLIN.

Legend:

- I - Heated in Air at 730° F for 12 Hours
- II - Critical Region Dried
- III - Oven Dried at 220° F for 24 Hours

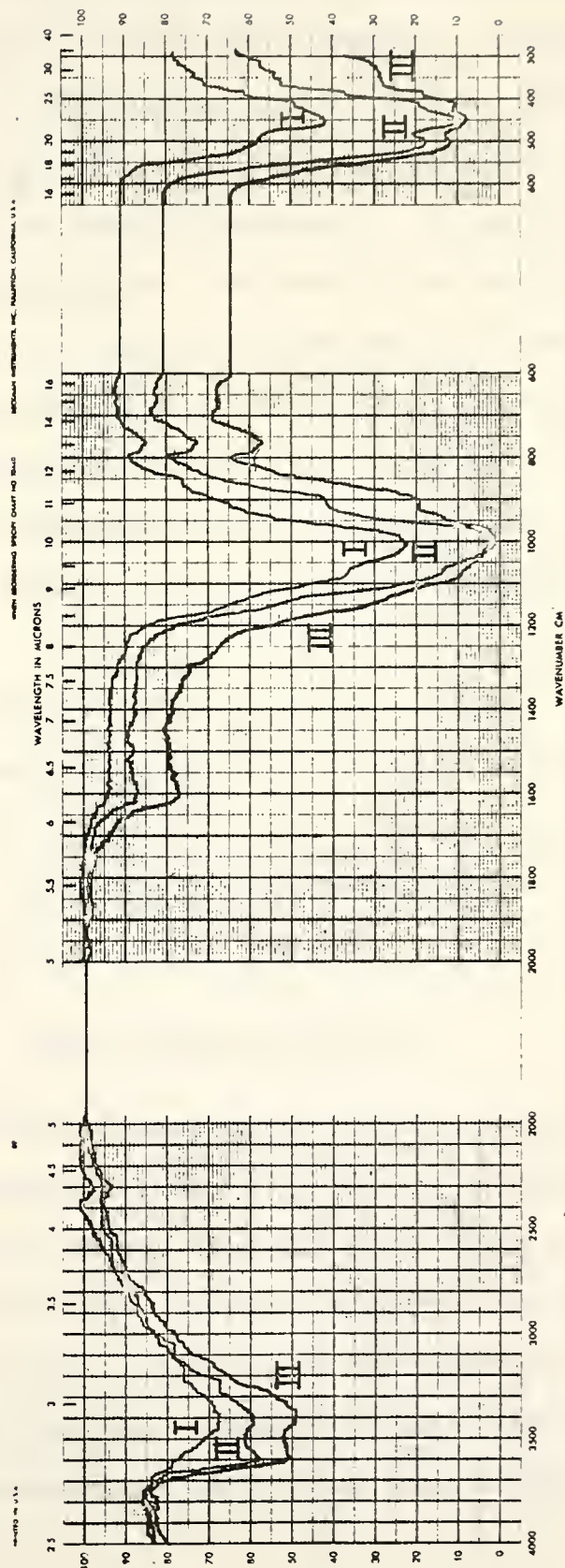


FIGURE V-6-INFRA-RED SPECTROGRAPHS OF OVEN DRIED, CRITICAL REGION DRIED AND 730° F HEATED GRUNDITE.

exhibit identical X-ray diffraction peaks for both the oven dried and the critical region dried samples. A typical X-ray diffractogram of grundite is included as Figure V-7. A comparison of X-ray diffractograms of air dried and critical region dried Volclay bentonite, Figure V-8, show that there are some changes. The basal spacing collapses to 9.7 \AA indicative of removal of the partial layer of inter-layer water present in the air dried state, and a fifth order basal peak appears at 1.86 \AA . A peak at 3.15 \AA in the air dried clay of unknown origin disappears. The hk peaks, characteristic of the crystal structure of montmorillonite, remain unaltered.

The above discussion regarding the changes in porosity and in the basic structure of clay minerals indicates that the critical region drying procedure does not cause recognizable changes in porosity or in crystal structure of the soil samples during the drying process.

Pore Size Distribution

The distribution of pore sizes (obtained after reduction of the mercury porosimeter data) is usually plotted as a cumulative intrusion curve, with the cumulative volume of pore space/gm of dry soil intruded in pore diameters larger than the equivalent pore diameter as the ordinate, and the equivalent cylindrical pore diameter as the abscissa. The curves are plotted with the equivalent pore diameter on a

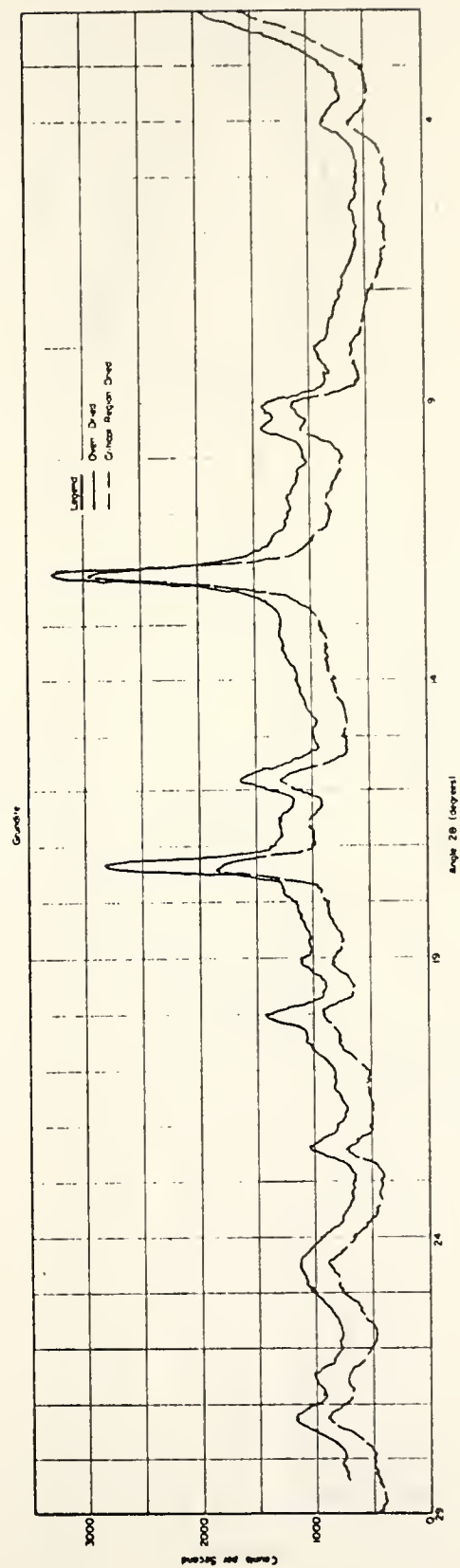


FIGURE 3.7 - X-RAY DIFFRACTOGRAMS OF OVEN DRIED AND CRITICAL REGION DRIED GROUNDNUT

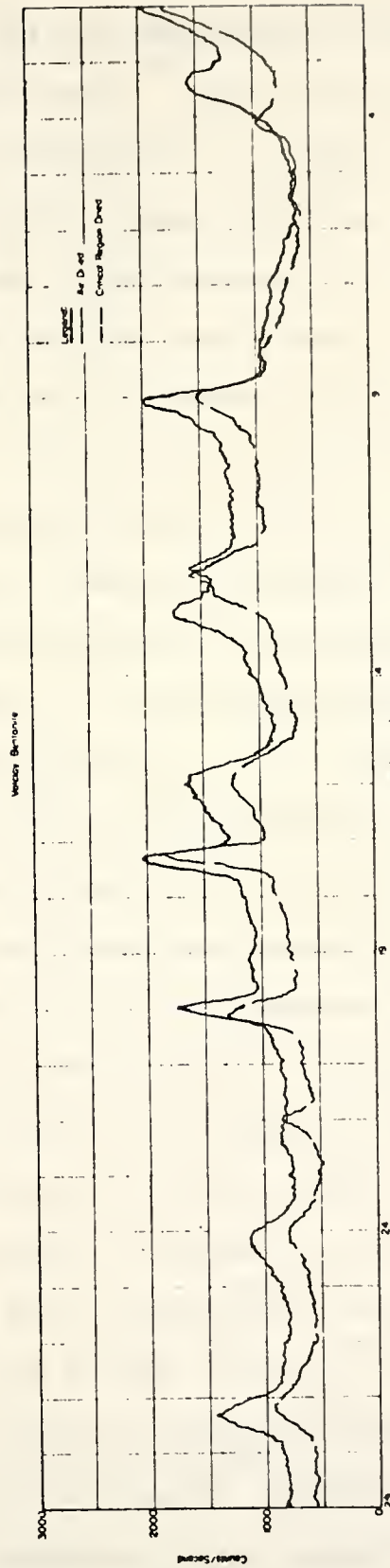


FIGURE 3-8 - X-RAY DIFFRACTOGRAMS OF AIR DRIED AND CRITICAL REGION DRIED VOLCANIC BENTONITE.

logarithmic scale, and the cumulative intrusion/gm of dry soil on an arithmetic scale. Such a plotting permits not only a convenient presentation of a range of diameters covering several orders of magnitude, but also a comparison of different pore size distributions for uniformity and for the relationships of certain pore sizes. The use of the logarithmic diameter scale, however, distorts the pore size distribution plots as the finer pore sizes exhibit a greater spread than that of an arithmetic plot.

The minimum pore diameter intruded in this study was limited by the maximum attainable pressure of about 15,000 psi in the porosimeter, and was approximately 0.016 micrometers. The maximum measurable pore diameter range was limited to between 600 and 150 micrometers, depending on the filling pressure range of 20 to 80 mm of mercury that was used. Most of the total pore space of the various samples was intruded within the pressure range of the equipment. The relatively small amount of unintruded porosity consisted either of "blind" pore space inaccessible to the sample surface or of pores of the range of size smaller than the minimum pore diameter intruded by the porosimeter.

Replicate pore size distribution determinations were generally made for all levels of the soil and compaction variables. It was observed that repeatability of the pore size distribution data was quite satisfactory. The pore size distribution data presented in the subsequent sections represent single but reliable determinations.

Influence of Soil Processing and Soil Mixing Artifacts on Pore Size Distribution

The possible influence of soil processing and soil mixing artifacts on pore size distribution could be evaluated using compacted samples of both unprocessed and processed Crosby silty clay. One portion of the soil was compacted completely without processing at its field moisture content of 24.4% by the Standard Proctor method (ASTM Designation: D 698-70, Method A). Another portion of the same soil was processed by air drying, pulverizing with a rubber-tipped pestle, and discarding the coarse material retained on the No. 40 U.S. Standard sieve. The processed soil was mixed with deionized water to a water content of 22.2% using the Patterson-Kelley twin-shell liquid-solids blender. The processed soil could not be mixed to the field moisture content, because water contents higher than about 23% resulted in a demonstrably non-uniform soil-water mix. The mix, made up of a spectrum of aggregation sizes, was cured in an atmosphere of nearly 100% relative humidity and at a constant temperature of approximately 21°C for about a week, and was then compacted by the Standard Proctor method (ASTM Designation: D 698-70, Method A). Specimens from the middle third layer of both compacted samples were critical region dried, and their pore size distributions determined. These are presented as cumulative intrusion curves in Figure V-9. The total porosity of the specimens indicated on the intrusion axis was obtained during the mercury

Standard Proctor Compaction
Critical Region Drying

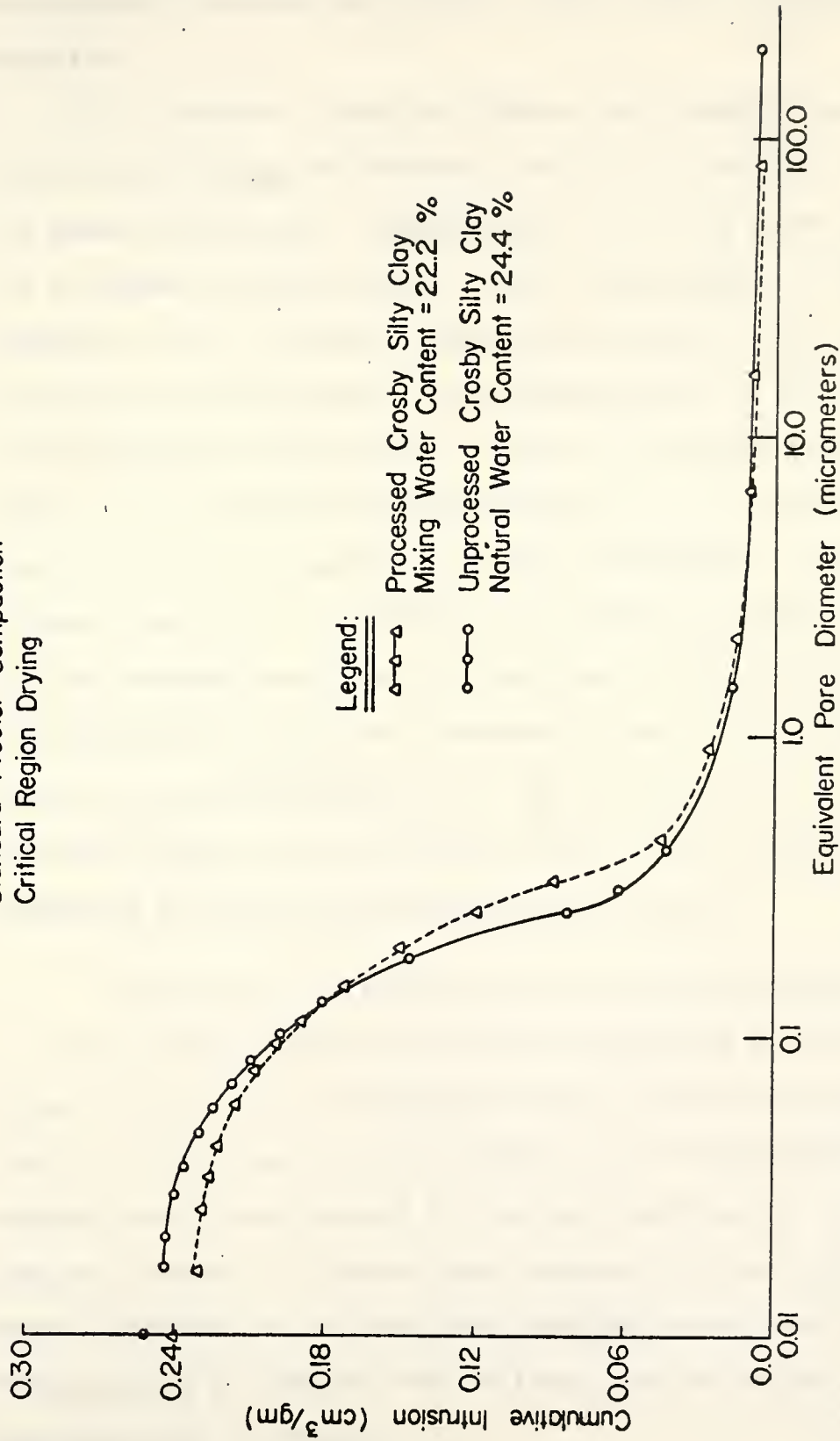


FIGURE V-9-CUMULATIVE INTRUSION CURVES FOR THE PROCESSED AND THE UNPROCESSED CROSBY SILTY CLAY COMPACTED AT THE MIXING AND THE NATURAL WATER CONTENTS OF 22.2 % AND 24.4 %, RESPECTIVELY, BY THE STANDARD PROCTOR METHOD.

porosimeter runs and was within $\pm 3\%$ of the "as-molded" porosity.

It is apparent from the Figure that despite the processing and mixing differences, the pore size distributions are almost identical. Essentially all of the pore space was intruded in both cases. Small differences in the distributions, i.e., a slightly less pore volume in the intermediate pore size range, i.e., between about 0.3 and 0.5 μm , and a slightly greater pore volume in the small pore size range, i.e., between about 0.025 and 0.1 μm , for the wetter sample, are to be expected for the differences in water content involved. The similarity of the pore size distributions demonstrates that the observed distributions do not significantly reflect soil processing and soil mixing artifacts but are representative of distributions that would be obtained after critical region drying field specimens compacted without such processing and mixing.

Pore Size Distributions of Soil Aggregations

Pore size distributions were determined for the space within individual soil aggregations, which were recovered from critical region dried samples of the aggregations. The samples were manufactured by tacking together of the aggregations formed at a given water content by low pressure static compaction, as described earlier under the section "Preparation of Samples for Critical Region Drying - Soil Aggregations" of Chapter IV.

Edgar Plastic kaolin and grundite aggregations formed at a number of water contents were studied for their pore size distributions. The cumulative intrusion curves for these aggregations are shown in Figures V-10 and V-11. The intrusion data in terms of pore content and percent distribution of space within the aggregations in equivalent pore diameter classes of 0.025 to 0.1, 0.1 to 0.4, 0.4 to 1.6, 1.6 to 6.4, and 6.4 to 25.6 μm are presented, respectively, in Tables A-1 and A-2 in Appendix A. These pore diameter classes, with the pore diameters varying by a factor of 4 in each class, were used for presentation in this study in preference to the pore diameter classes with pore diameters varying by a factor of 2, which were generally used for data analysis but were found to be inconvenient for tabular presentation. The space assigned to pore sizes below 0.025 μm in the above Tables consists of pore volume in pore sizes between about 0.016 and 0.025 μm and the unintruded pore volume. It is presumed that the unintruded pore volume could, in general, be reached with porosimeter of higher pressuring capacity. Table A-5 presents a division of total space into pore contents in pore sizes above and below 0.1 μm , and mean pore diameters of space in these sizes. This subdivision was dictated by relatively fixed pore content in pores smaller than 0.1 μm for each of the soils used, as will be seen later in this study.

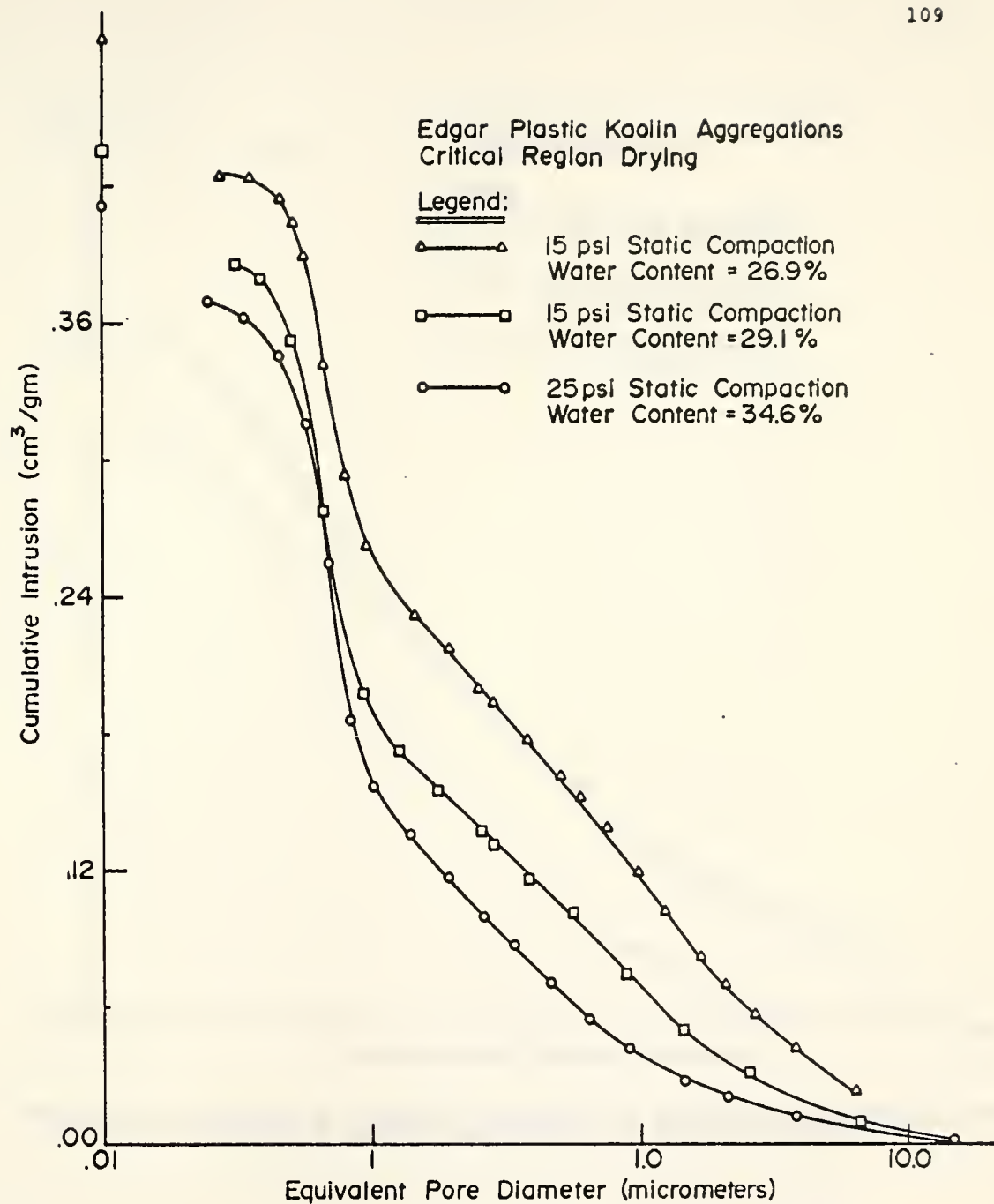


FIGURE V-10 - CUMULATIVE INTRUSION CURVES FOR EDGAR PLASTIC KAOLIN AGGREGATIONS FORMED AT THE MIXING WATER CONTENTS OF 26.9%, 29.1% AND 34.6%.

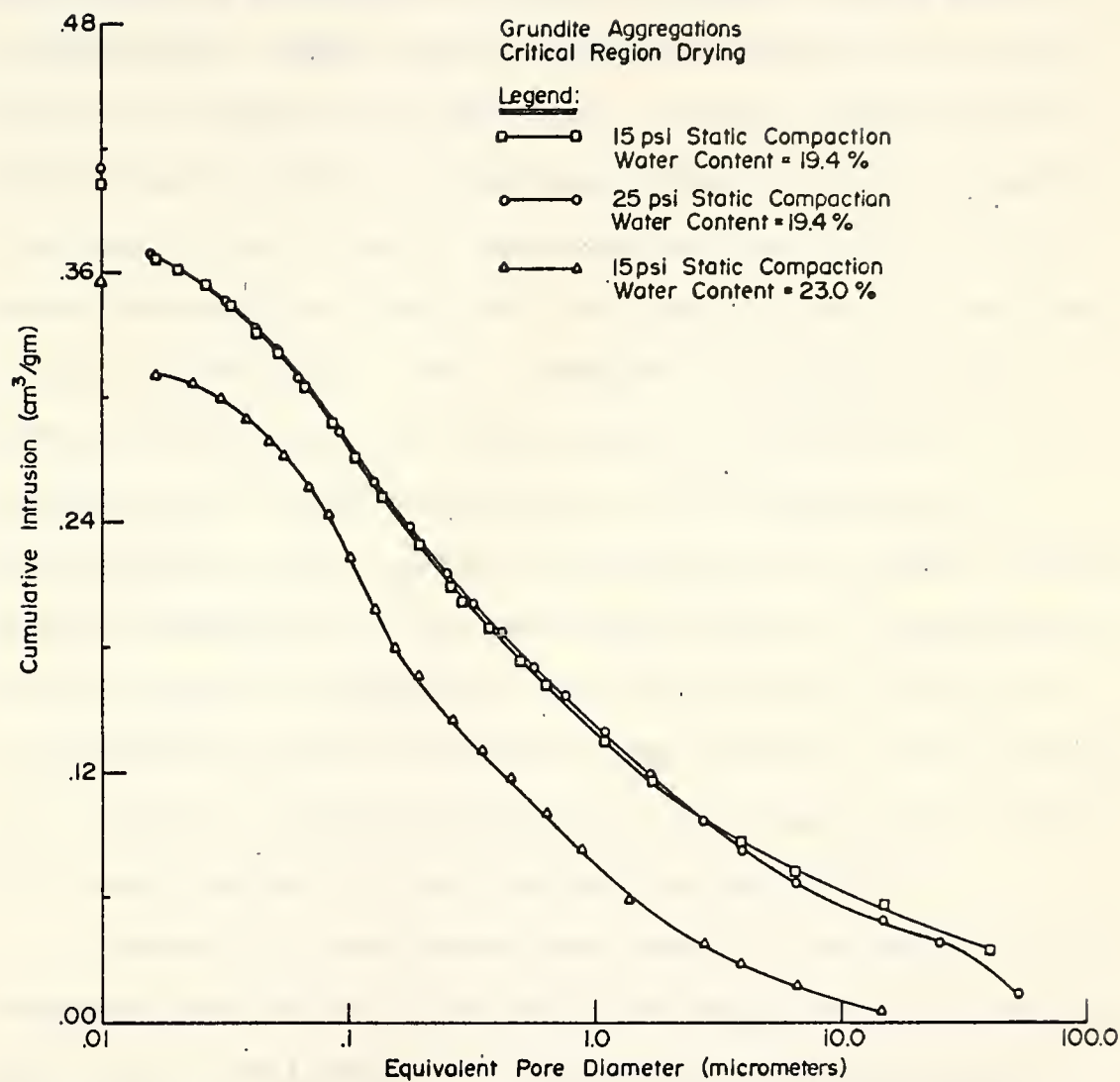


FIGURE V-II - CUMULATIVE INTRUSION CURVES FOR GRUNDITE AGGREGATIONS FORMED AT THE MIXING WATER CONTENTS OF 19.4% AND 23.0% .

The curves in Figures V-10 and V-11 and the data in Tables A-1, A-2, and A-5 indicate that Edgar Plastic kaolin and grundite aggregations formed at higher mixing water contents show lower total space, the reductions occurring mainly in large pore sizes, i.e., between 1 and 15 μm for Edgar Plastic kaolin and between 10 and 50 μm for grundite. The Edgar Plastic kaolin aggregations show for all of the water contents used similar size distributions of the space in pore sizes below 1 μm . Likewise, the grundite aggregations show basically similar size distributions of the space in pore sizes below about 2 μm , though these size distributions differ greatly from those of the Edgar Plastic kaolin aggregations. The unintruded space for aggregations of both soils is about 10%. The total space within the aggregations formed at a given water content is much higher than that of a sample of the same soil compacted at a similar water content by the Standard Proctor method.

Figure V-11 also shows that changing the modest static pressure from 15 to 25 psi has practically no effect on the pore size distribution of grundite aggregations formed at a water content of 19.4%.

Pore Size Distributions of Soils Compacted by the Standard Proctor Method

In this section, specimens of a number of soils compacted by the Standard Proctor method (ASTM Designation: D 698-70, Method A) at a number of water contents on both

sides of optimum were critical region dried, and their pore size distributions determined. The soils studied included Edgar Plastic kaolin, Crosby silty clay, Boston blue clay, grundite, and reddish-brown limestone residual clay. Pore size distributions of these soils will be presented as cumulative intrusion curves. The specimens of all of the soils used were observed to undergo only insignificant change in their "as-molded" porosity as a result of critical region drying, as discussed earlier under the section "Effects of drying Procedures." The total porosity indicated on the intrusion axis of the cumulative intrusion plots, therefore, represents the "as-molded" porosity of a soil compacted at a given water content. The pore size distribution data are also given in Tables A-3 and A-4 in terms, respectively, of pore content and percent pore space in equivalent standard pore diameter classes previously adopted. As indicated before, Table A-5 presents a division of total space into pore contents in pore sizes above and below $0.1\ \mu\text{m}$, and mean pore diameters of space in these sizes.

Edgar Plastic kaolin

Figures V-12 and V-13 present pore size distributions for Edgar Plastic kaolin compacted at a number of water contents on the dry side and on the wet side, respectively, of the Standard Proctor optimum (31.8%). The cumulative intrusion curves for different water contents are similar in shape. The distributions for water contents of 22.7 and

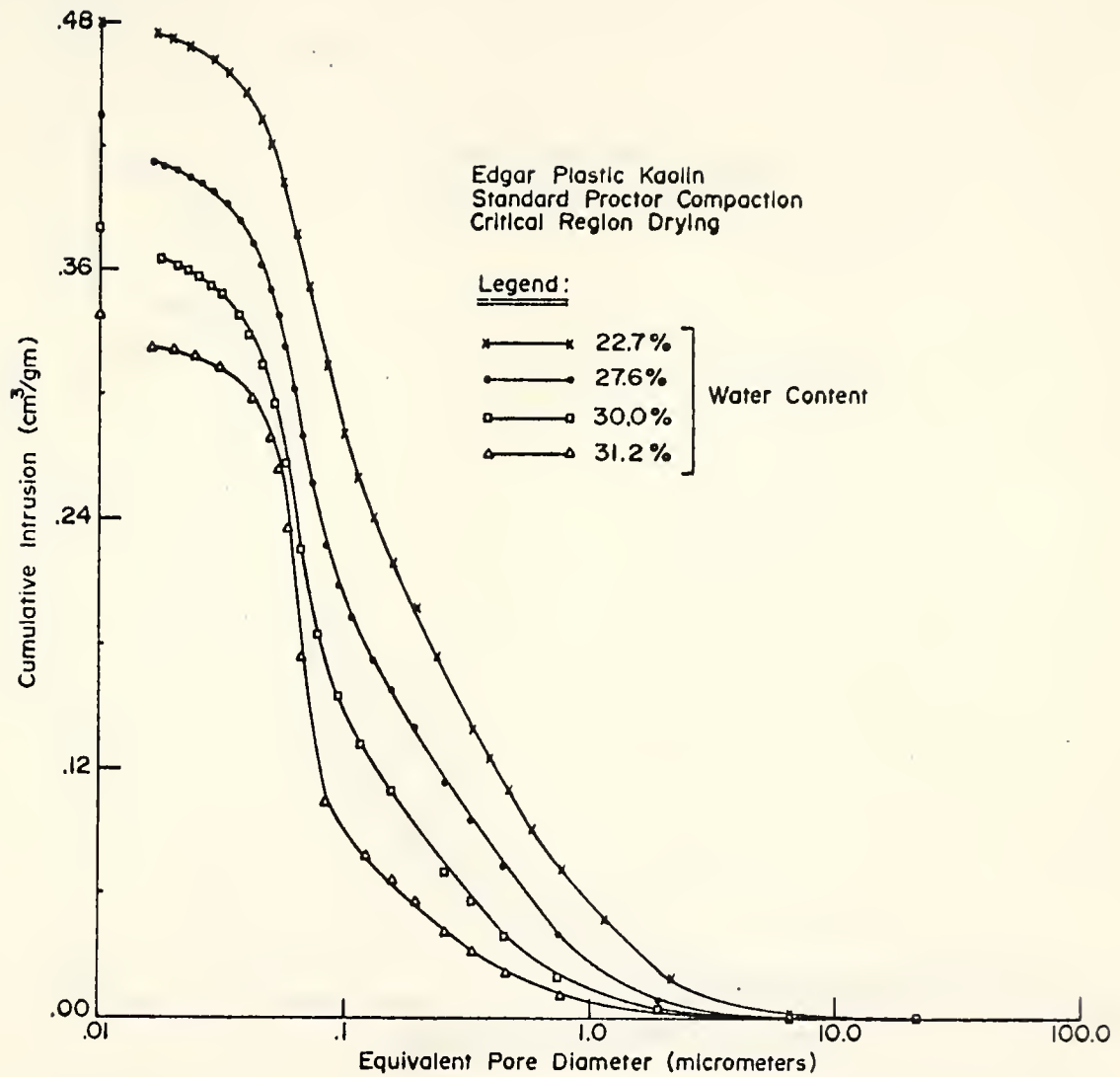


FIGURE V-12- CUMULATIVE INTRUSION CURVES FOR EDGAR PLASTIC KAOLIN COMPACTED AT DIFFERENT WATER CONTENTS BY THE STANDARD PROCTOR METHOD.

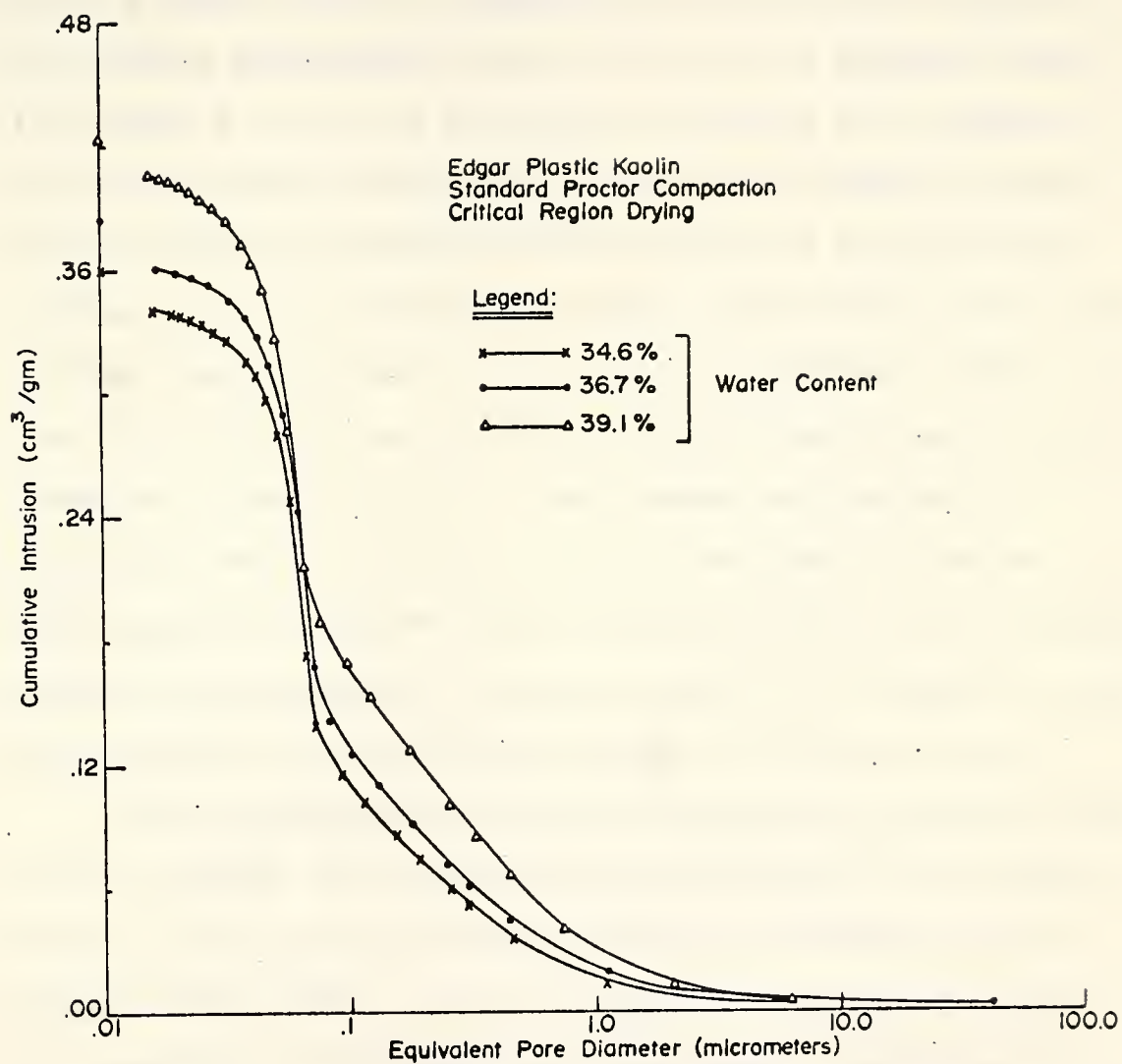


FIGURE V-13 - CUMULATIVE INTRUSION CURVES FOR EDGAR PLASTIC KAOLIN COMPACTED AT DIFFERENT WATER CONTENTS BY THE STANDARD PROCTOR METHOD.

27.6%, both on the dry side of the optimum, show four distinct slope regions (on the logarithmic diameter scale), i.e., a relatively flat slope for pore sizes above about 2 μm , a steep slope from about 2 to 0.1 μm , a steeper slope from about 0.1 to 0.05 μm , and a relatively flat slope for pore sizes below about 0.05 μm . The distributions for the rest of the water contents used also show 4 distinct slope regions, i.e., a flat slope for pore sizes above about 1 μm , a steep slope from about 1 to 0.08 μm , a steeper slope from about 0.08 to 0.05 μm , and a relatively flat slope for pore sizes below about 0.05 μm . The Figures and the data in Tables A-3 and A-4 indicate that all but about 5 percent of total space is intruded for all distributions in the pressure range of the equipment, and that roughly 75% or more of total space exists in the pore size range of 0.025 to 0.4 μm .

With increasing molding water contents on the dry side of the optimum, the cumulative distributions shift progressively to the left indicating increasing fineness and decreasing total space. These changes in the distributions are associated with significant progressive reductions in pore content largely in the pore size range between 0.1 and 2 μm and very small progressive increases in pore content in the pore size class of 0.025 to 0.1 μm . Calculated mean diameters for the part of total space in pore sizes above 0.1 μm exhibit a rather small reduction, i.e., from 0.32 to 0.23 μm , because compaction at successively increasing water

contents removes pores differentially, i.e., a greater content of pores is removed in smaller pore sizes. On the other hand, the mean pore diameters of the part of total space in sizes below $0.1\ \mu\text{m}$ are relatively consistent.

Above the optimum, total pore space increases with increasing moisture contents at compaction. These increases occur in pore sizes between 0.1 and $0.4\ \mu\text{m}$ for a water content of 34.6% and between 0.1 and $2\ \mu\text{m}$ for water contents of 36.7 and 39.1%.

Comparisons of interest can be made of the distributions for two parallel sets of specimens, viz., molding water contents of 30.0 and 36.7%, and 27.6 and 39.1%. Each set represents virtually identical total porosity obtained for compaction at water contents on either side of the optimum. The comparisons indicate that the dry-side samples exhibit greater space largely in the pore size range between 0.1 and $0.4\ \mu\text{m}$, and lesser space in pore sizes below $0.1\ \mu\text{m}$.

Crosby Silty Clay

Figures V-14 and V-15 show cumulative intrusion curves for Crosby silty clay compacted at a number of water contents on both sides of the Standard Proctor optimum (17.1%). It is apparent from the Figures and the data in Tables A-3 and A-4 that about 10 percent of the total space remains unintruded for each of the distributions. The distributions for compaction water contents of 13.4 and 15.6%, both on the dry

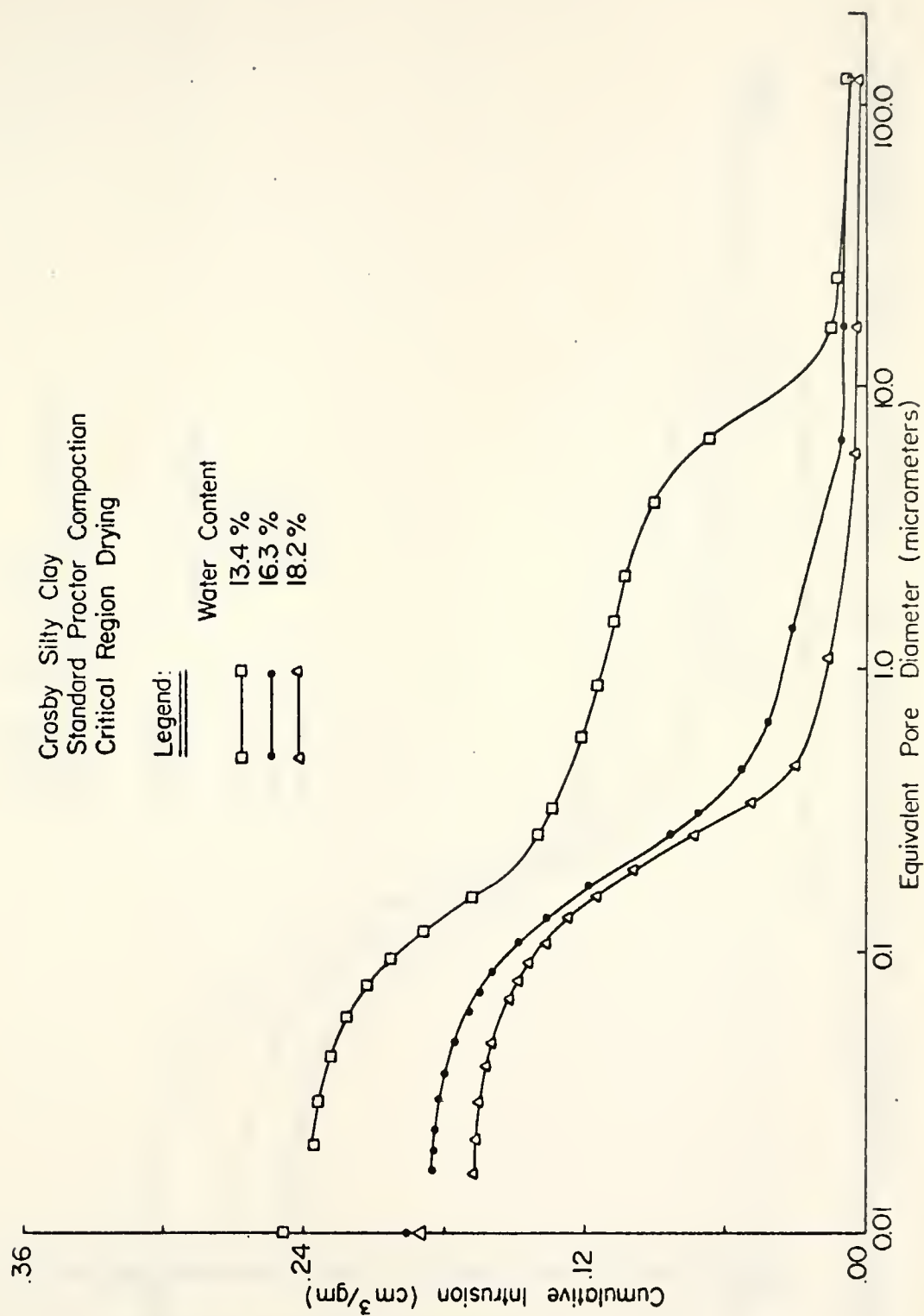


FIGURE V-14-CUMULATIVE INTRUSION CURVES FOR CROSBY SILTY CLAY COMPACTED AT DIFFERENT WATER CONTENTS BY THE STANDARD PROCTOR METHOD.

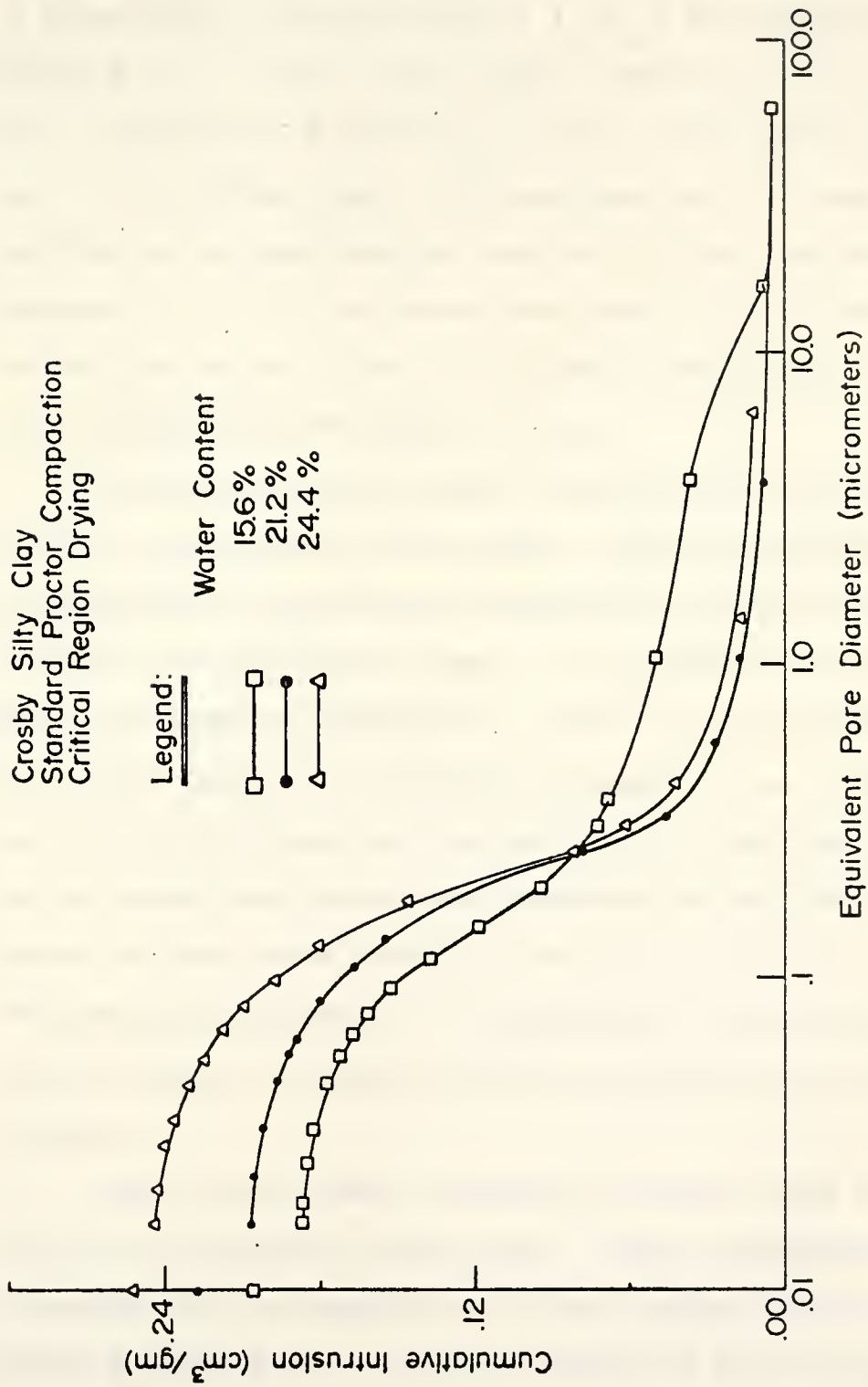


FIGURE V-15-CUMULATIVE INTRUSION CURVES FOR CROSBY SILTY CLAY COMPACTED AT DIFFERENT WATER CONTENTS BY THE STANDARD PROCTOR METHOD.

side of the optimum, show four distinct slope regions, i.e., a steep slope from about 20 to 4 μm , a flat slope from about 4 to 0.2 μm , a steep slope from about 0.2 to 0.1 μm , and a relatively flat slope for pore sizes below about 0.1 μm . On the other hand, the distributions for near-optimum and wet-of-optimum samples show only three distinct slope regions, i.e., a flat slope from about 4 to 0.4 μm , a steep slope from about 0.4 to 0.1 μm , and a relatively flat slope for pore sizes below about 0.1 μm .

Increasing molding water contents up to the optimum result in decreasing total space. These decreases are accompanied by significant progressive reductions of space in the large pore size range, i.e., between 4 and 20 μm , and small progressive increases of space in the intermediate pore size range, i.e., between 0.2 and 0.4 μm . These changes in the distributions are reflected by a significant reduction in the calculated mean pore diameters of the portion of total space in pore sizes above 0.1 μm , i.e., from 2.50 to 0.29 μm . The mean pore diameters of the portion of total space in pore sizes below 0.1 μm are relatively consistent for all distributions.

Above the optimum, increasing molding water contents result in increasing total space. These increases are reflections of the presence of greater space in pore sizes between 0.1 and 0.4 μm . The net effect of the increases is a small reduction in the mean pore diameters of the portion of total space in pore sizes above 0.1 μm .

Comparisons of the distributions for two parallel sets of specimens, each set exhibiting virtually identical total porosity, at compaction water contents of 13.4 and 24.4%, and 15.6 and 18.2% indicate that the dry-side samples exhibit greater space in the large pore size range and lesser space in the intermediate pore size range.

Boston Blue Clay

Figure V-16 presents cumulative intrusion curves for Boston blue clay compacted at a number of water contents on both sides of the Standard Proctor optimum (22.5%). The Figure shows that all but about 5 percent of the space is intruded for all distributions in the pressure range of the equipment. The distributions for compaction water contents of 15.0 and 19.6%, both on the dry side of the optimum, show three distinct slope regions, i.e., a steeper slope from about 1.5 to 0.2 μm , a steep slope from about 0.2 to 0.05 μm , and a relatively flat slope for pore sizes below about 0.05 μm . The distributions for near-optimum and wet-of-optimum samples also show three distinct slope regions, i.e., a flat slope from about 1.5 to 0.2 μm , a steep slope from about 0.2 to 0.05 μm , and a relatively flat slope for pore sizes below about 0.05 μm .

Decreasing total space results from increasing water contents up to the optimum. These decreases are accompanied by large progressive reductions of space in the intermediate pore size range, i.e., between 0.2 and 1.5 μm and small

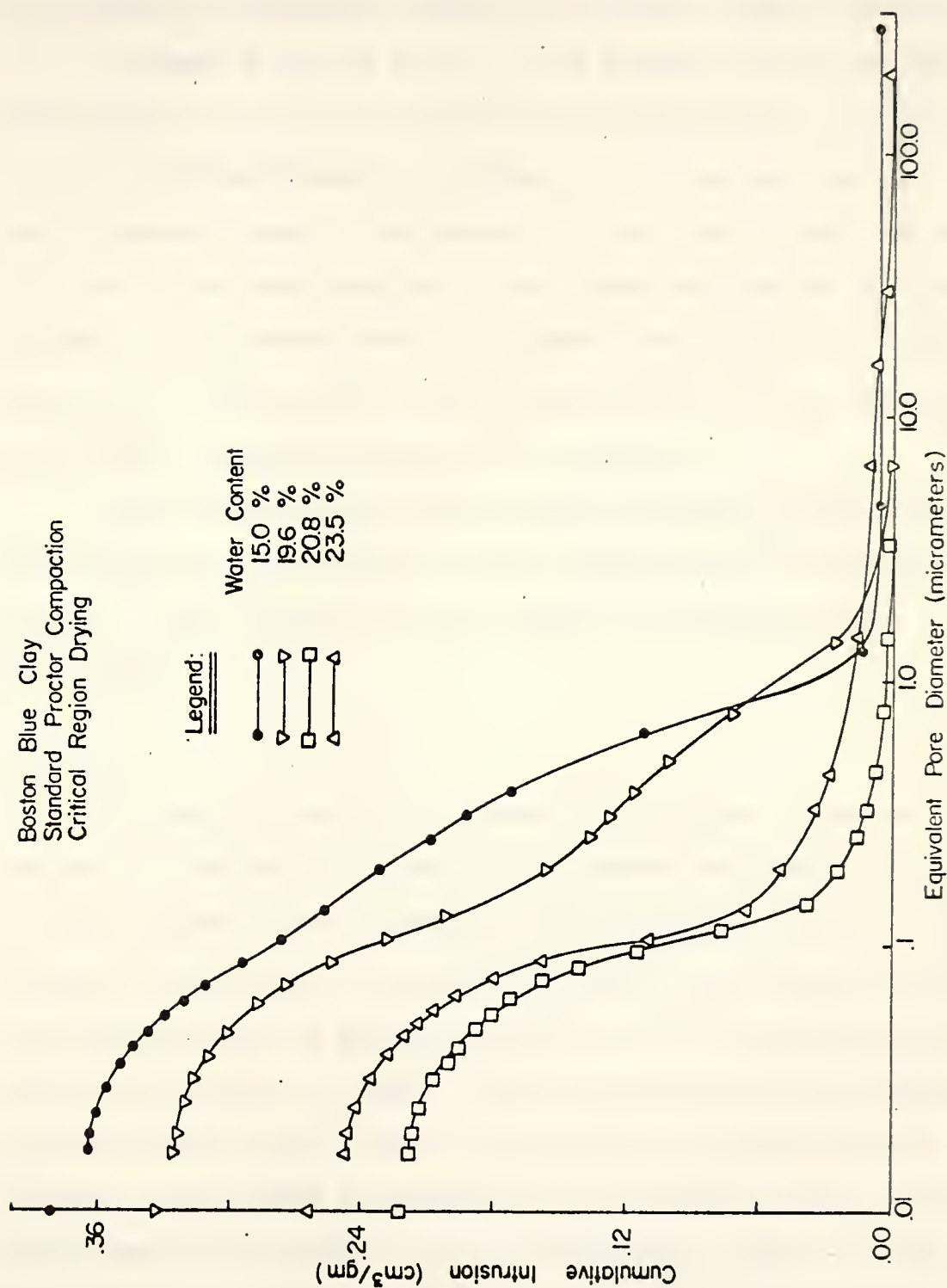


FIGURE V-16 - CUMULATIVE INTRUSION CURVES FOR BOSTON BLUE CLAY COMPACTED AT DIFFERENT WATER CONTENTS BY THE STANDARD PROCTOR METHOD.

progressive increases of space in the small pore size range, i.e., between 0.05 and 0.2 μm . The differences in the distributions are evident in terms of an appreciable reduction in the calculated mean pore diameters of the portion of total space in pore sizes above 0.1 μm , i.e., from 0.50 to 0.13 μm . The distribution of the finer portion of the pore system, as characterized by the mean pore diameter of the portion of total space in pore sizes below 0.1 μm , remains relatively unchanged for all distributions.

Above the optimum, total space increases slightly for an increase in compaction water content from the optimum to 23.5%. This increase occurs largely in the small pore size range.

Grundite

Figures V-17 and V-18 present cumulative intrusion curves for grundite compacted at a number of water contents on both sides of the Standard Proctor optimum (20.6%). The Figures and the data in Tables A-3 and A-4 show that there is unintruded space of about 15 percent. All distributions are basically similar in shape. The distributions for compaction water contents of 9.1 and 16.4%, both on the dry side of the optimum, show space continuously distributed in pore sizes below about 3 and about 1 μm , respectively. For the rest of the compaction water contents used, space is continuously distributed in pore sizes below about 0.2 μm .

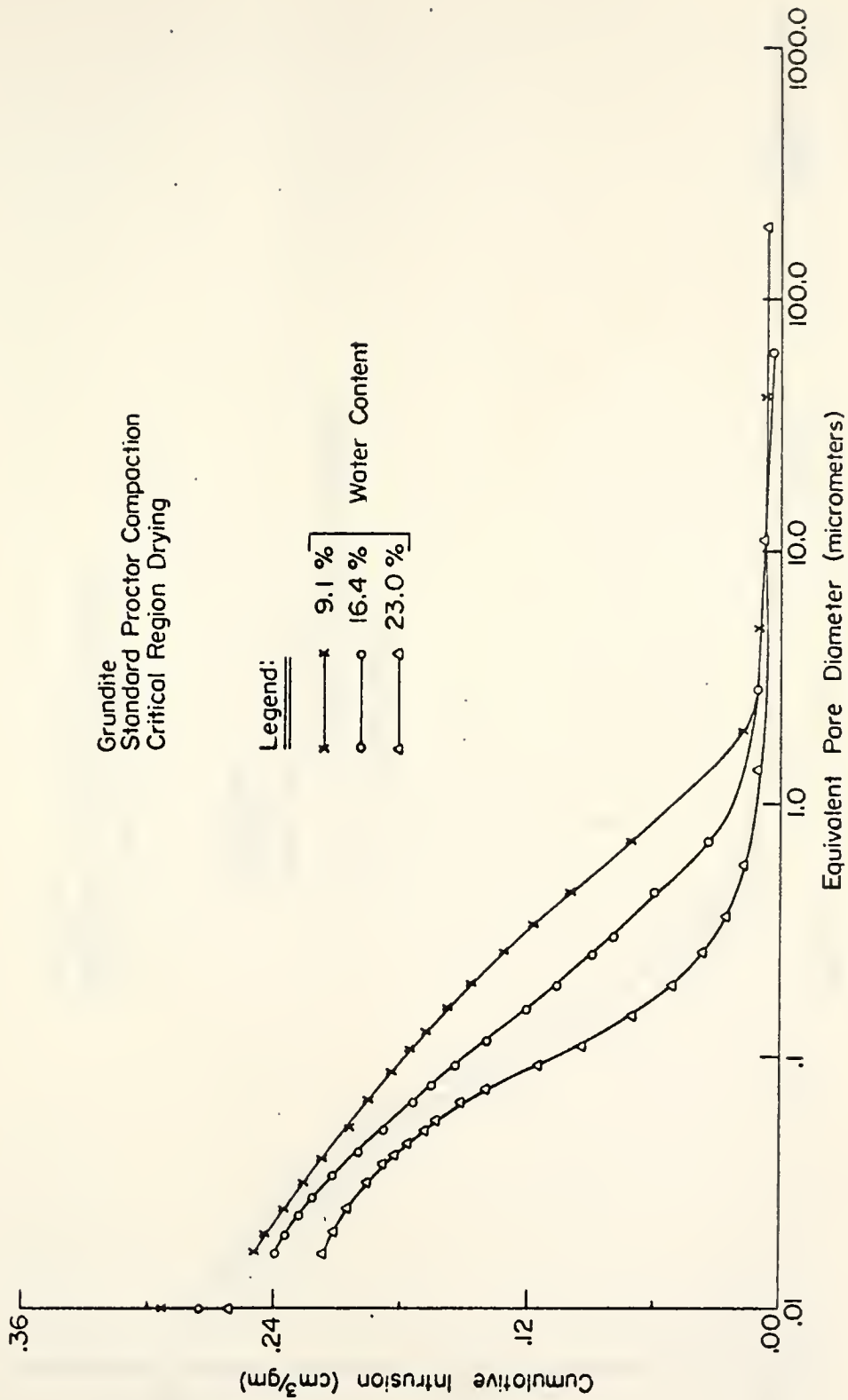


FIGURE X-17 - CUMULATIVE INTRUSION CURVES FOR GRUNDITE COMPACTED AT DIFFERENT WATER CONTENTS BY THE STANDARD PROCTOR METHOD.

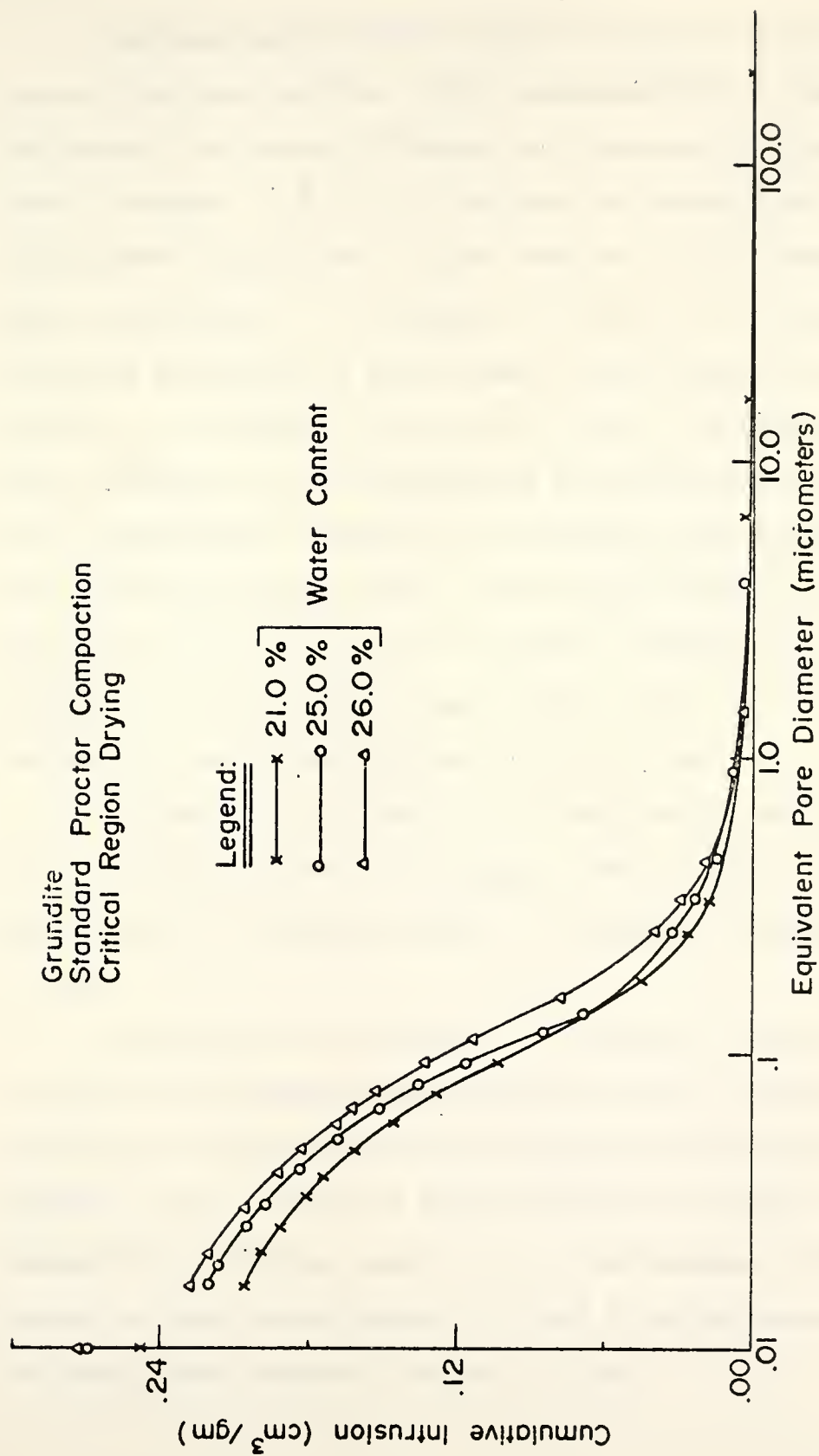


FIGURE V - 18 - CUMULATIVE INTRUSION CURVES FOR GRUNDITE COMPACTED AT DIFFERENT WATER CONTENTS BY THE STANDARD PROCTOR METHOD.

With increasing molding water contents up to the optimum, the distributions shift progressively to the left indicating increasing fineness and decreasing total space. These changes in the distributions are associated with large progressive reductions in pore content in the intermediate pore size range, i.e., between 0.2 and 3 μm , and small progressive increases of pore space in the small pore size range, i.e., between 0.025 and 0.1 μm . The reductions of pore content in the intermediate pore sizes are reflected by an appreciable reduction in the mean pore diameters of the portion of total space in pore sizes above 0.1 μm , i.e., from 0.51 to 0.17 μm . The mean pore diameters of the portion of total space in pore sizes below 0.1 μm are relatively consistent for all distributions.

Increasing total space results from increasing compaction water contents above the optimum. These increases are reflections of increasing space in pore sizes between 0.2 and 0.8 μm .

A comparison of interest can be made of the distributions for specimens exhibiting virtually identical total porosity at compaction water contents on either side of the optimum, such as at 16.4 and 25.0% water contents. The comparisons indicate that the dry-side samples show greater space in pore sizes between 0.2 and 3 μm and lesser space in pore sizes between 0.05 and 0.2 μm .

Reddish-Brown Limestone Residual Clay

Cumulative intrusion curves for reddish-brown limestone residual clay compacted at only three moisture contents, one at optimum (21.8%) and the others on either side of it are given in Figure V-19. Specimens at additional compaction moisture contents could not be prepared due to availability of only a limited quantity of the soil sample. It is apparent that about 9 to 18 percent of total space remains unintruded for distributions corresponding to compaction water contents increasing from 16.1 to 28.1%.

Again decreasing total space results from compaction water content increasing to the optimum and here again this decrease is associated with elimination of large pores. In this case at the low moisture content (16.1%) there is a continuous distribution of pores ranging in diameter from more than 100 μm to about 0.2 μm ; these are virtually eliminated on raising the compaction moisture content to the Standard Proctor optimum. There is also a small increase of space in the pore size class of 0.05 to 0.1 μm .

Above the optimum, there is again observed an increase in total space with increasing water content. Here this increase is associated with an increase in space in pore sizes below 0.2 μm .

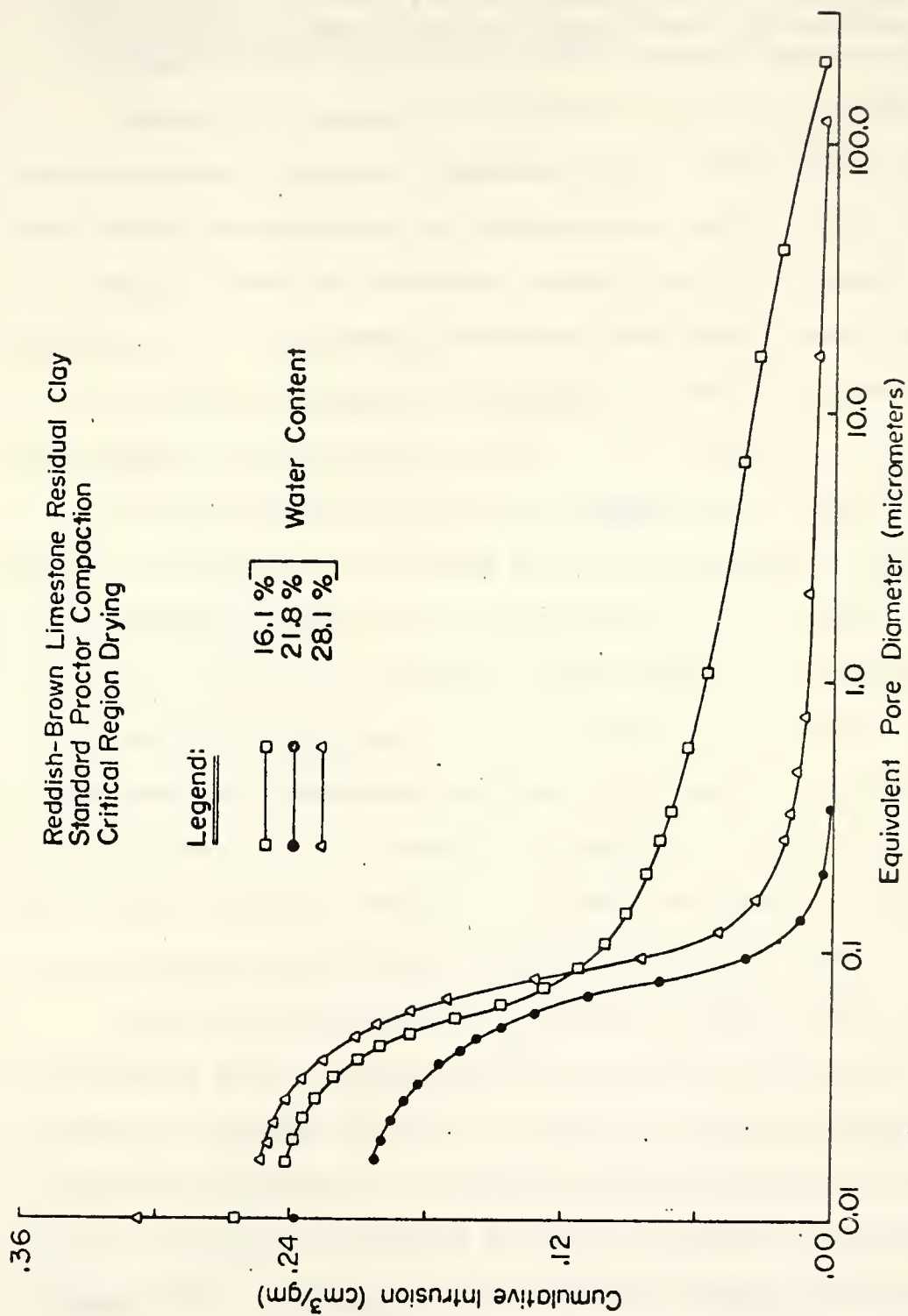


FIGURE X-19 - CUMULATIVE INTRUSION CURVES FOR REDDISH-BROWN LIMESTONE RESIDUAL CLAY COMPACTED AT DIFFERENT WATER CONTENTS BY THE STANDARD PROCTOR METHOD.

Comparisons of Pore Size Distributions of Different Soils
Compacted to Approximately Equal Total Porosities at
Different Water Contents by the Standard Proctor Method

Figure V-20 presents cumulative intrusion curves for reddish-brown limestone residual clay, Crosby silty clay, and grundite compacted to approximately equal total porosity at roughly identical moisture conditions with respect to optimum, i.e., the water contents considered range from about 75 to 80% of the respective optimums. The unintruded space for these distributions is about 15% or less.

The pore size distributions appear quite dissimilar. Most of the space for Crosby silty clay occurs in the two distinct pore size ranges of about 4 to 20 μm and of about 0.1 to 0.2 μm . For grundite, essentially all the space is distributed continuously in pore sizes below about 1 μm . For reddish-brown limestone residual clay, about one-third of the total space is distributed continuously in pore sizes between more than 100 μm to about 0.1 μm and the rest is confined to a narrow pore size range of about 0.025 to 0.1 μm .

Pore size distribution curves for Edgar Plastic kaolin and Boston blue clay compacted to virtually identical total porosity at water contents on the dry side of optimum, but representing dissimilar moisture conditions with reference to the respective Standard Proctor optimums, are given in Figure V-21. The unintruded space for these distributions is only about 5%. The distribution for Boston blue clay is coarser than that for Edgar Plastic kaolin, as is indicated

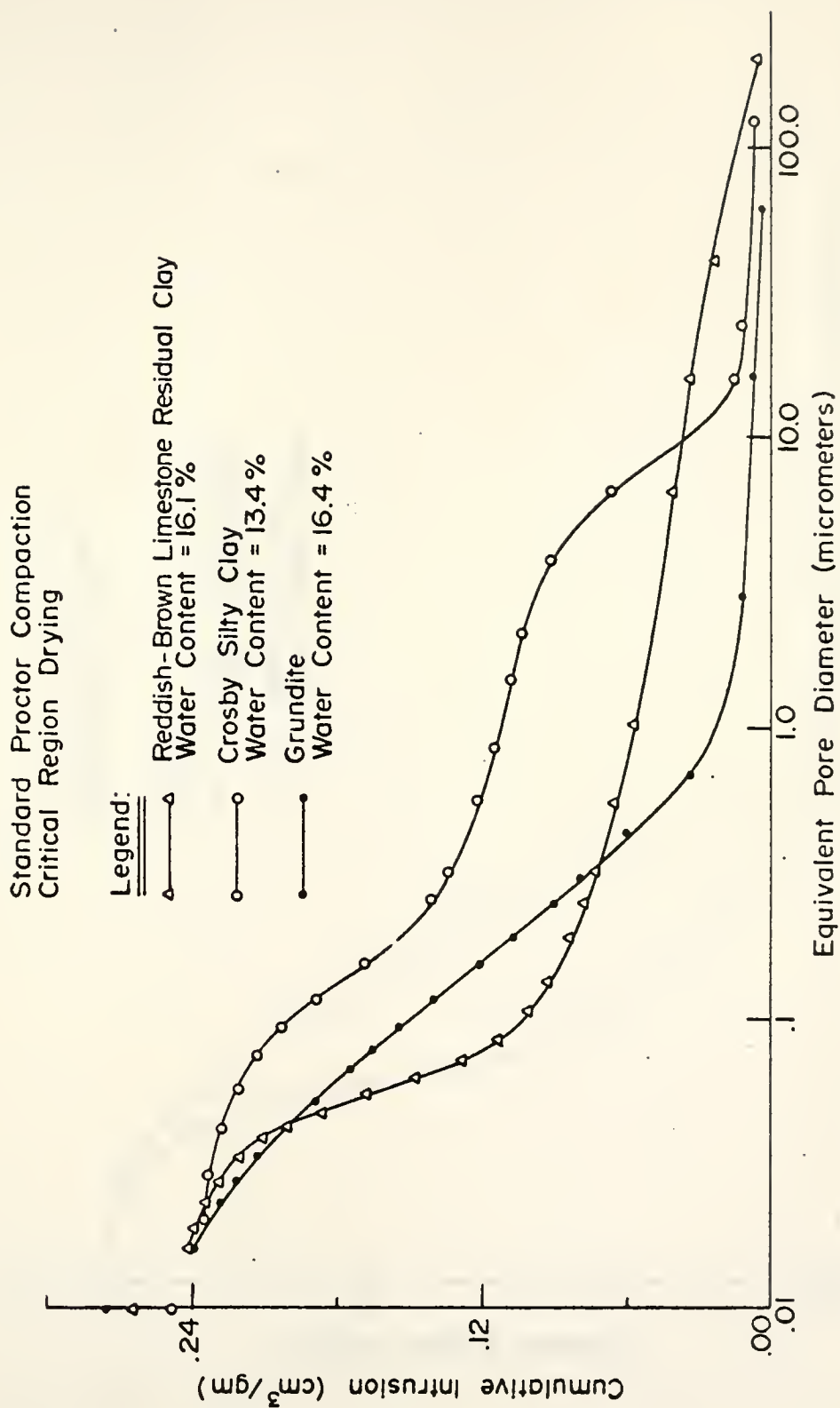


FIGURE Y-20- CUMULATIVE INTRUSION CURVES FOR REDDISH-BROWN LIMESTONE RESIDUAL CLAY, CROSBY SILTY CLAY AND GRUNDITE COMPACTED BY THE STANDARD PROCTOR METHOD AT THE WATER CONTENTS DRY OF THE OPTIMUM.

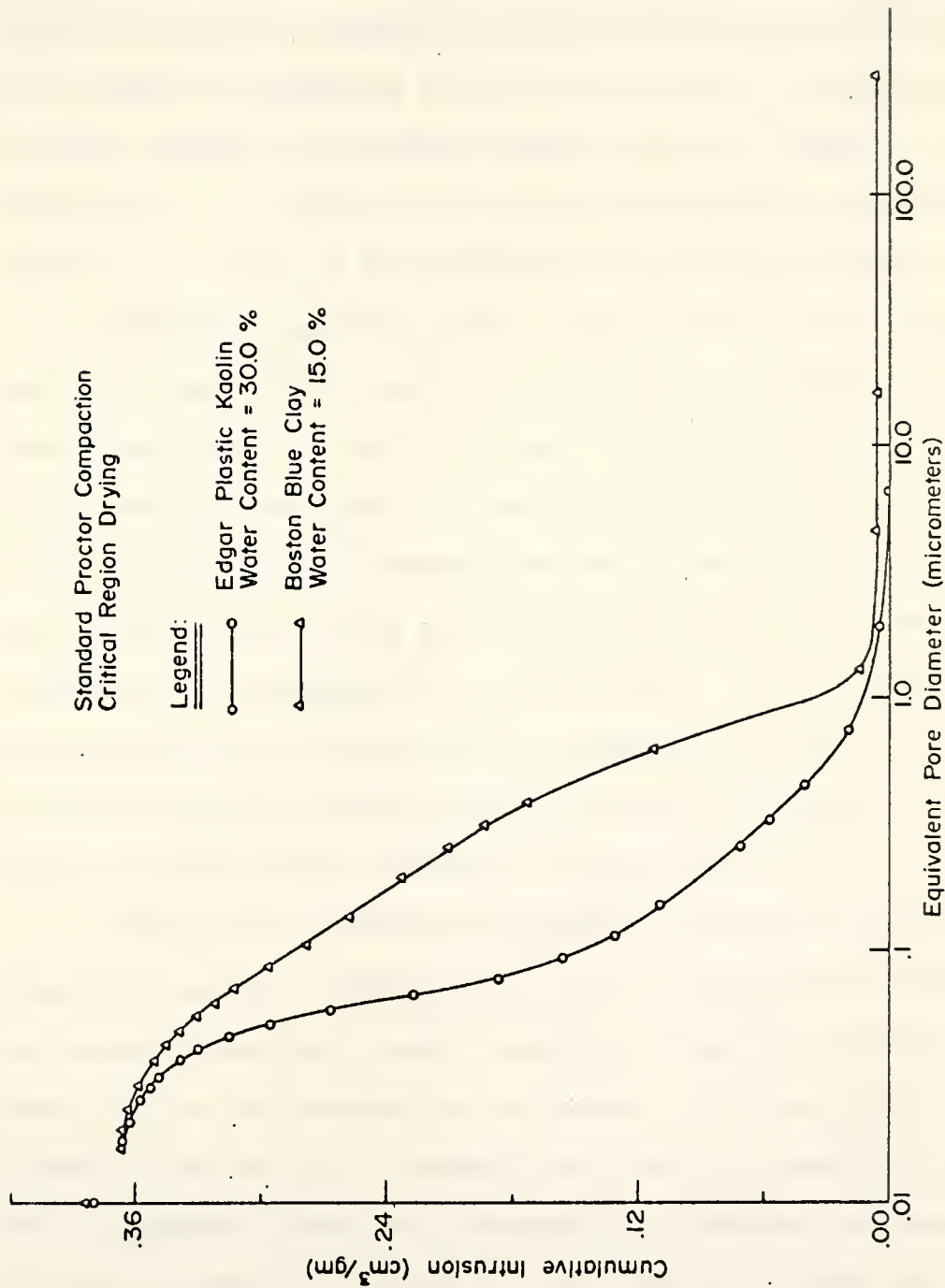


FIGURE V-21 - CUMULATIVE INTRUSION CURVES FOR EDGAR PLASTIC KAOLIN AND BOSTON BLUE CLAY COMPACTED BY THE STANDARD PROCTOR METHOD TO AN APPROXIMATE VOID RATIO OF 1.03 AT THE MOISTURE CONTENTS DRY OF THE OPTIMUM.

by the presence of a greater content of pores in sizes between about 0.2 and 1.5 μm .

Figure V-22 shows cumulative intrusion curves for Boston blue clay, reddish-brown limestone residual clay, and grundite compacted to about equal total porosity at roughly identical moisture conditions with respect to optimum, i.e., the water contents considered range from about 93 to 102% of the respective Standard Proctor optimums. The unintruded space is about 15% or less. For all distributions, essentially all of the space is confined to pore sizes smaller than about 0.4 μm . The differences in the distributions are small. The distribution for grundite is coarser than that of reddish-brown limestone residual clay, as is indicated by the presence of a greater content of pores in sizes between 0.1 and 0.4 μm . The distribution for Boston blue clay differs only slightly from that of reddish-brown limestone residual clay in having a slightly greater space in pore sizes between 0.1 and 0.2 μm .

Figure V-23 presents cumulative intrusion curves for Boston blue clay, Crosby silty clay, and grundite compacted to almost identical total porosity at water contents on the wet side of the respective optimums. The distribution for Crosby silty clay is coarser than that for Boston blue clay, as is apparent from the presence of a greater content of pores in sizes between 0.15 and 0.4 μm . The distribution for Boston blue clay exhibits a greater content of pores in

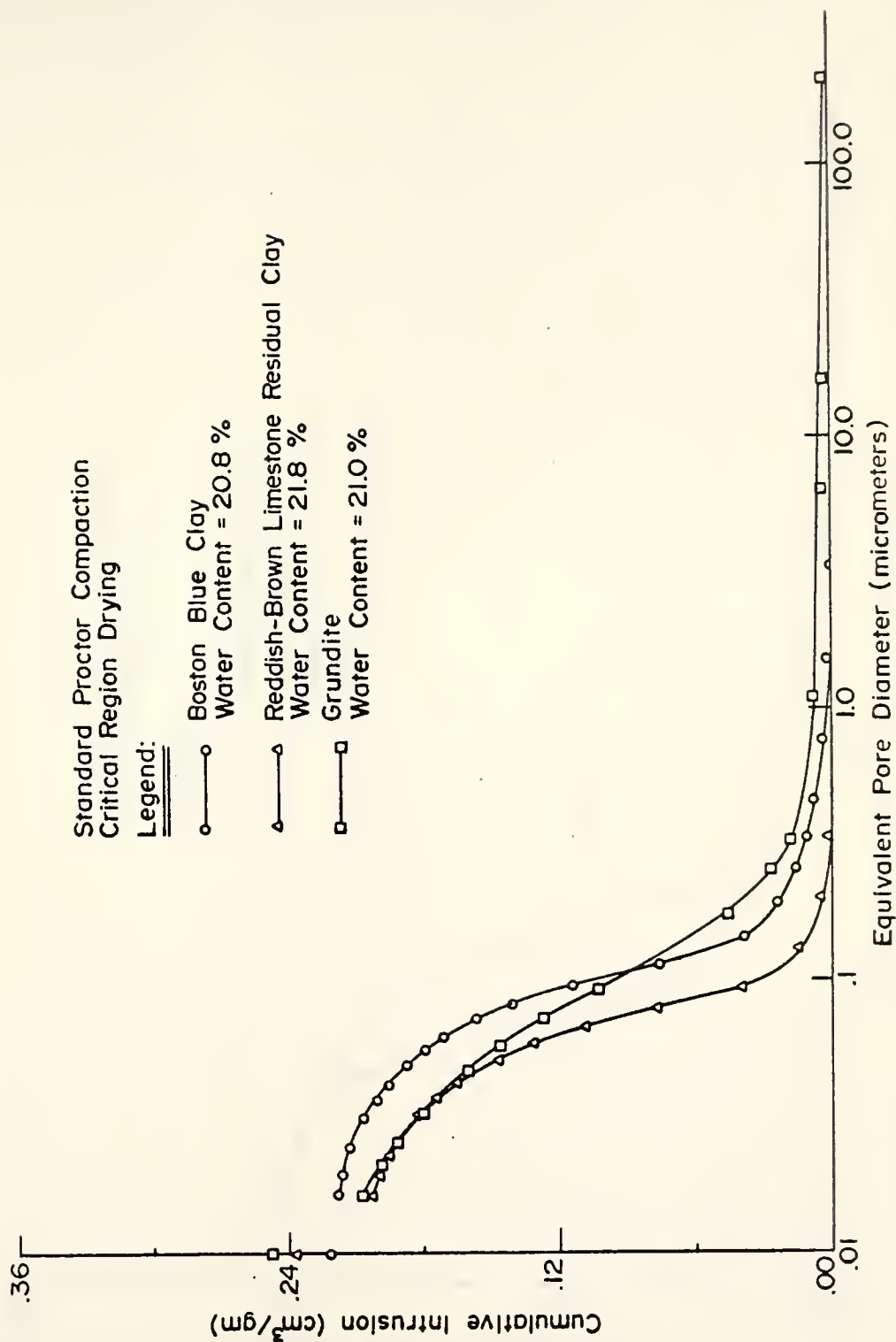


FIGURE V-22-CUMULATIVE INTRUSION CURVES FOR BOSTON BLUE CLAY, REDDISH-BROWN LIMESTONE RESIDUAL CLAY, AND GRUNDITE COMPACTED BY THE STANDARD PROCTOR METHOD AT THE WATER CONTENTS NEAR THE OPTIMUM.

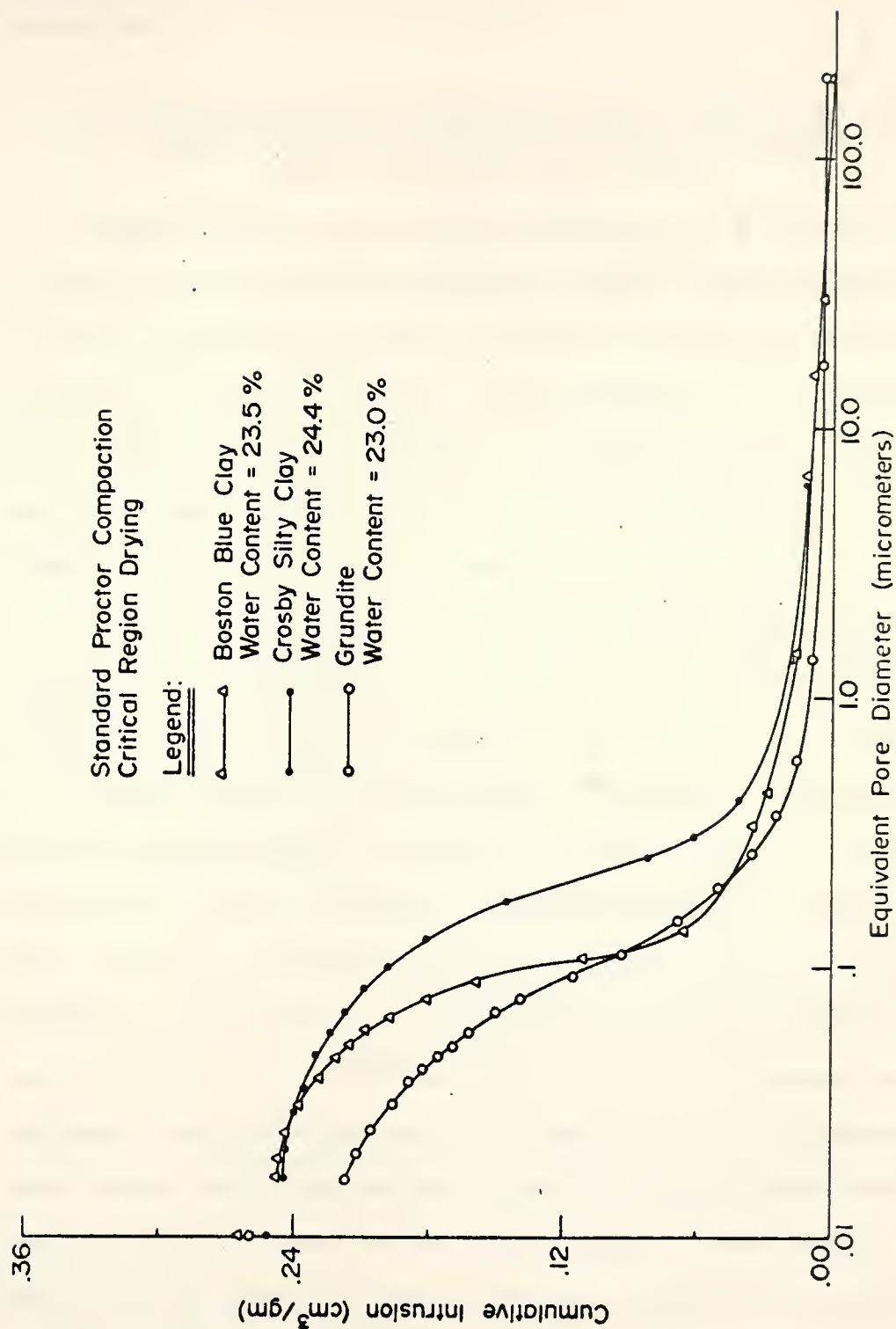


FIGURE V-23- CUMULATIVE INTRUSION CURVES FOR GRUNDITE, BOSTON BLUE CLAY, AND CROSBY SILTY CLAY COMPACTED AT THE WATER CONTENTS WET OF THE OPTIMUM BY THE STANDARD PROCTOR METHOD.

sizes between 0.05 and 0.2 μm that than apparent for grundite.

Pore Size Distributions of Edgar Plastic Kaolin
Compacted by the Modified Proctor Method
and by Methods Based on It

Edgar Plastic kaolin was compacted at a number of water contents by the Modified Proctor method (ASTM Designation: D 1557-70, Method A) and by methods based on it but using either 6 or 12 blows/layer. These methods of compaction were used to study the effect of varying applied energy in terms of number of blows/layer on total space and on size distribution of the total space.

Cumulative intrusion curves for Edgar Plastic kaolin compacted at a number of water contents by the Modified Proctor method and by the methods based on it but using 12 or 6 blows/layer are presented in Figures V-24 through V-27. The optimum moisture contents are 27.4, 29.5, and 32.6% in the order of the compaction methods mentioned. The intrusion data are also presented in Tables A-6 and A-7 in terms, respectively, of pore content and percent distribution of space in equivalent standard pore diameter classes previously adopted. Table A-8 shows the division of total space in pore sizes above and below 0.1 μm along with mean pore diameters of both parts of the total space. The results show that all but about 5 percent of total space is intruded for all distributions. It is also apparent that about half of the total space is present in pore sizes between 0.05 and

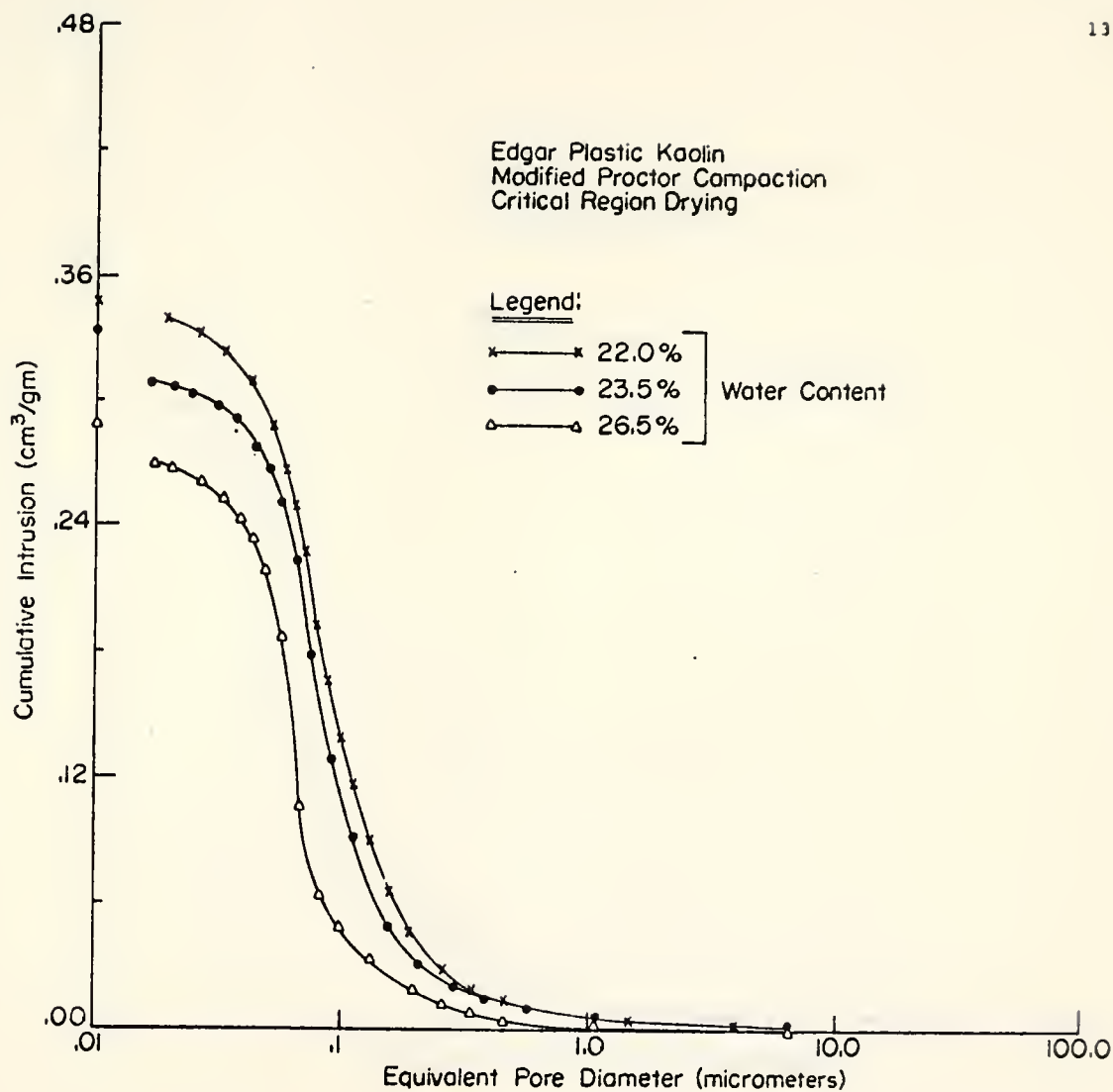


FIGURE IX-24 - CUMULATIVE INTRUSION CURVES FOR EDGAR PLASTIC KAOLIN COMPACTED AT DIFFERENT WATER CONTENTS BY THE MODIFIED PROCTOR COMPACTION METHOD.

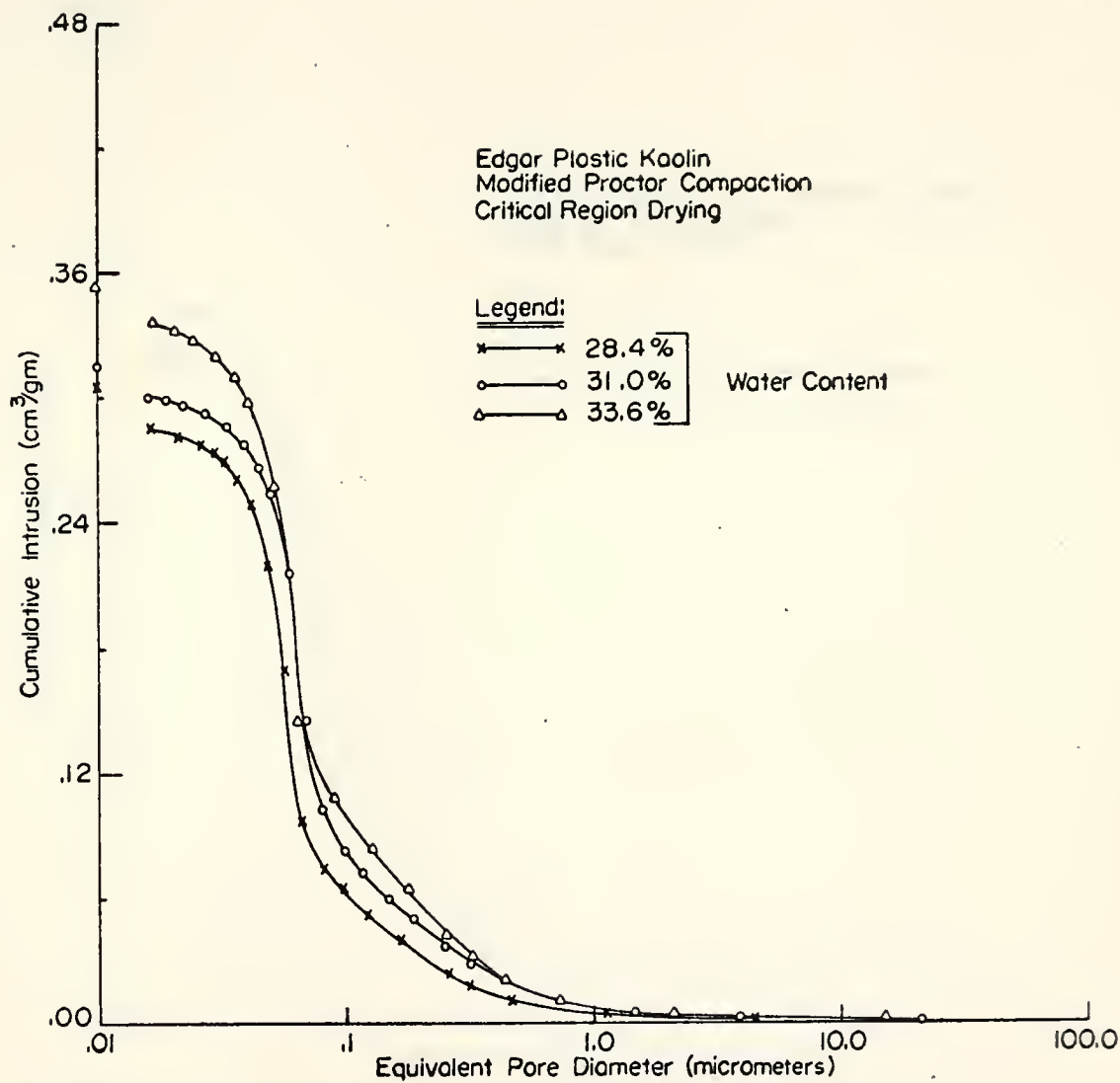


FIGURE V-25 - CUMULATIVE INTRUSION CURVES FOR EDGAR PLASTIC KAOLIN COMPACTED AT DIFFERENT WATER CONTENTS BY THE MODIFIED PROCTOR COMPACTION METHOD.

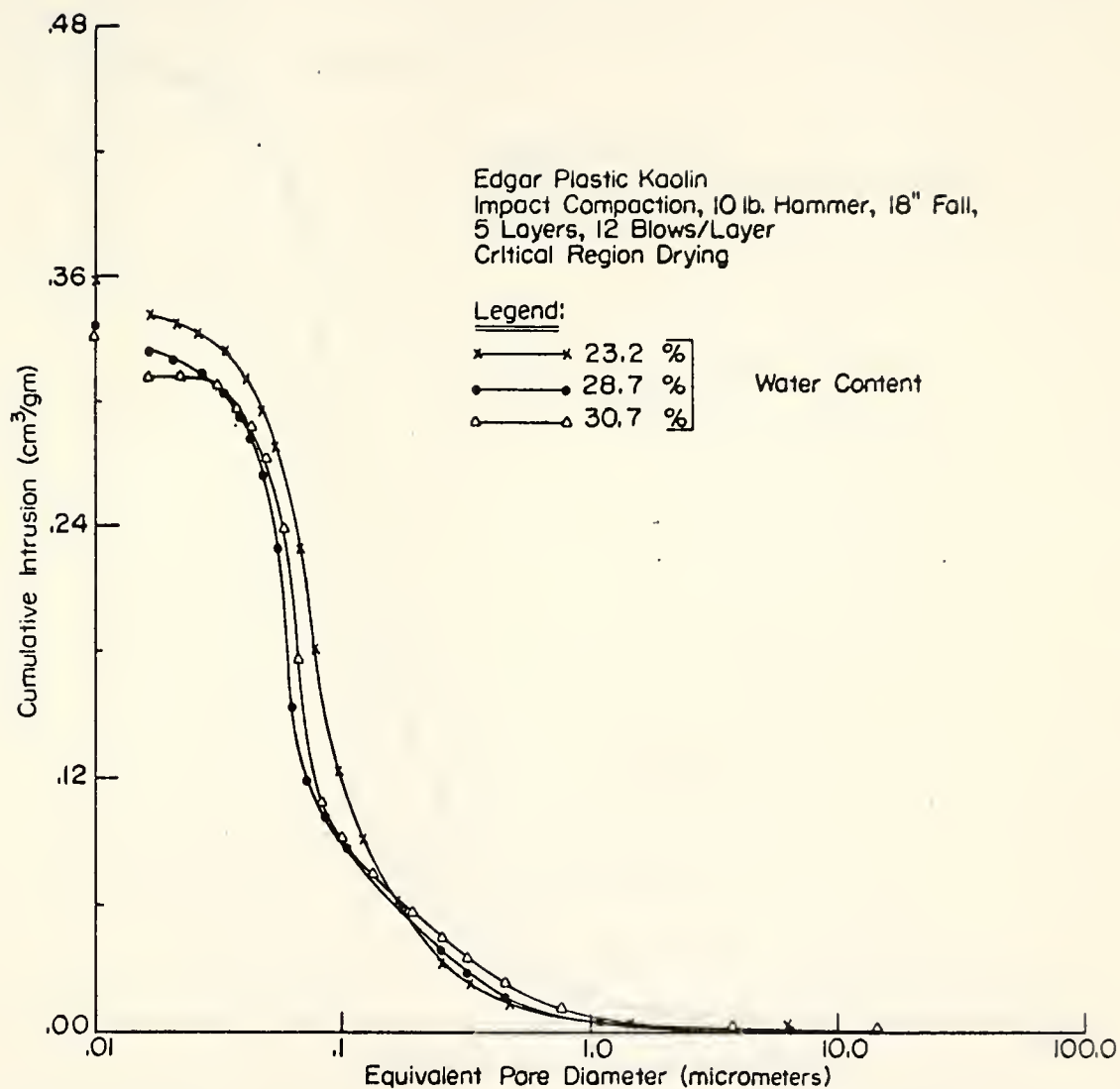


FIGURE V-26 - CUMULATIVE INTRUSION CURVES FOR EDGAR PLASTIC KAOLIN COMPACTED AT DIFFERENT WATER CONTENTS BY IMPACT COMPACTION WITH 10 LB. HAMMER, 18" FALL AND 12 BLOWS/ LAYER ON 5 LAYERS.

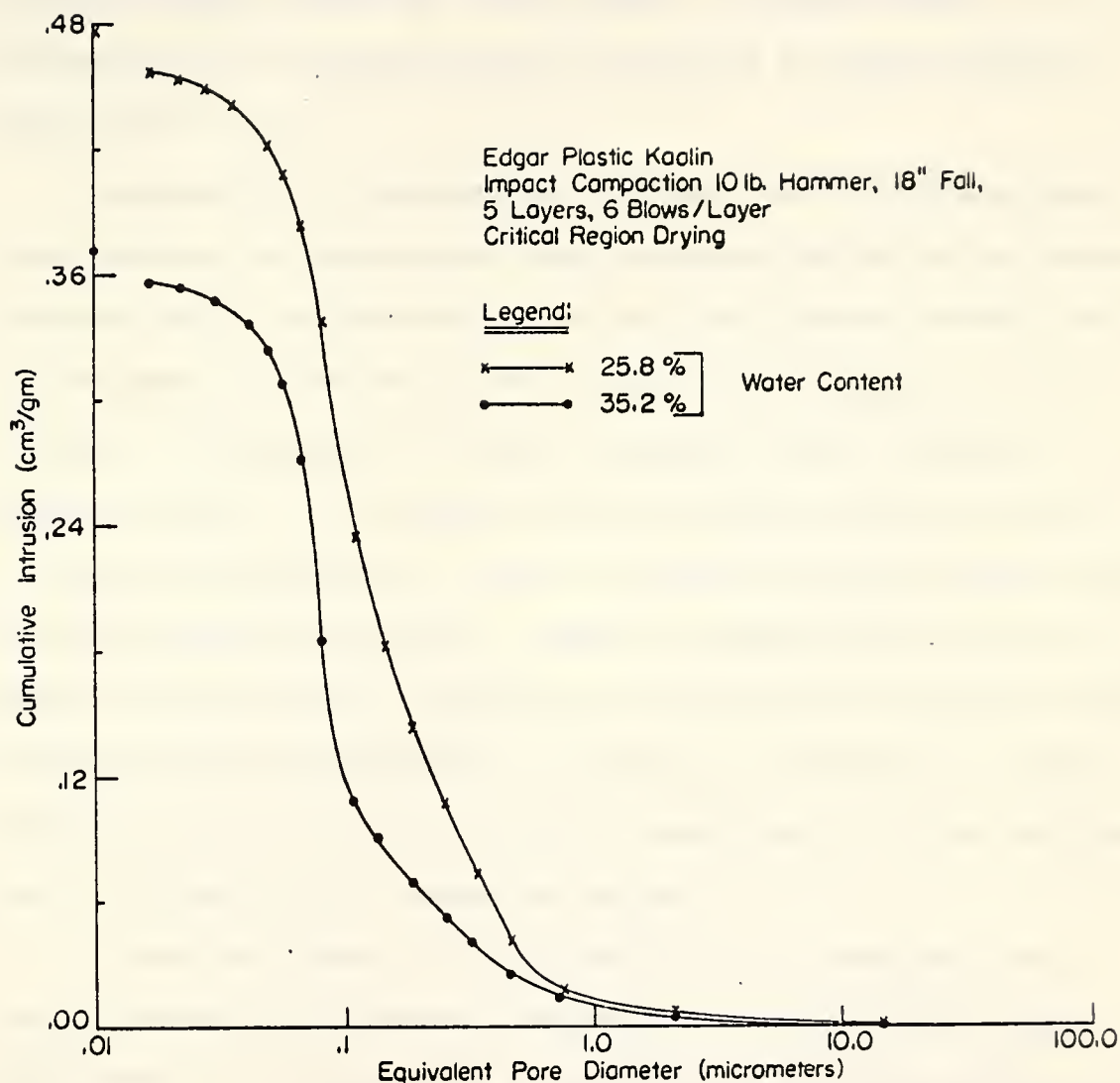


FIGURE V-27 - CUMULATIVE INTRUSION CURVES FOR EDGAR PLASTIC KAOLIN
COMPACTED AT DIFFERENT WATER CONTENTS BY IMPACT
COMPACTION METHOD USING 10 LB. HAMMER, 18" FALL AND 6 BLOWS/LAYER
ON 5 LAYERS.

0.08 μm at near-optimum (on dry side of optimum) and wet-of-optimum water contents for the Modified Proctor method and the method based on it but using 12 blows/layer. Essentially all of the space is confined to pores smaller than about 0.4 μm .

The pattern of changes in the pore size distributions with respect to compaction water contents exhibited by Edgar Plastic kaolin compacted by the Modified Proctor method and by the method based on it but using 12 blows/layer is consistent with that of the soil compacted by the Standard Proctor method. The magnitude of reduction of pore content in pore sizes above 0.1 μm with increasing water contents up to the optimum is, however, small in comparison to that for Edgar Plastic kaolin compacted by the Standard Proctor method. The mean pore diameters of the part of total space in pore sizes below 0.1 μm are relatively consistent, as was observed for Standard Proctor compacted soils.

Since the intent of this section is to evaluate the effectiveness of different compaction methods, pore size distributions of specimens prepared by different methods at about equal water contents will be compared with one another.

A comparison of the pore size distributions of two specimens, one compacted at a water content of 22.0% by the Modified Proctor method and the other at a water content of 22.7% by the Standard Proctor method, shows that a finer distribution with greatly reduced total space is obtained

for the Modified Proctor compacted sample. This reduction in total space is associated with significantly lesser space in pore sizes between 0.2 and 6.5 μm , which is reflected by a significant reduction in the mean pore diameter of the portion of space in pore sizes above 0.1 μm .

A specimen of Edgar Plastic kaolin compacted at a water content of 25.8% by 6 blows/layer in the Modified Proctor-based method exhibits much higher total space in comparison to that of a specimen compacted at a water content of 26.5% by the Modified Proctor method. The resulting differences in distribution are associated with lesser space in the intermediate pore size range, i.e., between 0.08 and 0.8 μm , for compaction at the high energy level. Because compaction at the high energy level removes pores differentially, i.e., a greater content of pores is removed in smaller pore sizes, the mean pore diameter of the portion of space in pore sizes above 0.1 μm suffers a small decrease.

A comparison of the pore size distributions of two specimens compacted to virtually identical total porosity, one at a water content of 25.8% by 6 blows/layer in the Modified Proctor-based method and the other at a water content of 22.7% by the Standard Proctor method, shows that the application of approximately equal compaction energy but with a heavier hammer results in a finer distribution, due to reduction of pore content in pore sizes between 0.4 and 6.5 μm . The differences in the distributions are

reflected by an appreciable reduction in the mean pore diameter of the portion of total space in pore sizes above 0.1 μm .

A comparison of the pore size distributions of two specimens compacted to slightly different porosities, one at a water content of 31.0% by the Modified Proctor method and the other at a water content of 31.2% by the Standard Proctor method, shows that the distributions are almost identical. Similar results were obtained for a set of specimens also compacted to slightly different porosities at respective water contents of 35.2, 33.6, and 34.6% by 6 blows/layer in the Modified Proctor-based method, Modified Proctor and Standard Proctor compaction, the minor differences in the distributions appearing mostly in the pore size range of 0.1 to 0.4 μm .

The pore size distributions of two parallel sets of specimens, the specimens in each set compacted to slightly different total porosities by the Modified Proctor-based method, one set compacted at respective water contents of 23.2 and 23.5% by 12 and 25 blows/layer, and the other set compacted at respective water contents of 30.7 and 31.0% by 12 and 25 blows/layer, reveal on comparison that the distributions are almost identical for each set.

The pore size distributions of a set of two specimens compacted by the Modified Proctor-based method to slightly different porosities, one at a water content of 28.7% by 12 blows/layer and the other at a water content of 28.4%

by 25 blows/layer, show on comparison that compaction at the high energy level results in a uniform reduction of pore content in pore sizes between 0.08 and 0.8 μm .

Pore Size Distributions of Compacted Soils After Soaking Under a Nominal Surcharge Pressure

Pore size distributions were determined on specimens obtained after exposing compacted soils to deionized water generally under a surcharge pressure of 3/4 psi, as described under the section "Soaking and Swelling of Compacted Samples" of Chapter IV. The compacted soils used included Edgar Plastic kaolin and grundite compacted at a number of water contents by the methods used in this study.

The cumulative intrusion curves for all soaked specimens are given in Figures V-28 through V-34. The intrusion data are also presented in Tables A-9 and A-10 in terms, respectively, of pore content and percent distribution of space in equivalent standard pore diameter classes previously outlined. Table A-11 shows the division of total space in pore sizes above and below 0.1 μm along with mean pore diameters of both parts of the total space. Table V-5 presents degrees of saturation of compacted specimens before and after soaking. Soaking is generally accompanied by an increase in total space and by raising of the degree of saturation to about 100%. The values of more than 100% reported in the Table are likely due to poor correspondence between water contents of the soaked sample and of the material sampled

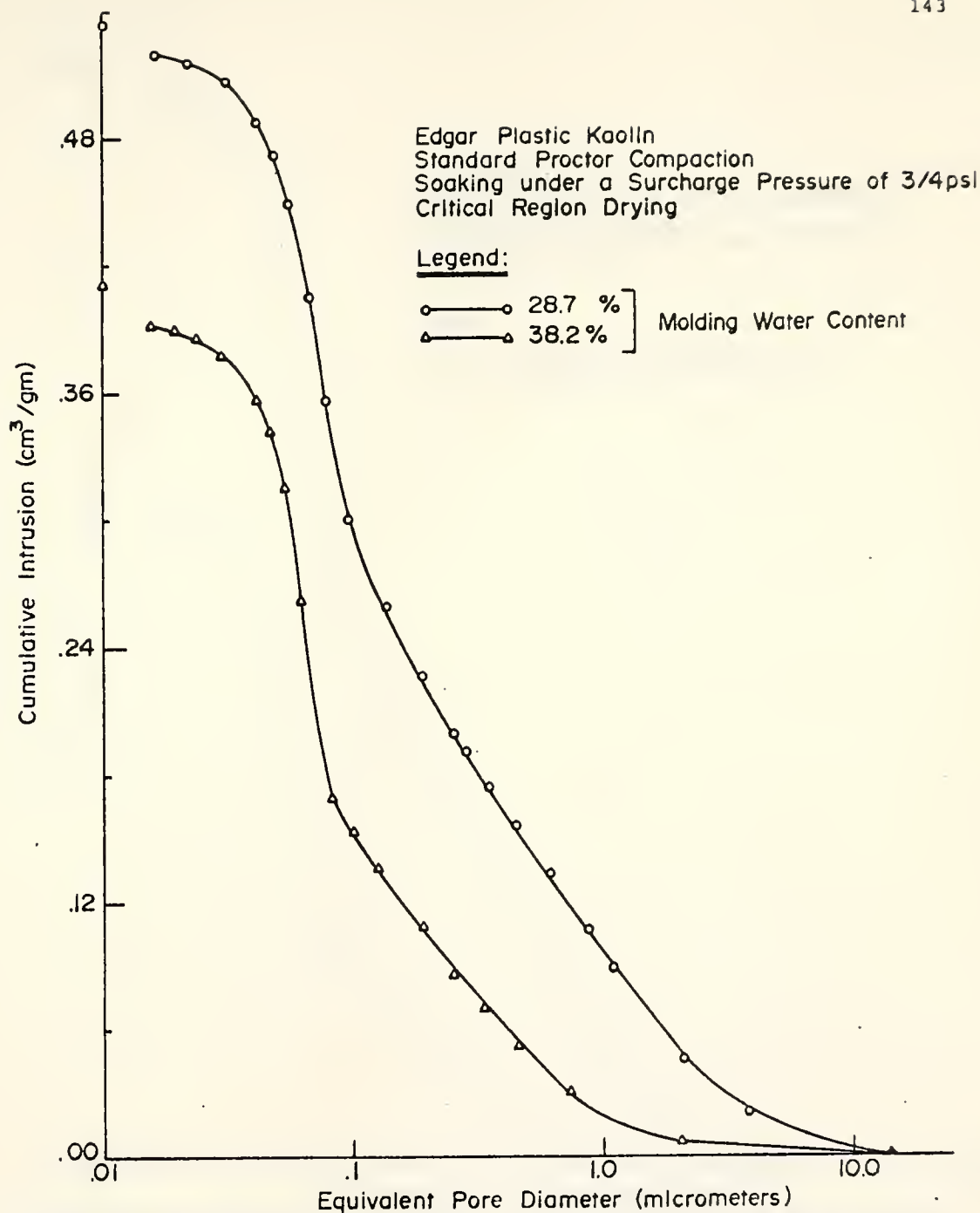


FIGURE V-28- CUMULATIVE INTRUSION CURVES FOR EDGAR PLASTIC KAOLIN COMPACTED AT DIFFERENT WATER CONTENTS BY THE STANDARD PROCTOR METHOD, AND SOAKED UNDER A SURCHARGE PRESSURE OF 3/4 PSI.

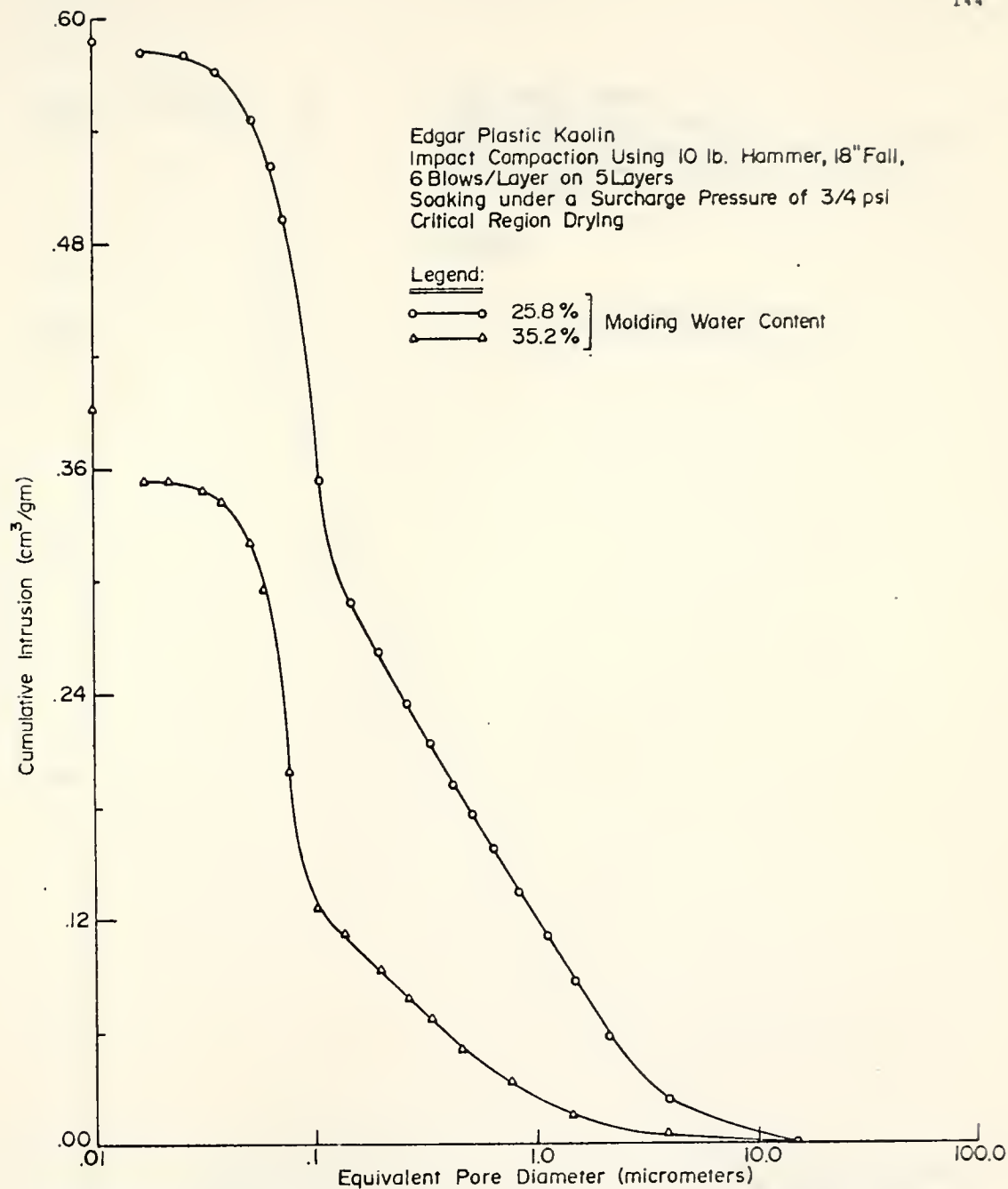


FIGURE V-29 - CUMULATIVE INTRUSION CURVES FOR EDGAR PLASTIC KAOLIN COMPACTED AT DIFFERENT WATER CONTENTS BY THE IMPACT COMPACTION METHOD USING 10 LB. HAMMER, 18" FALL, 6 BLOWS/LAYER ON 5 LAYERS, AND SOAKED UNDER A SURCHARGE PRESSURE OF 3/4 PSI.

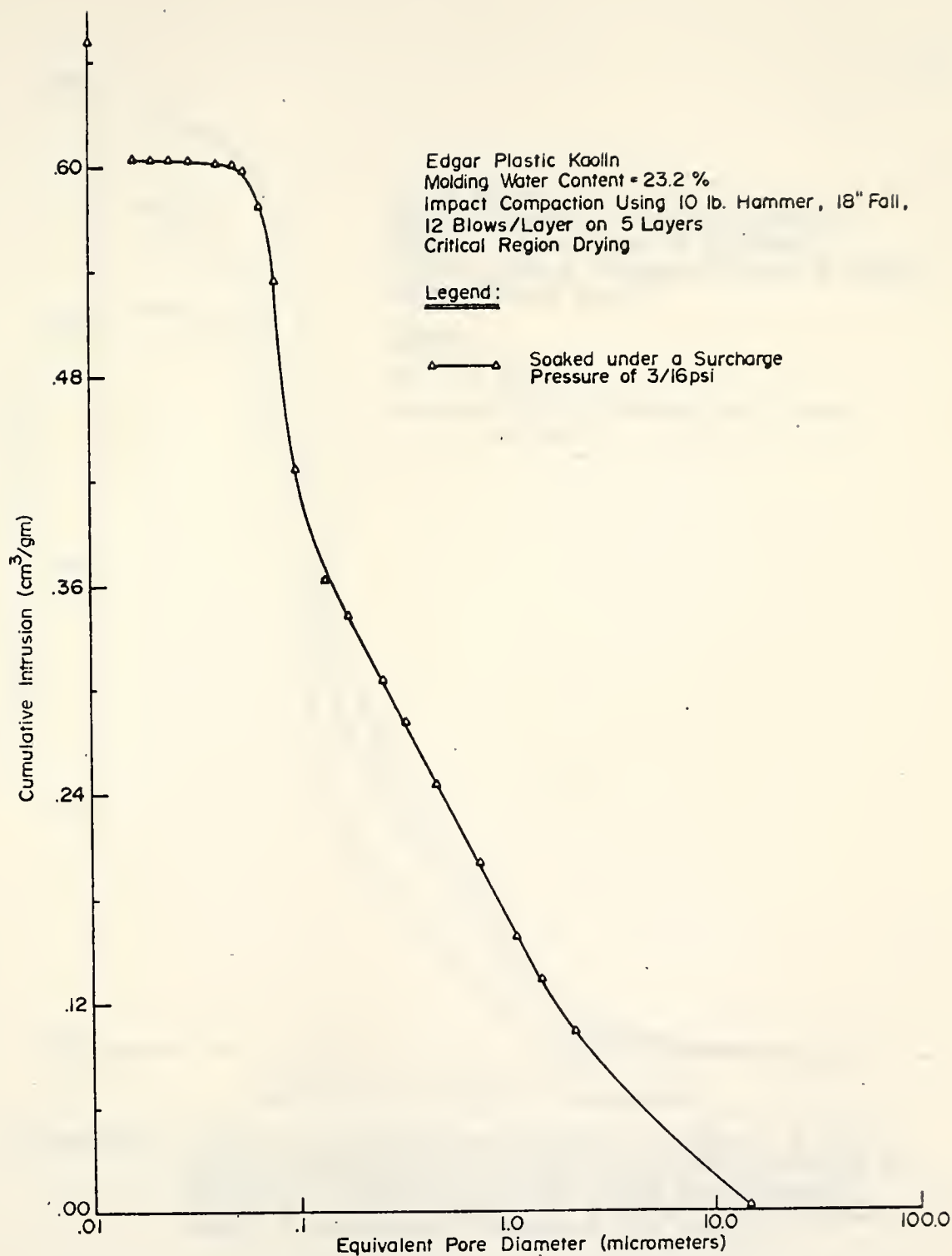


FIGURE V-30- CUMULATIVE INTRUSION CURVE FOR EDGAR PLASTIC KAOLIN COMPACTED AT A WATER CONTENT OF 23.2% BY THE IMPACT COMPACTION METHOD USING 10 LB. HAMMER, 18" FALL, 12 BLOWS/LAYER ON 5 LAYERS, AND SOAKED UNDER A SURCHARGE PRESSURE OF 3/16 PSI.

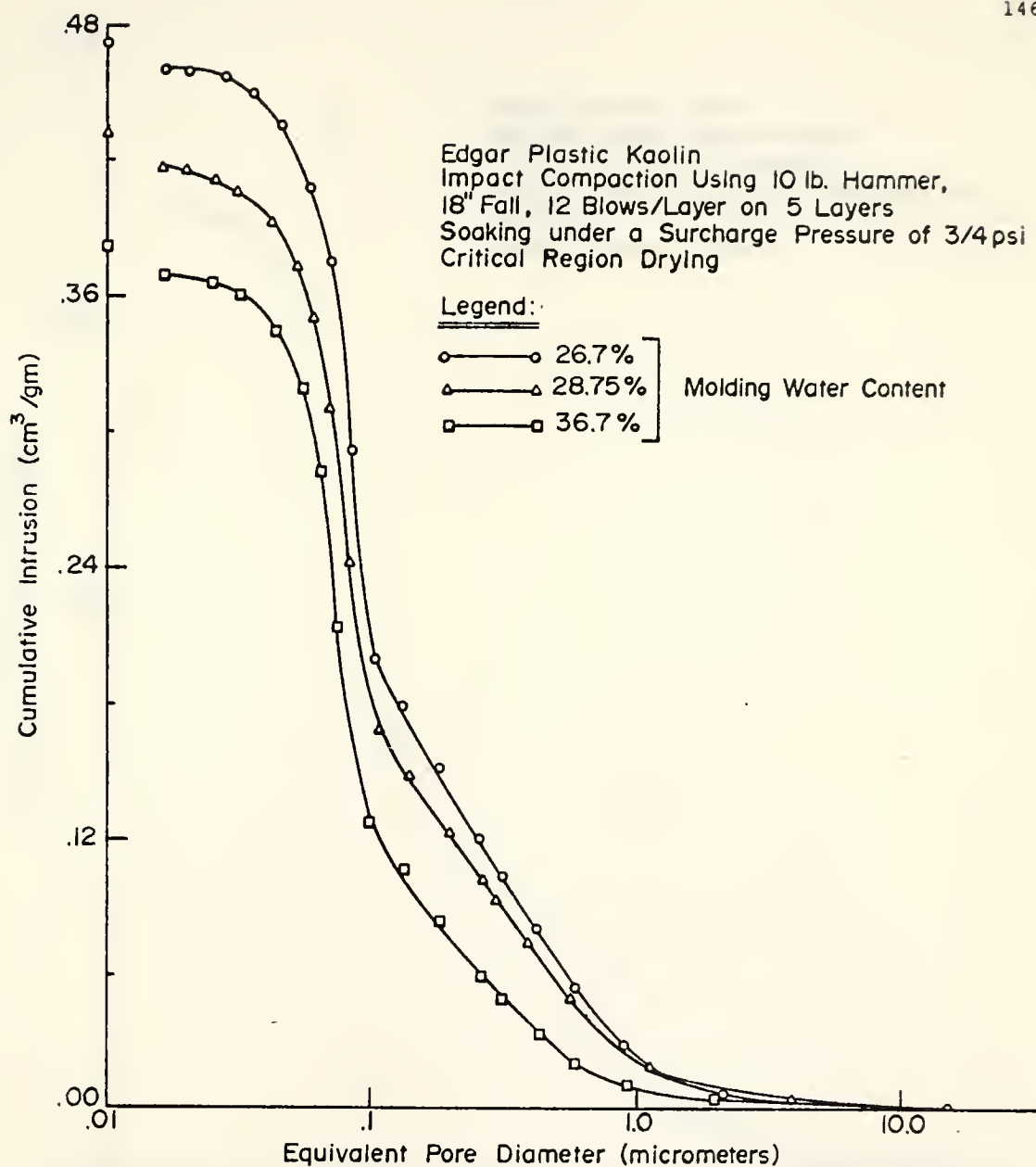


FIGURE X-31 - CUMULATIVE INTRUSION CURVES FOR EDGAR PLASTIC KAOLIN COMPACTED AT DIFFERENT WATER CONTENTS BY THE IMPACT COMPACTION METHOD USING 10 LB. HAMMER, 18" FALL, 12 BLOWS/LAYER ON 5 LAYERS, AND SOAKED UNDER A SURCHARGE PRESSURE OF 3/4 PSI.

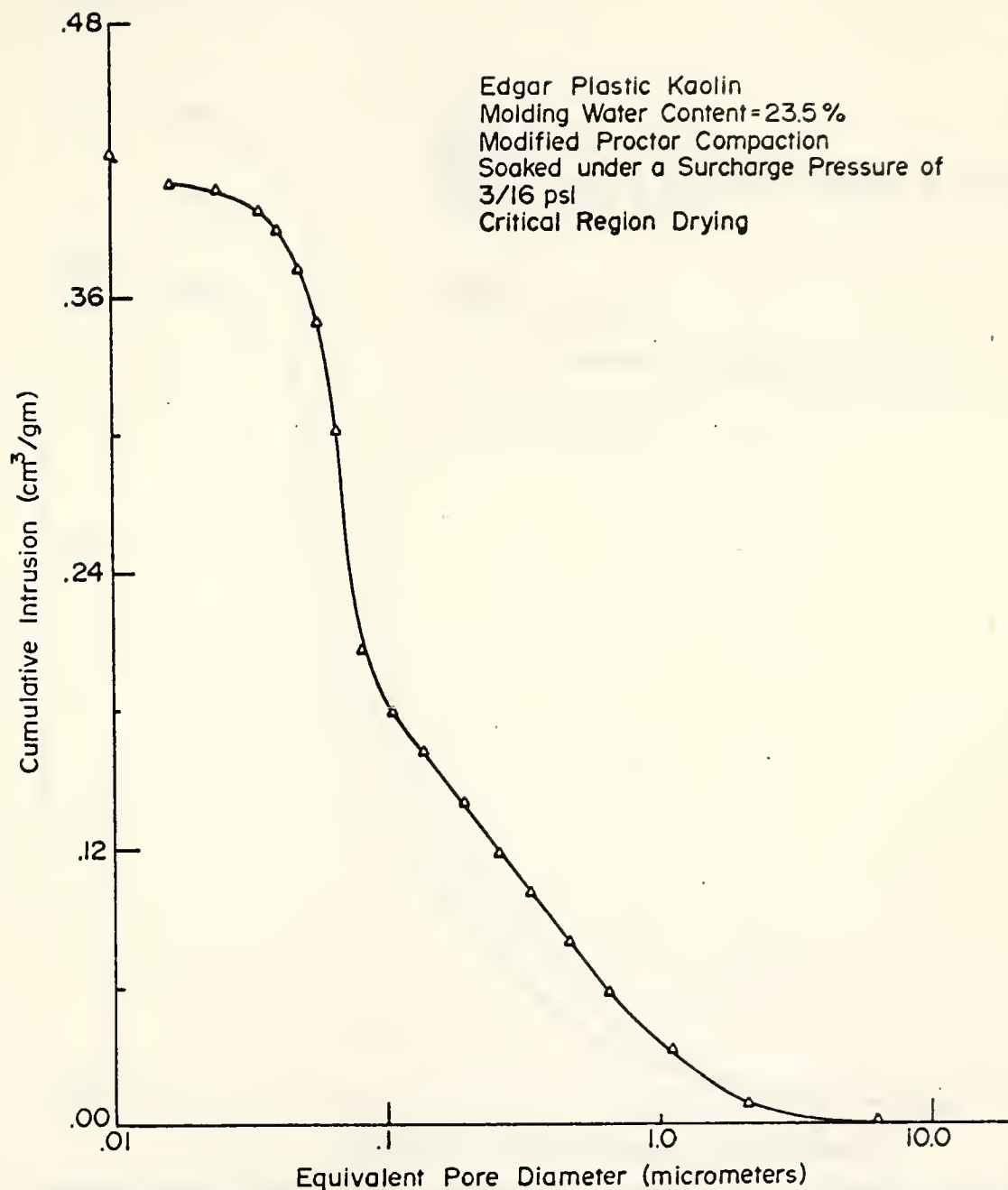


FIGURE X-32 - CUMULATIVE INTRUSION CURVES FOR EDGAR PLASTIC KAOLIN COMPACTED AT A WATER CONTENT OF 23.5% BY THE MODIFIED PROCTOR METHOD, AND SOAKED UNDER A SURCHARGE PRESSURE OF 3/16 PSI.

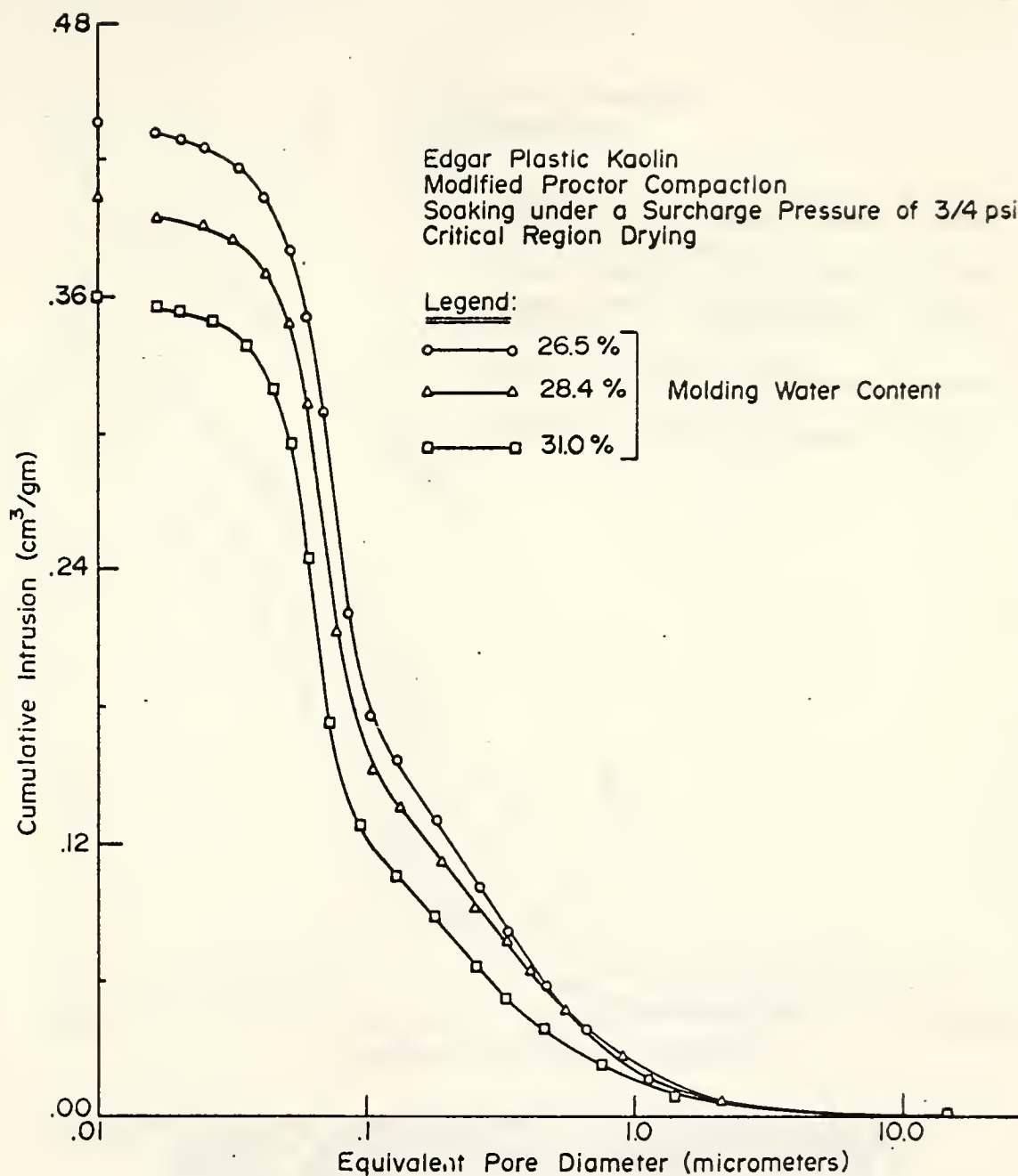


FIGURE V-33- CUMULATIVE INTRUSION CURVES FOR EDGAR PLASTIC KAOLIN COMPACTED AT DIFFERENT WATER CONTENTS BY THE MODIFIED PROCTOR METHOD, AND SOAKED UNDER A SURCHARGE PRESSURE OF 3/4 PSI.

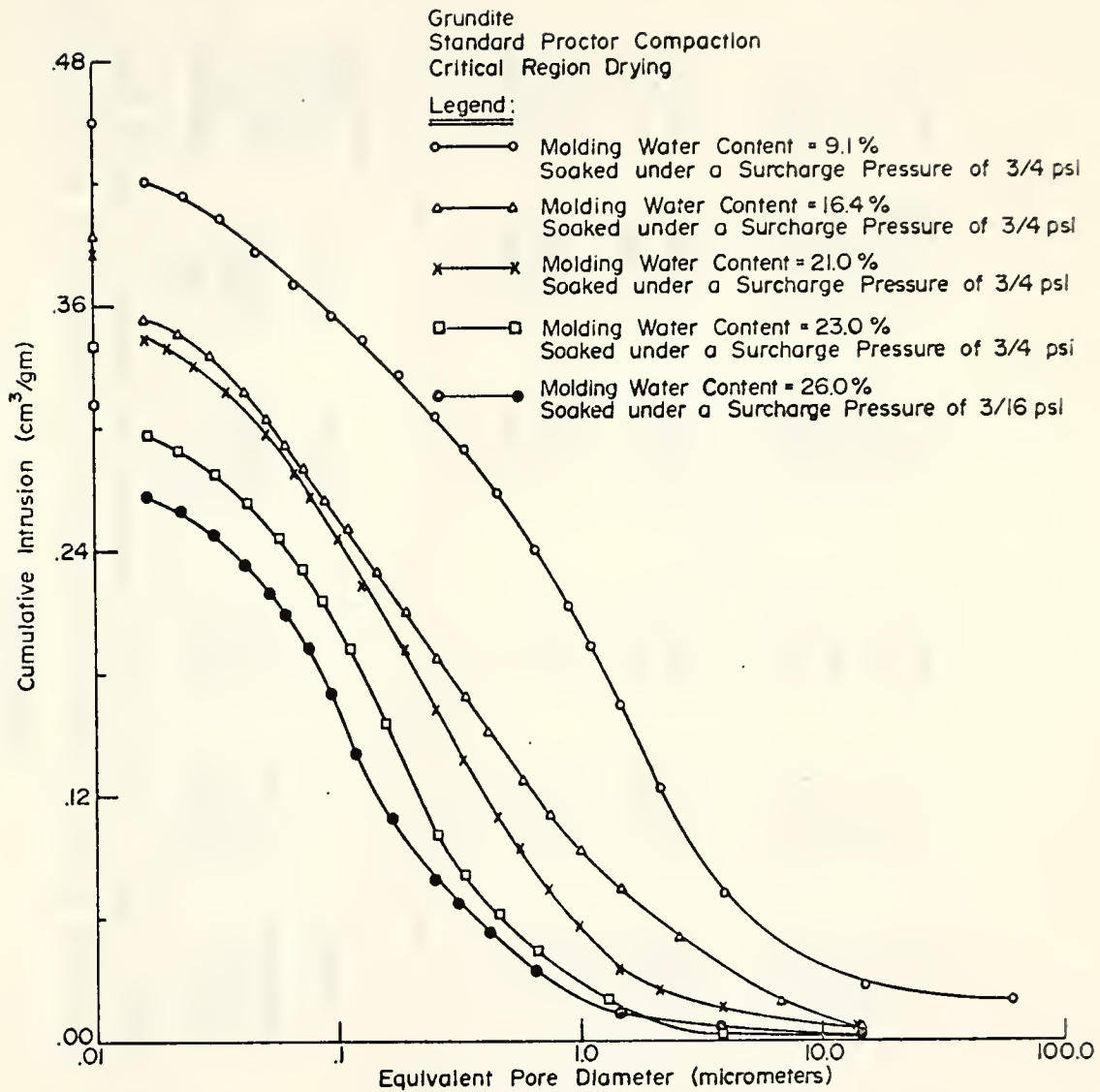


FIGURE V-34-CUMULATIVE INTRUSION CURVES FOR GRUNDITE COMPACTED AT DIFFERENT WATER CONTENTS BY THE STANDARD PROCTOR METHOD, AND SOAKED UNDER A SURCHARGE PRESSURE OF 3/4 OR 3/16 PSI.

TABLE V-5

Degrees of Saturation of Edgar Plastic Kaolin and Grundite Compacted at Different Water Contents, and Soaked Under a Surcharge Pressure of Either $\frac{3}{16}$ Or $\frac{3}{4}$ psi

Soil	Compaction Type and Level	Surcharge Pressure (psi)	Molding Water Content (%)	Soaking Water Content (%)	"As-Molded" Porosity (cm^3/gm)	"As-Soaked" Porosity (cm^3/gm)	Degree of Saturation After Compaction (%)	Degree of Saturation After Soaking (%)
Edgar Plastic Kaolin	Standard Proctor	3/4	28.7	55.4	0.364	0.535	79.0	103.5
		3/4	38.2	42.1	0.409	0.413	93.4	101.9
	Modified Proctor 6 Blows/Layer	3/4	25.8	64.4	0.477	0.588	54.0	109.5
		3/4	35.2	39.5	0.372	0.392	94.6	100.7
	Modified Proctor 12 Blows/Layer	3/16	23.2	62.9	0.357	0.673	65.0	93.5
		3/4	26.7	46.0	0.336	0.474	79.5	97.0
		3/4	28.7	45.0	0.309	0.433	93.0	103.9
		3/4	36.7	39.0	0.381	0.383	96.3	101.8

TABLE V-5

(Continued)

Soil	Compaction Type and Level	Sur- charge Pressure (psi)	Molding Water Content (%)	Soaking Water Content (%)	"As- Molded" Porosity (cm ³ /gm)	"As- Soaked" Porosity (cm ³ /gm)	Degree of Satur- ation After Compaction (%)	Degree of Satur- ation After Soaking (%)
Modified Proctor 25 Blows/Layer		3/16	23.5	42.4	0.334	0.425	70.3	99.8
		3/4	26.5	44.6	0.294	0.437	90.1	102.0
		3/4	28.4	39.5	0.302	0.405	94.0	97.5
		3/4	31.0	37.0	0.315	0.360	98.4	102.8
Grundite Standard Proctor		3/4	9.1	44.1	0.296	0.450	30.7	98.0
		3/4	16.4	38.8	0.282	0.394	58.2	98.5
		3/4	21.0	42.5	0.259	0.385	81.1	110.4
		3/4	23.0	33.7	0.273	0.339	84.2	99.4
		3/16	26.0	31.2	0.283	0.313	91.9	99.7

for critical region drying. The results show that all but about 5% or less and about 15% or less of total space is intruded for Edgar Plastic kaolin and grundite, respectively. Comparisons between pore size distributions of compacted soils and those of soaked specimens of these soils compacted at roughly identical water contents will be made separately for Edgar Plastic kaolin and grundite in the following section.

Edgar Plastic Kaolin

Figure V-28 gives pore size distributions for soaked specimens of Edgar Plastic kaolin compacted at a water content of 28.7% on the dry side and at a water content of 38.2% on the wet side of the Standard Proctor optimum. These distributions exhibit slope regions which are roughly the same as those of the soil compacted at about equal water contents. Soaking of the specimen compacted on the dry side of the optimum results in a large increase in total space. This increase is associated with a greater pore content largely in pore sizes between 1 and 15 μm and to a small extent in sizes between 0.1 and 1 μm . On the other hand, soaking of the specimen compacted on the wet side of the optimum causes a negligible change in the total space as well as in its distribution.

Figure V-29 presents cumulative intrusion curves for soaked specimens of the soil compacted at dry-side and wet-side water contents of 25.8 and 35.2%, respectively, by the

method based on Modified Proctor compaction but using 6 blows/layer. For the dry-side sample, the large increase in total space due to soaking is a reflection of greater space present largely in pore sizes between 0.8 and 15 μm . For the wet-side sample, the small increase in total space is associated with slightly greater pore content in pore sizes between 0.4 and 2 μm .

Cumulative intrusion curves are given in Figures V-30 and V-31 for soaked specimens of Edgar Plastic kaolin compacted at dry-side water contents of 23.2, 26.7, and 28.7%, and at a wet-side water content of 36.7% by the method based on Modified Proctor compaction but using 12 blows/layer. Unlike other specimens, the specimen at a compaction water content of 23.2% was soaked under a surcharge pressure of 3/16 psi. Soaking of the specimen compacted at a water content of 23.2% results in a very large increase in total space. This increase is accompanied by greater space in pore sizes between 0.2 and 15 μm . The presence of the large pores is reflected by a large increase in the mean pore diameter of the portion of total space in pore sizes above 0.1 μm . Soaking of the specimen compacted at a water content of 28.7% also resulted in a large increase in total space. This increase is associated with a greater pore content largely in pore sizes between 0.4 and 4 μm and to a small extent in pore sizes between 0.1 and 0.4 μm . No comparison could be made between pore size distributions of soaked and

unsoaked samples for the molding water contents of 26.7 and 36.7%, because distributions were not measured for the unsoaked samples. Figure V-31 shows that the distributions of soaked specimens shift progressively to the left with molding water contents increasing from 26.7 to 36.7%, indicating decreasing total space and increasing fineness. The differences in the distributions are associated with progressive reductions of space in pore sizes between 0.1 and 2 μm .

Figures V-32 and V-33 present cumulative intrusion curves for soaked specimens of Edgar Plastic kaolin compacted at dry-side water contents of 23.5 and 26.5% and at wet-side water contents of 28.4 and 31.0% by the Modified Proctor method. Unlike other specimens, the specimen at a compaction water content of 23.5% was soaked under a surcharge pressure of 3/16 psi. Soaking of the specimen compacted at a water content of 23.5% results in a large increase in total space. This increase is a reflection of greater pore content in pore sizes between 0.2 and 3 μm . The presence of the large pores is evidenced by a large increase in the mean pore diameter of the portion of space in pore sizes above 0.1 μm . Soaking of the specimens compacted at increasing water contents, i.e., from 26.5 to 31.0%, results in smaller increases in total space. The increases are associated with greater space in pore sizes between 0.08 and 2 μm .

Grundite

Figure V-34 presents cumulative intrusion curves for soaked specimens of grundite compacted at dry-side water contents of 9.1 and 16.4% and at wet-side water contents of 21.0, 23.0, and 26.0% by the Standard Proctor method.

Soaking of the specimens compacted on the dry side of the optimum results in large increases in total space. These increases decrease with increasing molding water contents and are reflections of greater pore contents largely in pore sizes between 1 and 15 μm and to a small extent in sizes below 1 μm . The presence of the large pores in the soaked specimens is reflected by large increases in the mean pore diameters of the portion of total space in pore sizes above 0.1 μm . Soaking of the specimens compacted at increasing water contents on the wet side of the optimum results in smaller increases in total space. These increases are associated with greater space in pore sizes between 0.2 and about 5 μm .

Comparisons of the Pore Size Distributions of Soaked Specimens of Edgar Plastic Kaolin Compacted at Nearly Equal Water Contents by Higher Compactive Efforts

A comparison of the pore size distributions of soaked specimens of Edgar Plastic kaolin compacted at a water content of about 26% by 6, 12, and 25 blows/layer in the Modified Proctor-based method shows that increasing the number of blows/layer from 6 to 12 is associated with a large reduction of pore content in sizes between 1 and 15 μm

and a small reduction of pore content in sizes between 0.1 and 1 μm . Increasing the number of blows/layer further, i.e., from 12 to 25, is accompanied by only a small decrease in space in pore sizes between 0.1 and 1 μm . Similar results are obtained when comparing the pore size distributions of soaked specimens of the soil compacted at a water content of about 28.5% by the Standard Proctor method and by 12 and 25 blows/layer in the Modified Proctor-based method.

A comparison of the pore size distributions of soaked specimens of Edgar Plastic kaolin compacted at water contents in excess of about 35% shows the distributions to be almost identical for all of the used compaction efforts.

CHAPTER VI

DISCUSSION OF RESULTS

The pore size distributions presented in the results represent, for the first time, an extensive series of measurements made on soils that demonstratably did not change pore volume as a result of drying prior to the determination.

Effectiveness of Critical Region Drying

The critical region drying method used in this study effectively removes soil water without phase change and hence without shrinkage occurring in the drying process. The drying method has been demonstrated to be effective in preventing changes in the total porosity of all of the soils used, except Volclay bentonite, in both the "as-compacted" and "as-soaked" conditions, i.e., over a large range of strengths of the soils. Volclay bentonite was specifically used to indicate the limitation of the drying method, i.e., that soils composed largely of expanding clay minerals could not be dried even by this method without volume change. Samples of this bentonite compacted at a number of water contents by the Standard Proctor method exhibited a more-or-less consistent reduction in total porosity of 15%. This

loss appears to be directly related to the loss of volume of about 16% within particles, as is indicated by a reduction in X-ray basal spacing from 11.6 to 9.7 Å on critical region drying of the as-supplied Volclay bentonite (Figure V-8).

Changes in total porosity were prevented for all other soils by careful development of the critical region drying technique. Because the drying method involves raising of temperature and pressure of soil water to values well within the critical region, efforts were made to minimize the adverse effects of these conditions with respect to maintaining unchanged the total porosity and the pre-existing distribution of total space for the soils used in this study. These adverse conditions include the effect of high temperature on the basic structure of clay minerals and the effect of high pressure on compacted soils.

The effect of high temperature on soils was studied using X-ray diffraction and infra-red spectral analysis. No changes were observed in the basic structure of all of the clay minerals present in the soils used, an expected result for the mostly hydrothermal conditions of exposure of critical region drying. The reversible thermal expansion of the clay minerals was also computed to be small for the temperature range used in the drying method.

The effect of high pressure on the fabric of saturated soils is likely to be minimal as hydrostatic pressure could be transmitted to the soil skeleton through an open interconnected network of channels present in soils. With this

in mind, as well as because of the fear that the fabric of compacted soils could be adversely affected during a critical region run by evaporation and subsequent expansion of the air initially dissolved by pressure application, it was thought desirable to replace most of the air in compacted soils initially by soaking them at constant volume. The small amount of air still remaining was brought in solution by pressuring water in the early part of the critical region run, and was kept in solution for all combinations of temperature and pressure leading to the critical region. The effect of high pressure on pore size distributions of the resulting saturated soils is likely to be small.

In addition, partially saturated soils exhibit a tendency to imbibe water and swell or slake, if free to do so, on exposure to water at the start of the critical region run. The original porosity of these soils was preserved by soaking them at constant volume under confinement; this resulted in increasing water contents approaching the saturation condition. It is thought that soaking at constant volume did not itself affect the pore size distributions of the compacted soils, judging from the consistent trends obtained for distributions corresponding to a wide range of molding water contents for all of the soils used.

As a further indication of the lack of influence of the soaking at constant volume on the pore structure of the specimens, a comparison was made of two specimens, one trimmed to dimensions of 1 inch diameter and 3/4 inch

thickness and the other to dimensions of 1/2 inch diameter and 1/2 inch thickness, of the same soil (Edgar Plastic kaolin) compacted at the same moisture content (31.2%). Both the specimens were soaked at constant volume and then critical region dried. Samples were taken from the middle of each of these specimens for mercury intrusion measurement, and the resulting pore size distributions are given in Figure VI-1. It is apparent from the Figure that the pore systems of the centers of the specimens, both soaked under restraint, are virtually identical. Since it is unlikely that the stress distribution obtained in soaking was the same in the center portions of both specimens, this result is evidence for the conclusion that the stresses involved in both cases were too small to materially affect the pore size distributions previously existing.

Changes in the Total Porosity of Compacted Soils
on Oven Drying and on Freeze Drying

The data reported on changes in the total porosity of Standard Proctor compacted soils resulting from oven drying and freeze drying (Table V-3) are consistent with those of Ahmed (1971). In both cases oven drying of grundite produced losses in total porosity of 20% for a similar dry-side water content, and about 40% or more for the optimum and wet-of-optimum water contents. Likewise the data show that freeze drying of grundite caused reductions in total porosity of between 15 and 25% for water contents up to the optimum

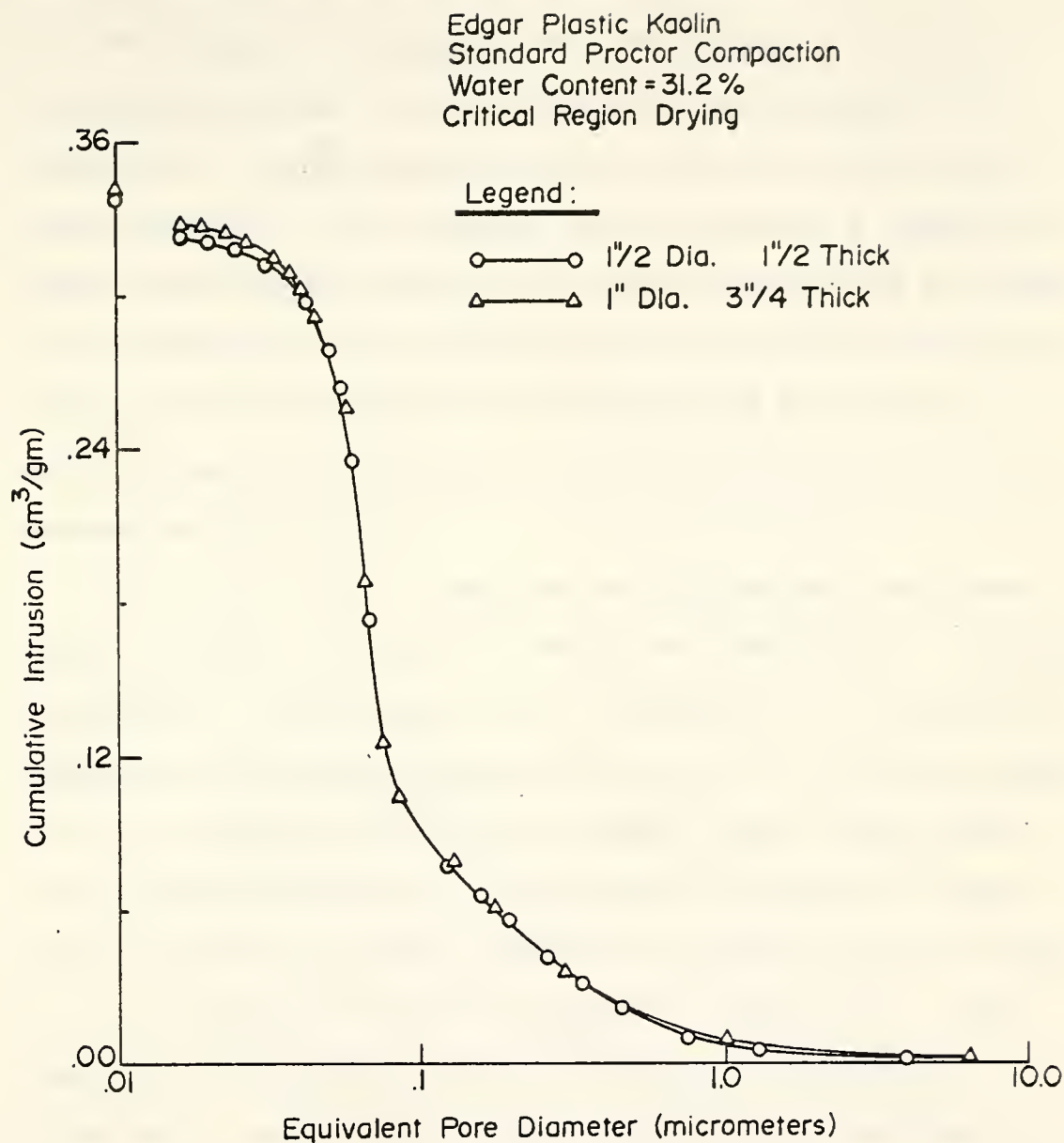


FIGURE VI-1 -CUMULATIVE INTRUSION CURVES FOR EDGAR PLASTIC KAOLIN COMPACTED AT A WATER CONTENT OF 31.2% BY THE STANDARD PROCTOR METHOD, AND TRIMMED TO DIFFERENT DIMENSIONS FOR CRITICAL REGION DRYING.

and of about 20% for wet-side water contents.

The above data relating to oven drying are also consistent with those of Diamond (1970), who obtained for another soil (Edgar Plastic kaolin) and for another compaction method (full coverage impact yielding a compaction curve lying between those of Standard Proctor and Modified Proctor methods but approximating that of the latter method) reductions in total porosity of about 10% for dry-side water contents and of about 30% for the optimum and wet-of-optimum water contents.

All of the soils compacted by the methods mentioned above have been observed to shrink on oven drying. Sridharan, Altschaeffl, and Diamond (1971) prevented such shrinkage by compacting statically Georgia kaolin at a low water content of 21% to densities (Table 2 of their paper) much higher than those obtained at a similar water content for Edgar Plastic kaolin by impact compaction (Diamond [1970], Table 4), or by Modified Proctor compaction (Table A-6). The degrees of saturation of the specimens of Sridharan, Altschaeffl, and Diamond (1971) ranged from a minimum of 65% to a maximum of 99% for the highest density, in comparison to the values of 68 and 62% for the specimens of Diamond (1971) and the writer, respectively. The former workers also oven dried without shrinkage Boston blue clay and grundite, each compacted to degrees of saturation of about 60%, but with a much higher density than that obtained at an identical

water content by the Standard Proctor method (Table A-3 and Figure V-3).

It is apparent from the above that a soil compacted to densities corresponding to those of the Standard Proctor and possibly Modified Proctor methods cannot be dried by oven drying or freeze drying and be counted on to maintain its original porosity. Under these conditions, critical region drying can be used with success.

Comparisons of Pore Size Distributions of Critical Region Dried and Oven Dried Soils

It was reported in the last section that oven drying causes significant reduction in the total porosity of soils compacted at water contents wet of optimum. Comparisons in this section will therefore be restricted to soils compacted at water contents dry of optimum, which have suffered relatively small shrinkage on oven drying.

Boston blue clay compacted at a water content of about 15% to total porosities of 0.26 and 0.38 cm³/gm by static compaction (Sridharan, Altschaeffl, and Diamond [1971], Figure 7) and by Standard Proctor compaction (Figure V-16), respectively, exhibited negligible shrinkage on oven drying and critical region drying. A comparison of the pore size distributions of the dried specimens shows that the lower porosity resulting from the use of a higher compactive effort is associated with lesser space largely in pore sizes between 0.2 and 1.5 μ m. It is in this size range that the

space was progressively reduced for increasing molding water contents up to the Standard Proctor optimum for critical region dried samples of Boston blue clay (Figure V-16). This similarity of response indicates that the pore size distributions obtained for the oven dried and critical region dried specimens are compatible with each other.

A similar comparison was made of the pore size distributions of Edgar Plastic kaolin compacted at a water content of about 22% by impact method (Diamond [1970], Figure 10, 30 blows/layer) and by the Standard Proctor method (Figure V-12). The resulting total porosities after oven drying and after critical region drying were respectively 0.26 and 0.48 cm³/gm. The lower porosity resulting from the impact compaction method is associated with lesser space largely in pore sizes between 0.1 and 2 μ m. This size range again corresponds to the range in which the space was progressively reduced for increasing molding water contents up to the Standard Proctor optimum for critical region dried samples of Edgar Plastic kaolin (Figure V-12). Thus, the similarity of response indicates once more the consistency of the pore size distributions obtained for the oven dried and critical region dried specimens.

Another comparison was made of the pore size distributions for grundite compacted statically at a water content of 7.0% (Hill [1960a], Figure 2a), and by the Standard Proctor method at a water content of 9.1% (Figure V-17).

The total porosities of the partly fired and critical region dried specimens were 0.24 and 0.29, respectively. The pore size distributions indicated slightly lesser space in pore sizes between 0.2 and 2 μm for the partly fired specimen. This size range is again in accord with that associated with progressive reductions in space for increasing molding water contents up to the Standard Proctor optimum for critical region dried samples of grundite. This shows that the pore size distributions of the partly fired and critical region dried specimens are consistent with each other. An abnormality was, however, found on comparing the pore size distribution of an oven dried specimen of grundite compacted statically at a molding water content of 13.9% to porosity of 0.21 cm^3/gm (Sridharan, Altschaeffl, and Diamond [1971], Figure 7) to that of a critical region dried specimen compacted by the Standard Proctor method at a molding water content of 16.4% to porosity of 0.28 cm^3/gm . For the critical region dried specimen, most of the space was measured in pore sizes below 1 μm . For the oven dried specimen, however, most of the space was measured in the pore size range of 1 to 10 μm .

The above discussion shows that in general the pore size distributions of critical region dried and oven dried soils are consistent with each other for soils compacted at low water contents.

Constancy of Space in Fine Pores for
Critical Region Dried Soils

A comparison of the distributions of pore sizes obtained for soil aggregations, compacted soils, and compacted soils after soaking shows that for each soil the distribution of the fine pores, as characterized by the mean pore diameter of the portion of total space in pore sizes below $0.1 \mu\text{m}$ (given in Tables A-5, A-8, and A-11), is relatively consistent. Moreover, the quantity of the fine pores appears to be reasonably constant and related to the clay content ($< 2 \mu\text{m}$) of the soils, i.e., $0.003 \text{ cm}^3/\text{gm}$ of space is contributed by about each percent of clay content for Edgar Plastic kaolin, Boston blue clay, and Crosby silty clay; the corresponding values are about 0.0025 and $0.005 \text{ cm}^3/\text{gm}$ for grundite and reddish-brown limestone residual clay, respectively. These facts suggest that for all of the soils used, the fine pores occur either within individual particles or within domains of roughly face to face oriented clay particles. The size range of the fine pores conforms roughly to the intradomainal pore size range of 300 to 800 \AA as determined by Diamond (1971) for Edgar Plastic kaolin. It appears that the fine pores are likely present within domains.

The relative constancy of the fine pores in all of the soils used in this study is in agreement with the findings of Rubin (1949), Sridharan (1968), and Diamond (1971), working respectively with a silty clay, Georgia kaolin, and

Edgar Plastic kaolin. The data of these workers show relationships between the space in the fine pores and the clay content of the soils, which are similar to those observed in this study.

Influence of Mixing Water Content on Total Porosity
and on Pore Size Distributions of Aggregations

The size distributions of aggregations found to be formed in the mixing sequence at higher water contents are coarser and are restricted to narrower size ranges, i.e., are more uniform (Figures V-1 and V-2), and are in general conformity with the findings of Hodek (1972), Figure A5. These larger aggregations obtained at higher water contents have lower total space and higher degrees of saturation (Table V-1). This means that the air content of the aggregations is decreasing with increasing water contents, i.e., the aggregations are being "internally" compacted in the mixing process due to numerous interactions between the larger and more plastic (deformable without fracture) aggregations. This densification is associated with reduction in the content of large pores, i.e., those of the order of a few micrometers (Figures V-10 and V-11), which are likely present among smaller aggregations constituting an individual large aggregation.

Influence of Compaction on Pore Size
Distributions of Aggregations

The pore size distribution representing both the inter-aggregation and intraaggregation space of aggregations compacted by the Standard Proctor method shows significantly lesser space in the large pores (Figures V-12 and V-13) than that present within the uncompacted aggregations for all of the water contents used. On the other hand, Modified Proctor compaction seems to completely eliminate the large pores (Figures V-24 and V-25) even at low water contents. This means that the shear strains accompanying Standard Proctor compaction bring the domains closer together, while the large strains accompanying Modified Proctor compaction eliminate nearly all of the interdomainal space, thus resulting in a structure in which essentially all of the space left is within the domains. This is in general agreement with conclusions reached earlier by Hodek (1972). Hodek compacted statically Edgar Plastic kaolin at a number of water contents (Table 8) to about Modified Proctor densities (Table A-6) and lower, and obtained for each of the two different sets of aggregation separates increased particle orientations with increasing water contents for the used compactive efforts.

Influence of Molding Water Content on Pore
Size Distributions of Compacted Soils

The pattern of changes in the pore size distributions for changes in the molding water content up to optimum is consistent for all of the soils, and for all of the levels of Proctor compaction variables used in this study. Increasing water contents up to optimum are accompanied by decreasing total space and by finer distributions of pore sizes, due mainly to progressive reductions in the content of relatively large pores. These pores occur in Standard Proctor compacted samples in the size range of about 0.2 to 3 μm for Edgar Plastic kaolin, grundite, and Boston blue clay, and in the larger ranges of about 4 to 20 μm and about 0.2 to more than 100 μm for Crosby silty clay and reddish-brown limestone residual clay, respectively. For Modified Proctor compacted samples, these pores occur in the size range of about 0.1 to 0.4 μm for Edgar Plastic kaolin. The distribution of pore sizes obtained at optimum represents the finest of all distributions obtained for water contents up to optimum.

The first few applications of the compaction effort remove a significant proportion of the air present in large pores (i.e., larger than about 3 μm for Edgar Plastic kaolin and grundite aggregations) existing between smaller aggregations constituting a large aggregation. (As previously indicated, the smaller aggregations get tacked together in the mixing process to form large aggregations.) These large pores are

removed from aggregations formed at all experimental water contents. The effectiveness of the subsequent applications of the compaction effort depends on the moisture condition of the aggregations relative to optimum. At low water contents, the aggregations are strong and do not deform plastically to fit into the interaggregation space. At high water contents, however, the aggregations are weaker and more deformable, and could, on adequate compaction, conform to the available interaggregation space.

The progressive reductions in the content of the relatively large pores with increasing molding water contents up to optimum are likely due to progressive closing in of the interaggregation space and the bringing closer of the randomly oriented domains present within aggregations, on deformation of weaker aggregations. For Standard Proctor compacted soils other than Crosby silty clay and reddish-brown limestone residual clay, the progressive reductions occur in the size range of about 0.2 to 3 μm , which appears to represent both interaggregation and interdomainal pores. For Crosby silty clay and reddish-brown limestone residual clay, however, the size ranges of about 4 to 20 μm and about 0.2 to more than 100 μm , respectively, appear to belong solely to interaggregation space. This might result from these soils having the soil mineral constituents present in well developed aggregations. For Modified Proctor compacted Edgar Plastic kaolin, the interaggregation space appears to

be completely eliminated and the size range of 0.1 to 0.4 μm pertains only to interdomainal space.

The presence of interaggregation space in the dry-side specimens prepared by the Standard Proctor method is apparent on comparing the degrees of saturation of Edgar Plastic kaolin compacted by the Standard Proctor and Modified Proctor methods with those of uncompacted individual aggregations formed at about the same water content. The degrees of saturation for Standard Proctor and Modified Proctor compacted samples are respectively 7 to 12% and 36 to 12% higher than those of the uncompacted individual aggregations (whose degrees of saturation increase from about 55 to 84%) for water contents increasing from about 27 to 34%. For this range of water contents, mere removal of the large pores from between the small aggregations constituting an individual large aggregation should have resulted in degrees of saturation higher by about 13 to 5% than those of the uncompacted individual aggregations.

The pattern of changes in the pore size distributions reported here for water contents dry of optimum is based on extensive data generated with critical region dried soils. These data are in accord with those of Diamond (1970, 1971) and of Ahmed (1971), who showed that samples compacted dry of optimum have an appreciable content of large pores. The data are also in conformity with the expectation of Lambe (1958) and Mitchell, Hooper, and Campanella (1965), based

on permeability studies, that samples compacted at water contents dry of optimum should have an appreciable proportion of total space in large pores.

The changes in the pore size distributions for changes in the molding water content wet of optimum also follow a consistent pattern for all of the soils and for all levels of Proctor compaction variables used in this study. Increasing water contents beyond optimum are associated with increasing total space, which in this case is a reflection of greater space in pores smaller than about $0.4\text{ }\mu\text{m}$. The only exceptions to this are the molding water content changes beyond 3 to 4% of optimum for Edgar Plastic kaolin and grundite. In these cases, greater space is present in sizes below about $2\text{ }\mu\text{m}$ and $0.8\text{ }\mu\text{m}$ for Edgar Plastic kaolin and grundite, respectively.

For water contents wet of optimum, the aggregations deform to fill in the available space between aggregations. In consequence, little interaggregation space remains. Within the aggregations the domains probably become progressively better oriented on compaction at increasing water contents. It is therefore likely that the greater space found in the small pore sizes for increasing water contents wet of optimum represents films of water between more nearly oriented domains developed in the compaction process.

The reported pattern of changes in the pore size distributions for changes in the molding water content wet of

optimum is consistent with that of Ahmed (1971), whose data also show that for grundite the increase in total space beyond the Standard Proctor optimum occurs in pore sizes below $0.8\text{ }\mu\text{m}$. The reported pattern was obtained with the data generated mostly with processed soils. It is likely that such a pattern would also be obtained for unprocessed soils because of the demonstrated similarity in the pore size distributions obtained for both processed and unprocessed Crosby silty clay (Figure V-9).

Comparisons of the Pore Size Distributions of Soils
Compacted to the Same Total Porosity on the Dry and
Wet Sides of Standard Proctor Optimum

Comparisons of the pore size distributions of a number of soils compacted by the Standard Proctor method show that for the same total porosity, a dry-side specimen exhibits greater space in relatively large pores than that present in the wet-side specimen. These large pores occur in pore sizes between 0.2 and $3\text{ }\mu\text{m}$ for Edgar Plastic kaolin and grundite, and between 4 and $20\text{ }\mu\text{m}$ for Crosby silty clay.

The presence of a greater content of large pores in a dry-side specimen results from such a specimen retaining, even after compaction, much of the structure of the initial individual aggregations, with large spaces present between the aggregations. In contrast, the interaggregation spaces are completely eliminated in a wet-side specimen and the space, other than that present within domains for the dry-side and wet-side specimens, exists between domains.

Influence of Soil Type on Pore Size Distributions
Obtained at About Standard Proctor Optimum

At Standard Proctor optimum, the compaction energy reduces the total space of a soil-water mix to a minimum value (for that energy), which may vary widely for different soils. Such values obtained for Boston blue clay, reddish-brown limestone residual clay, and grundite are quite close to one another. However, they are different from those of Edgar Plastic kaolin and Crosby silty clay, which soils exhibit values respectively higher and lower than those of the above soils. In spite of the differences in the total porosity at Standard Proctor optimum, all pore size distributions obtained at about these optimums exhibit most of the space in pore sizes below $0.4\text{ }\mu\text{m}$. The distributions for the three soils having virtually identical porosity at optimum (Figure V-22) differ only slightly from one another. The distributions for Edgar Plastic kaolin (Figure V-12) and Crosby silty clay (Figure V-14) show respectively greater and lesser contents of the fine pores as compared to those of the above distributions. Besides, Crosby silty clay shows a coarser distribution than the other soils in pore sizes between 0.1 and $0.4\text{ }\mu\text{m}$. Presumably, these differences in the distributions reflect differences in the clay fractions of the various soils. The factors contributing to the differences in the distributions probably include: shapes of the individual clay mineral particles, their degree of association, their intrinsic stiffness, and the possible

presence of cementation in holding some particles together in some soils.

Influence of Soil Type on Pore Size Distributions
Obtained for Dry-Side Samples Compacted to 95%
or Less of Standard Proctor Maximum Dry Density

Unlike the relatively small differences in pore size distributions obtained for samples compacted at about Standard Proctor optimum, different soils show largely different distributions of pore sizes for dry-side samples compacted to dry densities of about 95% or less of Standard Proctor maximum dry density (Figures V-20 and V-21). The differences in the distributions indicate that compaction specifications based on achievement of a certain percent of maximum dry density, irrespective of the soil type, do not yield identical pore structures. It is also apparent from the Figures that Crosby silty clay and reddish-brown limestone residual clay exhibit pores larger than 1 μm , likely present between well developed aggregations. In contrast, the rest of the soils, i.e., Edgar Plastic kaolin, grundite, and Boston blue clay, exhibit essentially all the space in pores smaller than about 1 μm . This strong dependence of pore size distributions of dry-side compacted samples on soil type is noteworthy.

Influence of Soil Type on Pore Size Distributions
Obtained for Wet-Side Samples Compacted to About
95% or Less of Standard Proctor Maximum Dry Density

The pore size distributions obtained for wet-side samples compacted to about 95% or less of Standard Proctor maximum dry density (Figures V-23, V-13 for water content of 36.7%, V-19) show trends similar to those of the samples compacted at about Standard Proctor optimum. Further, the differences in pore size distributions are relatively small for all soils tested.

Influence of Increasing Compactive Effort on Pore Size
Distributions of Edgar Plastic Kaolin

In this section, the effect of increasing compactive effort on pore size distributions will be discussed for Edgar Plastic kaolin at a series of about identical water contents. The results on which this discussion is based are reported under the section "Pore Size Distributions of Edgar Plastic Kaolin Compacted by the Modified Proctor Method and by Methods Based on It" of Chapter V.

The effectiveness of increasing compactive effort in causing greater densification of a soil mass depends on its water content. At dry-side water contents, Modified Proctor compaction effects a larger reduction in the total porosity and in the content of large pores, i.e., those lying between about 0.4 and 6.5 μm , than that achieved for Standard Proctor compaction. At wet-side water contents, however, both methods yield almost identical total porosity and pore

structure. The Modified Proctor compaction involves greater penetration of a heavier hammer into the soil mass, thus causing greater shear strains. At dry-side water contents, these shear strains likely deform the individual aggregations to fill in the interaggregation space. At wet-side water contents, however, the larger energy associated with Modified Proctor compaction does no additional densification and is wasted in unnecessary soil displacements.

Compaction of Edgar Plastic kaolin at about the same dry-side water content by the Standard Proctor method and by fewer (6) blows/layer of a heavier hammer in the Modified Proctor method, both of which apply approximately equal compaction energy, results in roughly the same total porosity. As expected, a finer pore size distribution with smaller content of the large pores is obtained for the sample compacted by the heavier hammer.

The effect of varying the compactive effort in terms of number of blows/layer in the Modified Proctor compaction method was investigated. It was found that raising the number of blows/layer from 6 to 12 for dry-side water contents is effective in causing additional densification and reduction in the content of intermediate pores, i.e., those in the size range of 0.08 to 0.8 μm . Additional raising of the number of blows/layer from 12 to 25 results in small changes in total porosity and almost identical pore size distribution. For wet-side water contents, however,

raising the number of blows/layer from 6 to 25 does not materially alter either the total porosity or the pore size distributions.

It appears that for dry-side water contents, the application of 12 blows/layer increases the density of soil to such a degree that it acts elastically in its response to further applications of blows, and the applied energy is lost as the soil rebounds instantaneously. For wet-side water contents, however, increasing compactive effort is wasted in unnecessary soil displacements.

Influence of Molding Water Content on Total Porosity of Soaked Samples of Compacted Soils

Two soils, i.e., Edgar Plastic kaolin and grundite, were investigated to determine the changes in total porosity and pore size distributions that occur as a result of soaking of compacted samples, generally under a modest surcharge pressure of $3/4$ psi. The increase in water content as a percentage of the original molding water content of the soaked samples decreases with increasing original molding water content from dry to wet of optimum (Table V-5). The percentage increase in water content is of the order of 100% for samples molded at about Standard Proctor optimum moisture content and of 50% for samples molded at about optimum moisture contents corresponding to the Modified Proctor method and the Modified Proctor-based method using 12 blows/layer. These data are in accord with the notion that the "deficiency"

of water in compacted soils decreases with increasing molding water content; in consequence lesser water is drawn in to satisfy this deficiency at higher water contents. The differences between the percentage increases in water content for samples originally molded at optimum moisture content by the Standard Proctor and Modified Proctor-based methods are significant. Since there is a high degree of saturation at both these optimums, the increase in water content appears to occur mainly by osmotic pressure. For the denser samples, the existence of a stronger mechanical force system between soil grains might be responsible for the decreased water intake.

Soaking results in increases of more than about 35% in the "as-molded" porosity for soils compacted at and on the dry side of optimum, and of much smaller values for water contents above optimum. These increases in porosity are volumetrically less than about 60% of the increase in water content at each molding water content for soils compacted by the Standard Proctor method. The corresponding values are about 80% for soils compacted by the Modified Proctor method and the Modified Proctor-based method using 12 blows/layer. These data are consistent with the findings of Ladd (1960) and Kayyal (1965) that the increase in porosity as a result of soaking was always smaller than the increase in water content.

The effect of soaking on total porosity was also investigated for samples compacted by decreasing effort, i.e., for

undercompacted samples. On soaking of the dry-side (molding water content of about 26%) samples of Edgar Plastic kaolin, the increase in porosity decreases by about 25% and the increase in water content nearly doubles for compactive effort decreasing from 25 or 12 to 6 blows/layer in the Modified Proctor-based method. For a molding water content of about 28.5%, however, the increase in porosity becomes larger by more than about 40% and the increase in water content more than doubles for the compactive effort decreasing from 25 or 12 blows/layer in the Modified Proctor-based method to the Standard Proctor method. The larger increase in pore volume obtained with the lower compactive effort for the molding water content of about 28.5% is due to the shifting of the water content to the dry side of optimum at the lower compactive effort.

Influence of Molding Water Content on Pore Size Distributions of Soaked Samples of Compacted Soils

The pore size distributions of soaked samples of compacted soils give information about the distribution of pore sizes for the additional space generated by soaking. Such pore size distributions of soils compacted at water contents on the dry side of Standard Proctor optimum and at water contents smaller by more than 5% with respect to optimums for the Modified Proctor-based methods indicate the generation of appreciable contents of large pores extending up to 15 μm in size. For water contents at and on the wet side of Standard Proctor optimum, the pore sizes extend to about

5 μm . For dry-side water contents within 5% of optimum and for wet-side water contents for the Modified Proctor-based methods, the pore sizes for the soaked condition are restricted to about 2 μm or less in size.

The presence of large pores extending up to 15 μm in the soaked samples initially molded at water contents on the dry side of optimum results mainly from elimination of the menisci present at air-water interfaces both between aggregations and within aggregations. The elimination of the menisci present at the soil surface sets up a hydraulic pressure gradient which causes water to flow into the sample. The flowing water not only eliminates the menisci present within the sample but also pressurizes the entrapped air. Both these factors would cause most of the swelling observed with dry-side samples. For the wet-side samples having high degrees of saturation, however, osmotic pressure is likely responsible for most of the swelling.

Summary of Results

Certain of the results seem to have a practical or engineering significance, and are emphasized here by re-statement in Summary.

1. Compaction of fine grained soils on the dry side of optimum, even to a density of about 95% of Standard Proctor maximum dry density, results in an appreciable content of relatively large pores. These large

pores are probably responsible for the higher permeabilities generally observed for the dry-side samples. On soaking under a nominal surcharge pressure, the samples compacted on the dry side of Standard Proctor optimum and at water contents smaller by more than 5% with respect to optimums for the Modified Proctor-based methods imbibe large amounts of water and swell considerably. These swelled samples exhibit appreciable contents of large pores in sizes up to 15 μm . The presence of such large pores along with large increases in water content are probably responsible for the observed significant loss of strength on soaking of the dry-side samples under a nominal surcharge pressure.

2. Samples compacted at optimum moisture content exhibit pore size distributions which are the finest of all distributions of pore sizes obtained for water contents ranging from dry to wet of optimum. Soaking under a nominal surcharge pressure of samples compacted at Standard Proctor optimum results in increases in space in pore sizes below about 5 μm . On the other hand, soils compacted at optimum and at the dry-side water contents within 5% of optimum by Modified Proctor or the Modified Proctor-based method using 12 blows/layer exhibit

similar increases in space in pore sizes below about 2 μm . Both the presence of increased porosity in pore sizes below about 2 μm and the smaller increase in water content on soaking, in comparison to that of soils compacted at Standard Proctor optimum, indicate that soils compacted at about optimum by the Modified Proctor-based methods probably retain considerable strength when exposed to water under a nominal surcharge pressure.

3. Soils compacted at a single dry-side water content to decreasing densities contain a greater content of large pores. These samples with decreasing densities likely exhibit greater permeability, and imbibe larger amounts of water and swell on soaking under a nominal surcharge pressure. The swelling introduces appreciable contents of large pores in samples compacted to lower densities. These factors are responsible for the relatively low strengths of the undercompacted soils after soaking.
4. The compaction of soils at a single wet-side high water content by increasing compactive efforts results in an almost identical total porosity. The pore size distributions of samples compacted with different types and levels of Proctor effort are almost identical and are insignificantly affected by soaking of the samples under a nominal surcharge

pressure. The soaked strengths are thus relatively low because of the high water contents, but these strengths are little reduced by soaking under nominal surcharge.

CONCLUSIONS

Based on the extensive series of pore size distributions measured in this study it was concluded that:

1. The techniques used in this study for measuring pore size distributions, and involving critical region drying and mercury intrusion, are reliable.
2. Different soils, compacted to a given percentage compaction (e.g., 95% of Standard Proctor maximum dry density) on the dry side of Standard Proctor optimum moisture content, have different total porosities. Furthermore, the pore size distributions of the various soils compacted in this manner are significantly different from each other.
3. Soils compacted at Standard Proctor optimum moisture contents varied considerably in total porosity, but had pore size distributions similar to each other in many respects. All pore sizes intruded were smaller than 0.4 μm . Between 0.1 and 0.4 μm , all the soils had a characteristic size distribution of pores. Below 0.1 μm , the content of pores varied with the clay fraction, and to some extent the type of soil.

4. Increase in compactive effort on the dry side of optimum moisture values decreased the total porosity and diminished the quantity of pores at the larger pore size end of the distribution. The largest pores present were about 6.5 μm for Standard Proctor compaction but were only about 0.4 μm for Modified Proctor compaction. Thus the increased energy applied resulted in a reduced maximum pore size and a finer pore size distribution.
5. Increasing the compactive effort on the wet side of optimum moisture values had little effect on either the total porosity or the distribution of pore sizes.
6. Compaction at optimum moisture content using the Modified Proctor method (or the Modified Proctor - based method using 12 blows/layer) resulted in a smaller maximum pore size and reduced porosity as compared with compaction at optimum moisture content using the Standard Proctor method.

The effect of soaking under a nominal surcharge pressure on soils compacted at about optimum moisture content by the Modified Proctor method (or the Modified Proctor-based method using 12 blows/layer) was less than that undergone by corresponding soils compacted at about optimum moisture content by the Standard Proctor method. The former

underwent a smaller increase in both the total porosity and maximum pore size than the latter.

7. After soaking under a nominal surcharge pressure, soils compacted on the dry side of optimum moisture values exhibited a higher porosity and a coarser pore size distribution than the soils compacted on the wet side of the optimum values.
8. The relative distributions of pore sizes effected by variables of moisture content, compactive effort, and soaking tend to agree with previous postulations, e.g., Lambe (1958) and Hodek (1972), with respect to compacted soil fabric.
9. The gross differences in pore size distributions occurring at the same percentage compactions, for different soils and compactive efforts, emphasize the lack of control over the compacted product exercised by most end result compaction specifications.

RECOMMENDATIONS FOR FURTHER STUDY

The work reported in this study pertains to laboratory Proctor compaction of a variety of processed soils, except for one soil (Crosby silty clay) which was compacted unprocessed at a single field water content. To verify the validity of the observed pore size distribution trends and to extend their applicability to field-compacted soils, the following research should be undertaken:

1. Measure pore size distributions for soils compacted by typical field rolling.
2. Investigate the dependence of important engineering properties of compacted subgrades and subbases such as strength, stiffness, compressibility, permeability, equilibrium moisture content, capillary rise, and frost-susceptibility on their pore size distributions.
3. Investigate the effect of simulated in-service conditions, like soaking and swelling, on the pore size distribution and deformation characteristics of compacted subgrades and subbase materials.

LIST OF REFERENCES

LIST OF REFERENCES

- Ahlrichs, J. L. and White, J. L., (1962), "Freezing and Lyophilizing Alters the Structure of Bentonite Gels", Science, Vol. 136, June, pp. 1116-1118.
- Ahmed, S., (1971), "Pore Size Distribution and Its Effect on the Behavior of a Compacted Clay", MSCE Thesis, Purdue University, Lafayette, Indiana, June, 200 pp.
- Ahmed, S., Lovell, C. W., Jr., and Diamond, S., (1974), "Pore Sizes and Strength of Compacted Clay", Journal of the Geotechnical Engineering Division, ASCE, Vol. 100, No. GT4, April, pp. 407-425.
- Altschaeffl, A. G., (1960), "Compressibility of Artificially Sedimented Clays", Ph.D. Thesis, Purdue University, Lafayette, Indiana, August, p. 24.
- Altschaeffl, A. G., and C. W. Lovell, Jr., (1968), "Compaction Variables and Compaction Specification", Proceedings, 54th Annual Road School, Engineering Bulletin, Extension Series No. 131, Purdue University, Lafayette, Indiana, pp. 116-133.
- American Society for Testing and Materials, (1971), "Standard Methods of Test for Moisture - Density Relations of Soils Using 5.5 lb. Rammer and 12-in. Drop", ASTM Standard Designation: D 698-70, Annual Book of ASTM Standards, Part 11, pp. 332-336.
- American Society for Testing and Materials, (1971), "Standard Methods of Test for Moisture-Density Relations of Soils Using 10 lb. Rammer and 18-in. Drop", ASTM Standard Designation: D 1557-70, Annual Book of ASTM Standards, Part 11, pp. 498-503.
- American Society for Testing and Materials, (1971), "Standard Methods of Test for Apparent Porosity, Water Absorption, Apparent Specific Gravity, and Bulk-Density of Burned Refractory Brick", ASTM Standard Designation: C 20-70, Annual Book of ASTM Standards, Part 13, pp. 6-8.
- Andersland, O. B., (1960), "The Clay Water System and the Shearing Resistance of Clays", Ph.D. Thesis, Purdue University, Lafayette, Indiana, January, pp. 35-36.

- Anderson, D. M., and Hoekstra, P., (1965), "Crystallization of Clay-Adsorbed Water", Science, Vol. 149, July, pp. 318-319.
- Anderson, D. M., and Hoekstra, P., (1965), "Migration of Interlamellar Water During Freezing and Thawing of Wyoming Bentonite", Soil Science Society Proceedings, Vol. 29, No. 5, pp. 498-503.
- Anderson, D. M., and Tice, A. R., (1971), "Low-Temperature Phases of Interfacial Water in Clay-Water Systems", Proceedings, Soil Science Society of America, Vol. 35, No. 1, January-February, pp. 47-54.
- Anderson, T. F., (1950), "A Method for Eliminating Gross Artifacts in Drying Specimens", Proceedings, First International Congress on Electron Microscopy, Paris, Communication No. 68, pp. 567-576.
- Anderson, T. F., (1951), "Techniques for the Preservation of Three-dimensional Structure in Preparing Specimens for the Electron Microscope", Transactions, New York Academy of Sciences, Series II, Vol. 13, No. 4, February, pp. 130-134.
- Andrews, T., (1869), "On the Continuity of the Gaseous and Liquid States of Matter", The Philosophical Transactions, Royal Society of London, Vol. 159, pp. 575-589.
- Andrews, T., (1876), "On the Gaseous State of Matter", The Philosophical Transactions, Royal Society of London, Vol. 166, pp. 421-449.
- Aylmore, L. A. G., and Quirk, J. P., (1960a), "Domain or Turbostratic Structure of Clays", Nature, Vol. 187, September, pp. 1046-1048.
- Aylmore, L. A. G., and Quirk, J. P., (1960b), "The Structural Status of Clay Systems", Ninth National Conference on Clays and Clay Minerals, pp. 104-129.
- Aylmore, L. A. G., and Quirk, J. P., (1967), "The Micropore Size Distributions of Clay Mineral Systems", The Journal of Soil Science, Vol. 18, No. 1, pp. 1-17.
- Baver, L. D., (1938), "Soil Permeability in Relation to Non-Capillary Porosity", Proceedings, Soil Science Society of America, Vol. 3, pp. 52-56.
- Bhasin, R. N., Lovell, C. W., Jr., and Toebe, G. H., (1969), "Erodability of Sand-Clay Mixtures as Evaluated by a Water Jet", Technical Report No. 8, Water Resources Research Center, Purdue University, Lafayette, Indiana, June, 207 pp.

- Borchardt, G. A., Theisen, A. A., and Harward, M. E., 1968, "Vesicular Pores of Pumice by Mercury Intrusion", Proceedings, Soil Science Society of America, Vol. 32, pp. 735-737.
- Bradfield, R., and Jamison, V. C., (1938), "Soil Structure - Attempts at Its Quantitative Characterization", Proceedings, Soil Science Society of America, Vol. 3, pp. 70-76.
- Bush, R. Y., (1950), "A Study of the Compaction Characteristics of Cohesive Soils", MSCE Thesis, Purdue University, Lafayette, Indiana, June, pp. 5-37.
- Call, F., (1953), "Preparation of Dry-Gels by Freeze-Drying", Nature, Vol. 172, pp. 126.
- Caro, J. H., and Freeman, H. P., (1961), "Physical Structure of Fertilizer Materials-Pore Structure of Phosphate Rock and Triple Superphosphate", Agricultural and Food Chemistry, Vol. 9, No. 3, May-June, pp. 182-186.
- Casagrande, A., (1932), "Research on the Atterberg Limits of Soils", Public Roads, Vol. 13, No. 7, September, pp. 121-130.
- Childs, E. C., and Collis-George, N., (1950), "The Permeability of Porous Materials", Proceedings of the Royal Society (London), Series A, Vol. 201, March-May, pp. 392-405.
- Cochran, C. N., and Cosgrove, L. A., (1957), "Pore Size Distribution of Porous Aluminum Oxides by Mercury Porosimeter and n-Butane Sorption", Journal of Physical Chemistry, Vol. 61, pp. 1417-1419.
- Commonwealth Scientific and Industrial Research Organization, Melbourne, Australia, (1960), "Discussion", Interparticle Forces in Clay-Water-Electrolyte Systems, pp. 3-13 to 3-26.
- Croney, D., and Coleman, J. D., (1954), "Soil Structure in Relation to Soil Suction", Journal of Soil Science, Vol. 5, No. 1, pp. 75-84.
- Dawson, R. F., (1960), "Some Laboratory Studies of the Moisture-Density Relations of Soil", Symposium on Soils for Engineering Purposes, Special Technical Publication 254, ASTM, pp. 308-317.
- Day, P. R., and Holmgren, G. G., (1952), "Microscopic Changes in Soil Structure During Compression", Proceedings, Soil Science Society of America, Vol. 16, No. 1, January, pp. 73-77.

- Diamond, S., (1970), "Pore Size Distributions in Clays", Clays and Clay Minerals, Vol. 18, pp. 7-23.
- Diamond, S., (1971), "Microstructure and Pore Structure of Impact-Compacted Clays", Clays and Clay Minerals, Vol. 19, pp. 239-249.
- Drake, L. C., (1949), "Pore-Size Distribution in Porous Materials", Industrial and Engineering Chemistry, Vol. 41, No. 4, April, pp. 780-785.
- Drake, L. C., and Ritter, H. L., (1945), "Macropore-Size Distributions in Some Typical Porous Substances", Industrial and Engineering Chemistry, Analytical Edition, Vol. 17, No. 12, December, pp. 787-791.
- DuBose, L. A., (1956), "Discussion of (Engineering Properties of Expansive Clays by Holtz, W. G., and Gibbs, H. J., Transactions, ASCE, Vol. 121, Proceedings Paper No. 2814, pp. 641-663)", Transactions, ASCE, Vol. 121, pp. 674-676.
- Eckert, E. R. G. and Drake, R. M., (1972), Analysis of Heat and Mass Transfer, McGraw Hill Book Co., 806 pp.
- Emmett, P. H., (1948), "Characteristics of Charcoal and Whetlerites", Chemical Reviews, Vol. 43, p. 93.
- Esmer, E., Walker, R. D., and Krebs, R. D., (1969), "Freeze-Thaw Durability of Lime-Stabilized Clay Soils", Highway Research Record, No. 263, pp. 27-36.
- Fraser, H. J., (1935), "Experimental Study of the Porosity and Permeability of Clastic Sediments", Journal of Geology, Vol. 43, No. 8, Part 1, November-December, pp. 910-1010.
- Gancy, A. B., (1972), "Aqueous Solutions under Extreme Conditions-High Temperature", Water and Aqueous Solutions, Structure, Thermodynamics, and Transport Processes (Horne, R. A., Editor), Wiley-Interscience, pp. 771-803.
- Gillott, J. E., (1969), "Study of the Fabric of Fine-Grained Sediments with the Scanning Electron Microscope", Journal of Sedimentary Petrology, Vol. 39, No. 1, March, pp. 90-105.
- Gillott, J. E. (1970), "Fabric of Leda Clay Investigated by Optical, Electron-Optical, and X-ray Diffraction Methods", Engineering Geology, Vol. 4, No. 2, April, pp. 133-153.
- Gillott, J. E., (1971), "Mineralogy of Leda Clay", Canadian Mineralogist, Vol. 10, Part 5, pp. 797-811.

- Girault, P., (1960), "A Study on the Consolidation of Mexico City Clay", Ph.D. Thesis, Purdue University, Lafayette, Indiana, June, pp. 17-20.
- Grady, J. D., (1949), "Discussion of (Effect of Reusing Soil on Moisture-Density Curves, by Nelson, G. H., and Sowers, G. F., Proceedings, Highway Research Board, Vol. 29, pp. 482-487), Proceedings, Highway Research Board, Vol. 29, pp. 488-490.
- Graton, L. C., and Fraser, H. J., (1935), "Systematic Packing of Spheres with Particular Relation to Porosity and Permeability", Journal of Geology, Vol. 43, No. 8, Part 1, November-December, pp. 785-909.
- Griffin, W. H., (1965), "A Study of the Strength Relationships of Critical-Region Dehydrated Clay Sediments", MSCE Thesis, Purdue University, Lafayette, Indiana, June, 61 pp.
- Grim, R. E., (1962), Applied Clay Mineralogy, McGraw-Hill Book Co., 422 pp.
- Grim, R. E., and Bradley, W. F., (1940), "Investigation of the Effect of Heat on the Clay Minerals Illite and Montmorillonite", Journal, American Ceramic Society, Vol. 23, No. 8, pp. 242-248.
- Hannigan, E. J., (1964), "A Critical Region Apparatus for the Dehydration of Clay Soils Without Particle Disturbance", MSCE Thesis, Purdue University, Lafayette, Indiana, June, 71 pp.
- Harkins, W. D., and Ewing, W. W., (1920), "The Surface Energy of Mercury and the Energy Relations at the Interface Between Mercury and Other Liquids", Journal, American Chemical Society, Vol. 42, pp. 2539-2547.
- Hatsopoulos, G. N. and Keenan, J. H., (1965), Principles of General Thermodynamics, John Wiley and Sons, Inc., 256 pp.
- Hilf, J. W., (1956), "An Investigation of Pore-Water Pressure in Compacted Cohesive Soils", Technical Memorandum No. 654, Bureau of Reclamation, Department of Interior, Denver, Colorado, October, 109 pp.
- Hill, R. D., (1960a), "A Study of Pore-Size Distribution of Fired Clay Bodies-I-The Effect of Clay Mineralogy on the Distribution", Transactions, British Ceramic Society, Vol. 59, pp. 189-197.
- Hill, R. D., (1960b), "A Study of Pore-Size Distribution of Fired Clay Bodies-II-An Improved Method of Interpreting Mercury Penetration Data", Transactions, British Ceramic Society, Vol. 59, pp. 198-212

- Hodek, R. J., (1972), "Mechanism for the Compaction and Response of Kaolinite", Ph.D. Thesis, Purdue University, Lafayette, Indiana, December, 269 pp.
- Hogentogler, C. A., Jr., (1936), "Essentials of Soil Compaction", Proceedings, Highway Research Board, Vol. 16, pp. 309-316.
- Holtz, W. G., (1968), "Soil as an Engineering Material", Journal of Materials, Vol. 3, No. 4, December, pp. 845-915.
- Holtz, W. G., and Ellis, W., (1963), "Comparison of the Shear Strengths of Laboratory-and Field-Compacted Soils", Laboratory Shear Testing of Soils, Special Technical Publication 361, ASTM, pp. 471-480.
- Holtz, W. G. and Gibbs, H. J., (1956), "Engineering Properties of Expansive Clays", Transactions, ASCE, Vol. 121, Proc. Paper No. 2814, pp 641-663.
- Hooper, J. R., (1971), Personal Communication.
- Hvorslev, M. J., (1949), Subsurface Exploration and Sampling of Soils for Engineering Purposes, Committee on Sampling and Testing, American Society of Civil Engineers, November, p. 105.
- Juhola, A. J., and Wiig, E. O., (1949), "Pore Structure in Activated Charcoal-Determination of Macro Pore Size Distribution", Journal, American Chemical Society, Vol. 71, June, pp. 2078-2080.
- Joyner, L. G., Barrett, E. P., and Skold, R., (1951), "The Determination of Pore Volume and Area Distributions in Porous Substances-Comparison Between Nitrogen Isotherm and Mercury Porosimeter Methods", Journal, American Chemical Society, Vol. 73, July, pp. 3155-3158.
- Kayyal, K. M., (1965), "Strength Characteristics of Soils Compacted by Four Methods", Ph.D. Thesis, University of Texas, Austin, Texas, 199 pp.
- Keenan, J. H., (1969), Steam Tables; Thermodynamic Properties of Water, Including Vapor, Liquid, and Solid Phases, John Wiley and Sons, Inc., 162 pp.
- Keenan, J. H. and Keyes, F. G., (1955), Thermodynamic Properties of Steam Including Data for the Liquid and Solid Phases, John Wiley and Sons, Inc., January, pp. 27-76.

- Kemball, C., (1946), "On the Surface Tension of Mercury", Transactions, Faraday Society, Vol. 42, pp. 526-537.
- Keyes, F. G., Smith, L. B., and Gerry, H. T., (1936), "The Specific Volume of Steam in the Saturated and Superheated Condition Together with Derived Values of Enthalpy, Entropy, Heat Capacity, and Joule-Thompson Coefficients", Proceedings of the American Academy of Arts and Sciences, Vol. 70, pp. 319-364.
- Kistler, S. S., (1932), "Coherent Expanded Aerogels", Journal of Physical Chemistry, Vol. 36, pp. 52-64.
- Klock, G. O., (1968), "Pore Size Distributions as Measured by the Mercury Intrusion Method and Their Use in Predicting Permeability", Ph.D. Thesis, Oregon State University, Corvallis, 91 pp.
- Klock, G. O., Boersma, L., and DeBacker, L. W., (1969), "Pore Size Distributions as Measured by the Mercury Intrusion Method and Their Use in Predicting Permeability", Proceedings, Soil Science, Vol. 33, No. 1, January, pp. 12-15.
- Ladd, C. C., (1957), "Swelling of Compacted Clays", M.S. Thesis, MIT, Cambridge, Massachusetts, pp. 3-30.
- Ladd, C. C., (1960), "Mechanisms of Swelling by Compacted Clay", Bulletin No. 245, Highway Research Board, pp. 10-26.
- Lambe, T. W., (1951), Soil Testing for Engineers, John Wiley & Sons, pp. 46-49.
- Lambe, T. W., (1953), "The Structure of Inorganic Soil", Proceedings, ASCE, Vol. 79, Separate No. 315, October, pp. 1-49.
- Lambe, T. W., (1958a), "The Structure of Compacted Clay", Journal of the Soil Mechanics and Foundations Division, ASCE, Vol. 84, No. SM2, pp. 1-34.
- Lambe, T. W., (1958b), "The Engineering Behavior of Compacted Clay", Journal of the Soil Mechanics and Foundations Division, ASCE, Vol. 84, No. SM2, May, pp. 1-35.
- Leamer, R. W., and Lutz, J. F., (1940), "Determination of Pore-Size Distribution in Soils", Soil Science, Vol. 49, pp. 347-360.
- Lee, P. Y., and Suedkamp, R. J., (1972), "Characteristics of Irregularly Shaped Compaction Curves of Soils", Highway Research Record, No. 381, pp. 1-9.

- Leonards, G. A., (1952), "Shearing Resistance of Partially Saturated Clays", Ph.D. Thesis, Purdue University, Lafayette, Indiana, February, 87 pp.
- Leonards, G. A., and Altschaeffl, A. G., (1964), "Compressibility of Clay", Journal of the Soil Mechanics and Foundations Division, ASCE, Vol. 90, No. SM5, September, pp. 133-155.
- Lincoln, J. B., Miller, R. J., and Tettenhorst, R., (1970), "Random Powder Mounts from Montmorillonite Aerogels", Clay Minerals, Vol. 8, pp. 347-348.
- Lovell, C. W., Jr., (1957), "Certain Characteristics of Partially Frozen Soil", Ph.D. Thesis, Purdue University, Lafayette, Indiana, January, 166 pp.
- Loxton, H. T., Beavis, H. M., and McNicholl, M. D., (1948), "A Procedure for Evaluating the Influence of the Moisture Content of the Subgrade on the Thickness Required for Flexible Pavements of Airfields", Proceedings, Second International Conference on Soil Mechanics and Foundation Engineering, Vol. 2, pp. 218-222.
- Marshall, T. J., (1958), "A Relation Between Permeability and Size Distribution of Pores", Journal of Soil Science, Vol. 9, No. 1, pp. 1-8.
- Massachusetts Institute of Technology, (1961), "Research on the Physical Properties of Marine Soils", Publication No. 117, Soil Engineering Division, Department of Civil and Sanitary Engineering, July, p. 28.
- Matyas, E. L., (1967), "Air and Water Permeability of Compacted Soils", Permeability and Capillarity of Soils, Special Technical Publication 417, ASTM, pp. 160-175.
- McKinstry, H. A., (1965), "Thermal Expansion of Clay Minerals", The American Mineralogist, Vol. 50, January-February, pp. 212-222.
- Michaels, A. S., (1959), "Discussion of (Physico-Chemical Properties of Soils: Soil-Water Systems by Rosenqvist, I.T., Journal of the Soil Mechanics and Foundations Division, ASCE, Vol. 85, No. SM2, April, pp. 31-53)", Journal of the Soil Mechanics and Foundations Division, ASCE, Vol. 85, No. SM2, April, pp. 91-102.
- Mikhail, R. S., Brunauer, S., and Bodor, E. E., (1968), "Investigations of a Complete Pore Structure Analysis", Journal of Colloid and Interface Science, Vol. 26, p. 45.

- Millington, R. J., and Quirk, J. P., (1959), "Permeability of Porous Media", Nature, Vol. 183, February, pp. 387-388.
- Mishu, L. P., (1963), "Collapse in One-Dimensional Compression of Compacted Clay upon Wetting", MSCE Thesis, Purdue University, Lafayette, Indiana, August, 105 pp.
- Mitchell, J. K., (1956), "The Importance of Structure to the Engineering Behavior of Clay", Sc. D. Thesis, MIT, Cambridge, Massachusetts, pp. 28-41.
- Mitchell, J. K., Hooper, D. R., and Campanella, R. G., (1965), "Permeability of Compacted Clay", Journal of the Soil Mechanics and Foundations Division, ASCE, Vol. 91, No. SM4, July, pp. 41-65.
- Nalezny, C. L., and Li, M. C., (1967), "Effect of Soil Structure and Thixotropic Hardening on the Swelling Behavior of Compacted Clay Soils", Highway Research Record, No. 209, pp. 1-22.
- Nelson, W. R., and Baver, L. D., (1940), "Movement of Water Through Soils in Relation to the Nature of the Pores", Proceedings, Soil Science Society of America, Vol. 5, pp. 69-76.
- Norrish, K., and Rausell-Colom, J. A., (1962), "Effect of Freezing on the Swelling of Clay Minerals", Clay Minerals Bulletin, Vol. 5, No. 27, July, pp. 9-16.
- Nowak, E. S., (1962), "An Equation of State and Certain Thermodynamic Properties for Water and Water Vapor in the Critical Region", Vol. I, Ph. D. Thesis, Purdue University, Lafayette, Indiana, June, 24 pp.
- Nutting, P. G., (1943), "Some Standard Thermal Dehydration Curves of Minerals", U. S. Geological Survey Professional Paper 197-E, pp. 197-216.
- Olson, R. E., and Langfelder, L. J., (1965), "Pore Water Pressures in Unsaturated Soils", Journal of the Soil Mechanics and Foundations Division, ASCE, Vol. 91, No. SM4, July, pp. 127-150.
- Olson, R. E., and Scott, J. D., (1961), "Discussion of (Structure and Strength Characteristics of Compacted Clays by Seed, H. B., and Chan, C. K., Journal of the Soil Mechanics and Foundations Division, ASCE, October, pp. 87-128)", Transactions ASCE, Vol. 126, Part I, pp. 1398-1404.

- Orr, C., Jr., (1970), "Application of Mercury Penetration to Materials Analysis", Powder Technology, Vol. 3, No. 3, pp. 117-123.
- Pacey, J. G., Jr., (1956), "The Structure of Compacted Soils", S. M. Thesis, MIT, Cambridge, Massachusetts.
- Parcher, J. V., and Liu, P., (1965), "Some Swelling Characteristics of Compacted Clays", Journal of the Soil Mechanics and Foundations Division, ASCE, Vol. 91, No. SM3, Proceedings Paper 4316, May, pp. 1-17.
- Perloff, W. H., (1966), "Study of Long Term Deformation of Compacted Cohesive Soil Embankments", Plan of Study, Joint Highway Research Project, Project No. C-36-5F, File No. 6-6-6, Purdue University, Lafayette, Indiana, pp. 28-35.
- Pray, H. A., Schweickert, C. E., and Minnich, B. H., (1952), "Solubility of Hydrogen, Oxygen, Nitrogen, and Helium in Water at Elevated Temperatures", Industrial and Engineering Chemistry, Vol. 44, No. 5, May, pp. 1146-1151.
- Proctor, R. R., (1933a), "Fundamental Principles of Soil Compaction", Engineering News Record, Vol. 111, No. 9, August, pp. 245-248.
- Proctor, R. R., (1933b), "Description of Field and Laboratory Methods", Engineering News Record, Vol. 111, No. 10, September, pp. 286-289.
- Purcell, W. R., (1949), "Capillary Pressures - Their Measurement Using Mercury and the Calculation of Permeability Therefrom", Journal of Petroleum Technology, Vol. 1, February, pp. 39-48.
- Pusch, R., (1966), "Quick-Clay Microstructure", Engineering Geology, Vol. 1, No. 6, pp. 433-443.
- Pusch, R., (1967), "A Technique for Investigation of Clay Microstructure", Journal De Microscopie, Vol. 6, pp. 964-983, (Reprinted in English by the Swedish Geotechnical Institute as Reprints and Preliminary Reports, No. 24, 1968).
- Pusch, R., (1972), "Discussion of (Pore Size Distribution Studies by Sridharan, A., Altschaeffl, A. G., and Diamond, S., (1971), Journal of the Soil Mechanics and Foundations Division, ASCE, Vol. 97, No. SM5, May)", Journal of the Soil Mechanics and Foundations Division, ASCE, Vol. 98, No. SM1, January, pp. 135-137.

- Quirk, J. P., and Panabokke, C. R., (1962), "Incipient Failure of Soil Aggregates", Journal of Soil Science, Vol. 13, No. 1, pp. 60-70.
- Rallings, R. A., (1971), "The Effect of Pretreatment Moisture Content on the Properties of Cement and Lime Stabilized Clay Soils", Australian Road Research, Vol. 4, No. 6, June, pp. 10-31.
- Ray, P. N., and Chapman, T. G., (1954), "The British Standard Compaction Test for Soils: A Study of Some Factors Affecting the Test Results", Geotechnique, Vol. 4, December, pp. 169-177.
- Rieke, R. and Mauve, L., (1942), "Zur Frage des Nachweises des mineralischen Bestandteile der Kaoline", Bericht Deutsche Keramischen Gesellschaft, Vol. 23, pp. 119-150.
- Ritter, H. L., and Drake, L. C., (1945), "Pore Size Distribution in Porous Materials", Industrial and Engineering Chemistry, Analytical Edition, Vol. 17, No. 12, December, pp. 782-786.
- Roberts, N. K., (1964), "The Surface Tension of Mercury and the Adsorption of Water Vapor and Some Saturated Hydrocarbons on Mercury", Journal, Chemical Society, June, pp. 1907-1915.
- Rootare, H. M., (1968), "A Short Literature Review of Mercury Porosimetry as a Method of Measuring Pore-Size Distributions in Porous Materials, and a Discussion of Possible Sources of Errors in This Method," Aminco Lab News, Vol. 24, No. 3, pp. 4A-4H.
- Rosenqvist, I. T., (1959), "Physico-Chemical Properties of Soils: Soil-Water Systems", Journal of the Soil Mechanics and Foundations Division, ASCE, Vol. 85, No. SM2, April, pp. 31-53.
- Ross, C. S., and Kerr, P. F., (1931), "The Kaolin Minerals", U. S. Geological Survey Professional Paper 165E, pp. 151-175.
- Rubin, J., (1949), "The Influence of Externally Applied Stresses upon the Structure of Confined Soil Materials", Ph.D. Thesis, University of California, Berkeley, California, August, pp. 115-128.
- Russell, M. B., (1942), "Pore Size Distribution as a Measure of Soil Structure", Proceedings, Soil Science Society of America, Vol. 6, pp. 108-112.

- Saddington, A. W., and Krase, N. W., (1934), "Vapor-Liquid Equilibria in the System Nitrogen-Water", Journal, American Chemical Society, Vol. 56, February, pp. 353-361.
- Schackel, B., (1969), "A Nuclear Method for Detecting Small Variations in Density Within Soil Specimens", Australian Road Research, Vol. 3, No. 9, March, pp. 12-34.
- Seed, H. B., and Chan, C. K., (1959), "Structure and Strength Characteristics of Compacted Clays," Journal of the Soil Mechanics and Foundations Division, ASCE, No. SM5, October, pp. 87-128.
- Seed, H. B., and Chan, C. K., (1959), "Undrained Strength of Compacted Clays After Soaking", Journal of the Soil Mechanics and Foundations Division, ASCE, Vol. 85, No. SM6, December, pp. 31-47.
- Seed, H. B., Chan, C. K., and Lee, C. E., (1962), "Resilience Characteristics of Subgrade Soils and Their Relation to Fatigue Failures in Asphalt Pavements", International Conference on the Structural Design of Asphalt Pavements, Ann Arbor, Michigan, pp. 1-37.
- Seed, H. B., Mitchell, J. K., and Chan, C. K., (1962), "Studies of Swell and Swell Pressure Characteristics of Compacted Clays," Bulletin No. 313, Highway Research Board, pp. 12-39.
- Seed, H. B., Woodward, R. J., and Lundgren, R., (1962), "Prediction of Swelling Potential for Compacted Clays", Journal of the Soil Mechanics and Foundations Division, ASCE, Vol. 88, No. SM3, June, pp. 53-87.
- Sengers, J. V., and Sengers, A. L., (1968), "The Critical Region", Chemical and Engineering News, June, pp. 104-118.
- Sloane, R. L., and Kell, T. R., (1966), "The Fabric of Mechanically Compacted Kaolin", Clays and Clay Minerals, Vol. 26, pp. 289-296.
- Smalley, I. J., and Cabrera, J. G., (1969), "Particle Association in Compacted Kaolin", Nature, Vol. 222, April, pp. 80-81.
- Smith, R. M., Browning, D. R., and Pohlman, G. G., (1944), "Laboratory Percolation Through Undisturbed Soil Samples in Relation to Pore-Size Distribution", Soil Science, Vol. 57, pp. 197-213.

- Sowers, G. F., and Nelson, G. H., (1949), "Effect of Re-using Soil on Moisture-Density Curves", Proceedings, Highway Research Board, Vol. 29, pp. 482-487.
- Sridharan, A., (1968), "Some Studies on the Strength of Partly Saturated Clays", Ph.D. Thesis, Purdue University, Lafayette, Indiana, August, 179 pp.
- Sridharan, A., Altschaeffl, A. G. and Diamond, S., (1971), "Pore Size Distribution Studies", Journal of Soil Mechanics and Foundations Division, ASCE, Vol. 97, No. SM5, May, pp. 771-787.
- Stanley, H. E., (1971), Introduction to Phase Transitions and Critical Phenomena, Oxford University Press, pp. 1-7.
- Stringer, I., (1966), "The Accuracy of Volume Measurement by Mercury Displacement," Journal, Australian Ceramic Society, Vol. 2, No. 2, pp. 47-51.
- Swanson, C. L. W., and Peterson, J. B., (1942), "The Use of the Micrometric and Other Methods for the Evaluation of Soil Structure", Soil Science, Vol. 53, pp. 173-185.
- Tamez, E. G., (1957), "Some Factors Affecting the Dynamic Compaction Test", Conference on Soils for Engineering Purposes, Special Technical Publication 232, ASTM, pp. 62-66.
- Terzaghi, C., (1925), "Principles of Soil Mechanics: III-Determination of Permeability of Clay", Engineering News Record, Vol. 95, No. 21, pp. 832-836.
- Thompson, J. N., (1941), "An Investigation of Compaction in Highway Construction", Proceedings, Fourth Texas Conference on Soil Mechanics and Foundation Engineering, Part I, The University of Texas, Austin, Texas, February, 17 pp.
- Tovey, N. K., and Yan, W. K., (1973), "The Preparation of Soils and Other Geological Materials for the Scanning Electron Microscope", Proceedings, International Symposium on Soil Structure, Gothenburg, Sweden, pp. 59-67.
- Townsend, D. L., (1959), "The Performance and Efficiency of Standard Compaction Equipment", Report No. 6, Queen's University, Kingston, Ontario, January, pp. 3-27.
- Trollope, D. H., and Chan, C. K., (1960), "Soil Structure and the Step-Strain Phenomenon", Journal of the Soil Mechanics and Foundations Division, ASCE, Vol. 86, No. SM2, April, pp. 1-39.

- Turnbull, J. M., (1960), "Discussion of (Compacted Clay: Structure by Lambe, T. W., (1960), Transactions, ASCE, Vol. 125, pp. 682-717)", Transactions, ASCE, Vol. 125, pp. 743-746.
- Ulmer, G. C., and Smothers, W. J., (1967), "Application of Mercury Porosimetry to Refractory Materials", Bulletin, American Ceramic Society, Vol. 46, No. 7, pp. 649-652.
- Walker, F. C., and Holtz, W. G., (1953), "Control of Embankment Material by Laboratory Testing", Transactions, ASCE, Vol. 118, pp. 1-11.
- Warshaw, C. M., Rosenberg, P. E., and Roy, R., (1960), "Changes Effected in Layer Silicates by Heating Below 550°C", Clay Minerals Bulletin, Vol. 4, No. 23, July, pp. 113-126.
- Washburn, E. W., (1921), "Note on a Method of Determining the Distribution of Pore Sizes in a Porous Material", Proceedings, National Academy of Sciences, Vol. 7, pp. 115-116.
- Waterways Experiment Station, Vicksburg, Mississippi, (1949a), "Compaction Studies on Clayey Sands", Soil Compaction Investigation, Technical Memorandum No. 3-271, Report No. 1, 36 pp.
- Waterways Experiment Station, Vicksburg, Mississippi, (1949b), "Compaction Studies on Silty Clay", Soil Compaction Investigation, Technical Memorandum No. 3-271, Report No. 2, 49 pp.
- Watson, A., May, J. O., and Butterworth, B., (1957), "Studies of Pore Size Distribution", Transactions, British Ceramic Society, Vol. 56, pp. 37-52.
- Weiss, A., Fahn, R., and Hofmann, U., (1952), "Nachweis der Gerueststruktur in Thixotropen Gelen", Naturwissenschaften, Vol. 39, No. 15, pp. 351-352.
- Wiebe, R., Gaddy, V. L., and Heins, C., Jr., (1933), "The Solubility of Nitrogen in Water at 50°, 75°, and 100°C From 25 To 1000 Atmospheres", Journal, American Chemical Society, Vol. 55, March, pp. 947-953.
- Willis, E. A., (1946), "Discussion of (A Study of Lateritic Soils by Fruhauf, B., (1946), Proceedings, Highway Research Board, Vol. 26, pp. 579-589)", Proceedings, Highway Research Board, Vol. 26, pp. 589-593.

- Winslow, D. N., (1969), "The Pore Size Distribution of Portland Cement Paste", MSCE Thesis, Purdue University, Lafayette, Indiana, January, 102 pp.
- Winslow, D. N., and Diamond, S., (1970), "The Pore Size Distribution of Portland Cement Paste", Journal of Materials, Vol. 5, No. 3, pp. 564-585.
- Winslow, N. M., and Shapiro, J. J., (1959), "An Instrument for the Measurement of Pore-Size Distribution by Mercury Penetration", ASTM Bulletin 236, February, pp. 39-54.
- Wu, T. H., Douglas, A. G., Goughnour, R. D., (1962), "Friction and Cohesion of Saturated Clays", Journal of the Soil Mechanics and Foundations Division, ASCE, Vol. 88, No. SM3, June, pp. 1-33.

APPENDIX A

TABULATED PORE SIZE
DISTRIBUTION DATA

TABLE A-1

Distribution of Pore Space for Edgar Plastic Kaolin and Grundite Aggregations
Manufactured at Different Water Contents, and Dried by the Critical Region Method

Pore Content (cm^3/gm) in Equivalent
Pore Diameter (micrometers) Ranges of

Soil	Mixing Water Content (%)	Total Porosity (cm^3/gm)	< 0.025	0.025 - 0.1	0.1 - 0.4	0.4 - 1.6	1.6 - 6.4	6.4 - 25.6
Edgar Plastic Kaolin	26.9	0.485	0.043	0.186	0.081	0.090	0.065	0.020
	29.1	0.436	0.048	0.200	0.074	0.068	0.038	0.008
	34.6	0.411	0.042	0.212	0.080	0.052	0.020	0.005
Grundite	19.4	0.404	0.066	0.072	0.090	0.069	0.054	0.029
	23.0	0.356	0.053	0.085	0.097	0.073	0.036	0.012

TABLE A-2

Percent Distribution of Pore Space for Edgar Plastic Kaolin and Grundite Aggregations Manufactured at Different Water Contents, and Dried by the Critical Region Method

Percent Pore Space in Equivalent Pore Diameter (micrometers) Ranges of

Soil	Mixing Water Content (%)	< 0.025	0.025 - 0.1	0.1 - 0.4	0.4 - 1.6	1.6 - 6.4	6.4 - 25.6
Edgar Plastic Kaolin	26.9	8.9	38.4	16.7	18.6	13.3	4.1
	29.1	11.0	45.9	17.0	15.6	8.7	1.8
	34.6	10.2	51.6	19.5	12.6	4.9	1.2
Grundite	19.4	16.3	17.8	22.3	17.1	13.4	7.2
	23.0	14.9	23.9	27.2	20.5	10.1	3.4

TABLE A-3

Distribution of Pore Space for Edgar Plastic Kaolin, Crosby Silty Clay, Boston Blue Clay, Grundite, and Reddish-Brown Limestone Residual Clay Compacted at Different Water Contents by the Standard Proctor Method, and Critical Region Dried

Pore Content (cm^3/gm) in Equivalent
Pore Diameter (micrometers) Ranges of

Soil	Molding Water Content (%)	Total Porosity (cm^3/gm)	<0.025	0.025 - 0.1	0.1 - 0.4	0.4 - 1.6	1.6 - 6.4	6.4 - 25.6
Edgar Plastic Kaolin								
	22.7	0.479	0.016	0.195	0.150	0.090	0.028	-
	27.6	0.437	0.032	0.210	0.117	0.063	0.015	-
	30.0	0.382	0.024	0.213	0.096	0.043	0.006	-
	31.2	0.340	0.022	0.228	0.056	0.030	0.003	-
	34.6	0.360	0.027	0.228	0.071	0.028	0.006	-
	36.7	0.386	0.032	0.230	0.075	0.041	0.004	-
	39.1	0.424	0.032	0.230	0.093	0.055	0.014	-
Crosby Silty Clay								
	13.4	0.248	0.018	0.038	0.075	0.015	0.042	0.057
	15.6	0.206	0.024	0.038	0.081	0.022	0.017	0.023
	16.3	0.196	0.023	0.033	0.093	0.030	0.016	0.001
	18.2	0.199	0.037	0.025	0.105	0.024	0.006	0.001
	21.2	0.228	0.026	0.035	0.131	0.025	0.006	0.003
	24.4	0.252	0.021	0.045	0.153	0.030	0.003	0.000

TABLE A-3
(Continued)

Soil	Molding Water Content (%)	Total Porosity (cm ³ /gm)	<0.025	0.025 - 0.1	0.1 - 0.4	0.4 - 1.6	1.6 - 6.4	6.4 - 25.6
Boston Blue Clay	15.0	0.382	0.026	0.080	0.111	0.161	0.004	-
	19.6	0.335	0.015	0.087	0.126	0.088	0.019	-
	20.8	0.223	0.011	0.108	0.096	0.007	0.001	-
	23.5	0.265	0.023	0.117	0.096	0.015	0.005	-
Grundite	9.1	0.293	0.065	0.057	0.075	0.078	0.016	-
	16.4	0.275	0.052	0.078	0.084	0.050	0.007	-
	21.0	0.247	0.058	0.096	0.081	0.008	0.003	-
	23.0	0.262	0.065	0.105	0.078	0.013	0.001	-
	25.0	0.270	0.066	0.099	0.090	0.011	0.003	-
	26.0	0.273	0.063	0.087	0.102	0.021	0.000	-
Reddish-Brown Limestone Residual Clay	16.1	0.265	0.043	0.132	0.034	0.017	0.014	0.009
	21.8	0.237	0.045	0.162	0.030	0.000	0.000	0.000
	28.1	0.308	0.069	0.180	0.050	0.004	0.004	0.001

TABLE A-4

Percent Distribution of Pore Space for Edgar Plastic Kaolin, Crosby Silty Clay, Boston Blue Clay, Grundite, and Reddish-Brown Limestone Residual Clay Compacted at Different Water Contents by the Standard Proctor Method, and Critical Region Dried

Percent Pore Space in Equivalent Pore Diameter
(micrometers) Ranges of

Soil	Molding Water Content (%)	< 0.025	0.025 - 0.1	0.1 - 0.4	0.4 - 1.6	1.6 - 6.4	6.4 - 25.6
Edgar Plastic Kaolin	22.7	3.4	40.7	31.3	18.8	5.8	-
	27.6	7.3	48.1	26.7	14.4	3.4	-
	30.0	6.3	55.7	25.1	11.2	1.6	-
	31.2	6.5	67.1	16.7	8.8	0.9	-
	34.6	7.5	63.3	19.7	7.8	1.7	-
	36.7	8.3	59.5	19.4	10.6	1.0	-
	39.1	7.5	54.2	21.9	12.9	3.3	-
Crosby Silty Clay	13.4	7.2	15.3	30.3	6.0	16.9	23.0
	15.6	11.6	18.5	39.3	10.7	8.3	11.2
	16.3	11.7	16.8	47.5	15.3	8.2	0.5
	18.2	18.6	12.6	52.8	12.1	3.0	0.5
	21.2	11.4	15.4	57.5	11.0	2.6	1.3
	24.4	8.3	17.9	60.7	11.9	1.2	0.0

TABLE A-4
(Continued)

Soil	Molding Water Content (%)	< 0.025	0.025 - 0.1	0.1 - 0.4	0.4 - 1.6	1.6 - 6.4	6.4 - 25.6
Boston Blue Clay	15.0	6.8	21.0	29.0	42.2	1.0	-
	19.6	4.6	26.0	37.6	26.2	5.6	-
	20.8	4.9	48.4	43.0	3.1	0.5	-
	23.5	8.6	44.2	36.2	5.6	1.9	-
Grundite	9.1	22.2	19.5	25.6	26.6	5.5	-
	16.4	18.9	28.4	30.5	18.2	2.5	-
	21.0	23.5	38.9	32.8	3.4	1.4	-
	23.0	24.8	40.0	29.8	4.9	0.3	-
	25.0	24.4	36.7	33.3	4.0	1.1	-
	26.0	23.1	31.9	37.4	7.7	0.0	-
Reddish-Brown Limestone Residual Clay	16.1	16.3	49.8	12.8	6.4	5.3	3.4
	21.8	18.9	68.4	12.7	0.0	0.0	0.0
	28.1	22.4	58.5	16.2	1.3	1.3	0.3

TABLE A-5

Mean Pore Diameters of the Space in Pore Sizes Above and Below 0.1 Micrometers for Edgar Plastic Kaolin and Grundite Aggregations; and for Edgar Plastic Kaolin, Crosby Silty Clay, Boston Blue Clay, Grundite, and Reddish-Brown Limestone Residual Clay Compacted at Different Water Contents by the Standard Proctor Method; and Critical Region Dried

Soil	Water Content (%)	Space in Pore Sizes below 0.1 μm		Space in Pore Sizes above 0.1 μm	
		Pore Content (cm^3/gm)	Mean Pore Diameter (μm)	Pore Content (cm^3/gm)	Mean Pore Diameter (μm)
Edgar Plastic Kaolin Aggregations	26.9	0.229	0.060	0.256	0.830
	29.1	0.240	0.062	0.188	0.590
	34.6	0.254	0.062	0.157	0.400
Grundite Aggregations	19.4	0.138	0.037	0.266	1.050
	23.0	0.138	0.036	0.218	0.500
Edgar Plastic Kaolin	22.7	0.211	0.062	0.268	0.320
	27.6	0.242	0.059	0.195	0.305
	30.0	0.237	0.062	0.145	0.248
	31.2	0.250	0.060	0.090	0.235
	34.6	0.255	0.060	0.105	0.280
	36.7	0.262	0.060	0.124	0.325
	39.1	0.262	0.058	0.162	0.370
Crosby Silty Clay	13.4	0.056	0.051	0.192	2.500
	15.6	0.062	0.044	0.144	0.285
	16.3	0.056	0.051	0.140	0.290
	18.2	0.062	-	0.137	0.270
	21.2	0.061	0.039	0.167	0.245
	24.4	0.066	0.052	0.186	0.235

TABLE A-5
(Continued)

Soil	Water Content (%)	Space in Pore Sizes below 0.1 μm		Space in Pore Sizes above 0.1 μm	
		Pore Content (cm^3/gm)	Mean Pore Diameter (μm)	Pore Content (cm^3/gm)	Mean Pore Diameter (μm)
Boston Blue Clay	15.0	0.106	0.054	0.276	0.505
	19.6	0.102	0.062	0.233	0.360
	20.8	0.119	0.067	0.104	0.133
	23.5	0.140	0.065	0.125	0.142
Grundite	9.1	0.122	0.025	0.171	0.510
	16.4	0.130	0.032	0.145	0.318
	21.0	0.154	0.038	0.093	0.173
	23.0	0.170	0.039	0.092	0.182
	25.0	0.165	0.037	0.105	0.178
	26.0	0.150	0.034	0.123	0.190
Reddish-Brown Limestone					
Residual Clay	16.1	0.175	0.051	0.090	1.850
	21.8	0.207	0.057	0.030	0.127
	28.1	0.249	0.056	0.059	0.147

TABLE A-6

Distribution of Pore Space for Edgar Plastic Kaolin Compacted at Different Water Contents by Methods Based on the Modified Proctor Compaction Method, and Critical Region Dried

Pore Content (cm^3/gm) in Equivalent Pore Diameter (micrometers) Ranges of

No. of Blows / Layer	Molding Water Content (%)	Total Porosity (cm^3/gm)	< 0.025	0.025 - 0.1	0.1 - 0.4	0.4 - 1.6	1.6 - 6.4
6	25.8	0.472	0.049	0.155	0.215	0.046	0.007
	35.2	0.372	0.022	0.226	0.094	0.024	0.006
12	23.2	0.357	0.021	0.216	0.102	0.015	0.003
	28.7	0.336	0.021	0.223	0.072	0.017	0.003
	30.7	0.331	0.020	0.219	0.065	0.023	0.004
25	22.0	0.355	0.021	0.204	0.117	0.011	0.002
	23.5	0.334	0.031	0.198	0.092	0.010	0.003
	26.5	0.289	0.025	0.213	0.044	0.005	0.002
	28.4	0.302	0.025	0.217	0.050	0.007	0.003
	31.0	0.315	0.020	0.210	0.063	0.020	0.002
	33.6	0.354	0.027	0.228	0.076	0.021	0.002

TABLE A-7

Percent Distribution of Pore Space for Edgar Plastic Kaolin Compacted at Different Water Contents by Methods Based on the Modified Proctor Compaction Method, and Critical Region Dried

Percent Pore Space in Equivalent Pore Diameter (micrometers) Ranges of

No. of Blows /Layer	Molding Water Content (%)	< 0.025	0.025 - 0.1	0.1 - 0.4	0.4 - 1.6	1.6 - 6.4
6	25.8	10.4	32.8	45.6	9.7	1.5
	35.2	5.9	60.8	25.3	6.4	1.6
12	23.2	5.9	60.5	28.6	4.2	0.8
	28.7	6.3	66.4	21.4	5.0	0.9
	30.7	6.0	66.2	19.6	7.0	1.2
25	22.0	5.9	57.5	33.0	3.1	0.5
	23.5	9.3	59.3	27.5	3.0	0.9
	26.5	8.7	73.7	15.2	1.7	0.7
	28.4	8.3	71.9	16.5	2.3	1.0
	31.0	6.4	66.7	20.0	6.3	0.6
	33.6	7.6	64.4	21.5	5.9	0.6

TABLE A-8

Mean Pore Diameters of the Space in Pore Sizes Above and
Below 0.1 Micrometers for Edgar Plastic Kaolin
Compacted by the Methods Based on Modified Proctor
Compaction, and Critical Region Dried

No. of Blows /Layer	Molding Water Content (%)	Space in Pore Sizes below 0.1 μm		Space in Pore Sizes above 0.1 μm	
		Pore Content (cm^3/gm)	Mean Pore Diameter (μm)	Pore Content (cm^3/gm)	Mean Pore Diameter (μm)
25	22.0	0.225	0.065	0.130	0.152
6	25.8	0.204	0.069	0.268	0.205
25	26.5	0.238	0.060	0.051	0.173
6	35.2	0.248	0.071	0.124	0.222
25	33.6	0.255	0.056	0.099	0.230
12	23.2	0.237	0.064	0.120	0.172
25	23.5	0.229	0.065	0.105	0.149
12	28.7	0.244	0.056	0.092	0.225
25	28.4	0.242	0.055	0.060	0.197
12	30.7	0.239	0.062	0.092	0.242
25	31.0	0.230	0.062	0.085	0.235

TABLE A-9

Distribution of Pore Space for Edgar Plastic Kaolin and Grundite Compacted at Different Water Contents, and Soaked Under a Surcharge Pressure of Either $\frac{3}{16}$ Or $\frac{3}{4}$ psi

		Pore Content (cm ³ /gm) in Equivalent Pore Diameter (micrometers) Ranges of								
Soil	Compaction Type and Level	Molding Water Content (%)	Sur-charge Pressure (psi)	Total Porosity (cm ³ /gm)	<0.025	0.025 - 0.1	0.1 - 0.4	0.4 - 1.6	1.6 - 6.4	6.4 - 25.6
Edgar Plastic Kaolin	Standard Proctor	28.7	3/4	0.535	0.022	0.217	0.132	0.100	0.053	0.011
		38.2	3/4	0.413	0.030	0.232	0.095	0.046	0.010	0.000
	Modified Proctor	25.8	3/4	0.588	0.020	0.204	0.181	0.117	0.065	0.001
		35.2	3/4	0.392	0.045	0.224	0.070	0.043	0.010	0.000
	12 Blows/Layer	23.2	3/16	0.673	0.075	0.178	0.165	0.135	0.089	0.031
		26.7	3/4	0.474	0.019	0.248	0.125	0.071	0.011	0.000
		28.7	3/4	0.433	0.022	0.227	0.114	0.059	0.010	0.001
		36.7	3/4	0.383	0.019	0.241	0.089	0.030	0.004	0.000

TABLE A-9
(Continued)

Soil	Compaction Type and Level	Molding Water Content (%)	Sur- charge Pressure (psi)	Total Porosity (cm ³ /gm)	0.025 - 0.1	0.1 - 0.4	0.4 - 1.6	1.6 - 6.4	6.4 -25.6
Modified Proctor 25 Blows/Layer		23.5	3/16	0.425	0.035	0.204	0.096	0.074	0.015
		26.5	3/4	0.437	0.016	0.244	0.110	0.060	0.007
		28.4	3/4	0.405	0.016	0.227	0.098	0.054	0.010
		31.0	3/4	0.360	0.012	0.227	0.079	0.036	0.006
Grundite Standard Proctor		9.1	3/4	0.450	0.068	0.058	0.077	0.121	0.102
		16.4	3/4	0.394	0.060	0.085	0.102	0.084	0.052
		21.0	3/4	0.385	0.055	0.090	0.123	0.090	0.023
		23.0	3/4	0.339	0.057	0.084	0.130	0.054	0.014
		26.0	3/16	0.313	0.055	0.095	0.108	0.042	0.011

TABLE A-10

Percent Distribution of Pore Space for Edgar Plastic Kaolin and Grundite Compacted at Different Water Contents, and Soaked Under a Surcharge Pressure of Either $\frac{3}{16}$ Or $\frac{3}{4}$ psi

		Percent Pore Space in Equivalent Pore Diameter (micrometers) Ranges of									
Soil	Compaction Type and Level	Molding Water Content (%)	Surcharge Pressure (psi)	< 0.025	0.025 - 0.1	0.1 - 0.4	0.4 - 1.6	1.6 - 6.4	6.4 - 25.6	25.6 - 63.1	63.1 - 250
Edgar Plastic Kaolin	Standard Proctor	28.7	3/4	4.1	40.6	24.7	18.7	9.9	2.0		
		38.2	3/4	7.3	56.2	23.0	11.1	2.4	0.0		
	Modified Proctor	25.8	3/4	3.4	34.7	30.8	19.9	11.0	0.2		
		35.2	3/4	11.5	57.1	17.9	11.0	2.5	0.0		
	6 Blows/Layer										
	Modified Proctor										
	12 Blows/Layer	23.2	3/16	11.2	26.5	24.5	20.0	13.2	4.6		
		26.7	3/4	4.0	52.3	26.4	15.0	2.3	0.0		
		28.7	3/4	5.1	52.4	26.3	13.6	2.3	0.2		
		36.7	3/4	5.0	62.9	23.2	7.8	1.0	0.0		
	Modified Proctor	23.5	3/16	8.3	48.0	22.6	17.4	3.5	0.2		
		26.5	3/4	3.7	55.8	25.2	13.7	1.6	0.0		
	25 Blows/Layer	28.4	3/4	4.0	56.0	24.2	13.3	2.5	0.0		
		31.0	3/4	3.3	63.1	22.0	10.0	1.6	0.0		

TABLE A-10
(Continued)

Soil	Compaction Type and Level	Molding Water Content (%)	Surcharge Pressure (psi)	< 0.025	0.025 - 0.1	0.1 - 0.4	0.4 - 1.6	1.6 - 6.4	6.4 -25.6
Grundite	Standard Proctor	9.1	3/4	15.1	12.9	17.1	26.9	22.7	5.3
		16.4	3/4	15.2	21.6	25.9	21.3	13.2	2.5
		21.0	3/4	14.3	23.3	32.0	23.4	6.0	1.0
		23.0	3/4	16.8	24.8	38.3	15.9	4.1	0.0
		26.0	3/16	17.6	30.3	34.5	13.4	3.5	0.6

TABLE A-11

Mean Pore Diameters of the Space in Pore Sizes Above and Below 0.1 Micrometers for Edgar Plastic Kaolin and Grundite Compacted at Different Water Contents, and Soaked Under a Surcharge Pressure of Either $\frac{3}{16}$ Or $\frac{3}{4}$ psi

Soil	Compaction Type and Level	Molding Water Content (%)	Surcharge Pressure (psi)	Space Below 0.1 μ m		Space Above 0.1 μ m	
				Pore Content (cm^3/gm)	Mean Pore Diameter (μ m)	Pore Content (cm^3/gm)	Mean Pore Diameter (μ m)
Edgar Plastic Kaolin	Standard Proctor	28.7	3/4	0.239	0.063	0.296	0.500
		38.2	3/4	0.262	0.060	0.151	0.295
	Modified Proctor, 6 Blows/Layer	25.8	3/4	0.224	0.075	0.364	0.425
		35.2	3/4	0.269	0.066	0.123	0.235
	Modified Proctor, 12 Blows/Layer	23.2	3/16	0.253	0.073	0.420	0.615
		26.7	3/4	0.267	0.075	0.207	0.300
		28.7	3/4	0.249	0.069	0.184	0.290
		36.7	3/4	0.260	0.068	0.123	0.247
	Modified Proctor, 25 Blows/Layer	23.5	3/16	0.239	0.066	0.186	0.375
		26.5	3/4	0.260	0.069	0.177	0.295
		28.4	3/4	0.243	0.067	0.162	0.295
		31.0	3/4	0.239	0.063	0.121	0.277

TABLE A-11
(Continued)

Soil	Compaction Type and Level	Molding Water Content (%)	Surcharge Pressure (psi)	Space Below 0.1 μ		Space Above 0.1 μ	
				Pore Content (cm^3/gm)	Mean Pore Diameter (μm)	Pore Content (cm^3/gm)	Mean Pore Diameter (μm)
Grundite	Standard Proctor	9.1	3/4	0.126	0.034	0.324	1.290
		16.4	3/4	0.145	0.036	0.249	0.550
		21.0	3/4	0.145	0.036	0.240	0.380
		23.0	3/4	0.141	0.036	0.198	0.258
		26.0	3/16	0.150	0.039	0.163	0.249

COVER DESIGN BY ALDO GIORGINI